https://ntrs.nasa.gov/search.jsp?R=19680023321 2020-03-12T06:35:09+00:00Z

NASA CONTRACTOR REPORT

NASA CR-1123

NASA CR-1123

FACILITY FORM 602

N68-23293 (ACCESSION NUMBER)

(THRU)

131 (PAGES)

1 (CODE)

CR-1123 (NASA CR OR TMX OR AD NUMBER)

27 (CATEGORY)

ANALYTICAL PREDICTIONS OF DELIVERED SPECIFIC IMPULSE

by Victor Quan

Prepared by
TRW SYSTEMS
Cleveland, Ohio
for Manned Spacecraft Center

GPO PRICE $

CFSTI PRICE(S) $

Hard copy (HC) 3.00

Microfiche (MF) .65

ff 653 July 65

SEP 1968
RECEIVED
NASA STI FACILITY
INPUT BRANCH

NATIONAL AERONAUTICS AND SPACE ADMINISTRATION • WASHINGTON, D. C. • AUGUST 1968

NASA CR-1123

ANALYTICAL PREDICTIONS OF DELIVERED SPECIFIC IMPULSE

By Victor Quan

Distribution of this report is provided in the interest of information exchange. Responsibility for the contents resides in the author or organization that prepared it.

Issued by Originator as Report No. 02874-6008-R000

Prepared under Contract No. NAS 9-4358 by
TRW SYSTEMS
Cleveland, Ohio

for Manned Spacecraft Center

NATIONAL AERONAUTICS AND SPACE ADMINISTRATION

For sale by the Clearinghouse for Federal Scientific and Technical Information
Springfield, Virginia 22151 – CFSTI price $3.00

PRECEDING PAGE BLANK NOT FILMED.

FOREWORD

The computer programs described in this report were developed for NASA/MSC under contract NAS 9-4358. Many parts of this final report are taken or summarized from reports previously published under the contract. In each instance, the original reference is given. The tasks of analysis, programming, and writing have been performed by many persons as indicated below. V. Quan coordinated the final efforts and edited the program document reports and this final report for the contract.

J.R. Kliegel initiated the efforts in developing the programs and served as program manager since the contract beginning in June 1965 until his leave from TRW Systems in December 1966. V. Quan succeeded Kliegel as program manager until the completion of the contract in September 1967. The original NASA/MSC technical monitor was W.R. Scott and the technical monitor at contract completion was R. Kahl.

The engineering analyses for these programs were performed by J.R. Kliegel, V. Quan, S.S. Cherry, and P.I. Gold. The computer programming was performed by H.M. Frey, J.E. Melde, and G.R. Nickerson. In addition, T.J. Tyson, C.T. Weekley, T.J. McCarron, R.W. Burnett, and P.C. Hanzel have made significant contributions to the completion of the programs. Other staff members have also provided support in various ways. For their infinite patience, ready cooperation, and dedicated effort, all of which enabled the contract to be brought to completion, the program manager would like to express his sincere gratitude. He also wishes to acknowledge the helpful discussions with the former program manager, J.R. Kliegel, in preparing this final report.

PRECEDING PAGE BLANK NOT FILMED.

CONTENTS

	Page
FOREWORD	iii
NOMENCLATURE	ix
1. INTRODUCTION	1-1
2. CHEMICAL SPECIES AND CHEMICAL REACTIONS STUDY	2-1
2.1 Chemical Species Study	2-2
2.2 Chemical Reaction Study	2-4
2.3 Chemical Reaction Rate Study	2-5
3. IMPLICIT INTEGRATION METHOD	3-1
3.1 Stability Considerations	3-1
3.2 Derivation of Numerical Method	3-5
4. TRANSONIC ANALYSES	4-1
4.1 Uniform Expansions	4-1
4.2 Two-Zone Expansions	4-9
5. PROGRAM ANALYSES	5-1
5.1 One-Dimensional Reacting Gas Program	5-1
5.2 One-Dimensional Two-Phase Reacting Gas Program	5-7
5.3 Axisymmetric Reacting Gas Program	5-14
5.4 Axisymmetric Two-Phase Perfect Gas Program	5-27
5.5 Axisymmetric Two-Phase Reacting Gas Analysis	5-34
6. PROGRAM LIMITATIONS	6-1
7. ILLUSTRATIONS OF RESULTS	7-1
8. CONCLUDING REMARKS	8-1
REFERENCES	R-1

ILLUSTRATIONS

		Page
7-1	Velocity Versus Area Ratio	7-3
7-2	Pressure Versus Area Ratio	7-3
7-3	Density Versus Area Ratio	7-4
7-4	Temperature Versus Area Ratio	7-4
7-5	Vacuum Specific Impulse Versus Area Ratio	7-5
7-6	Mole Fraction of H Versus Area Ratio	7-5
7-7	Velocity Lag Versus Axial Position	7-6
7-8	Temperature Lag Versus Axial Position	7-6
7-9	Density Ratio Versus Axial Position	7-7
7-10	Vacuum Specific Impulse Versus Area Ratio	7-7
7-11	Two-Zone Nozzle Performance	7-8
7-12	Nozzle Efficiency as a Function of Nozzle Throat Geometry	7-9
7-13	Nozzle Efficiency as a Function of Nozzle Inlet Geometry	7-9
7-14	Nozzle Efficiency as a Function of Nozzle Contouring	7-9

TABLES

		Page
2-1	Propellant Systems Studied at Chamber Pressures of 100 and 1000 psia to Identify Significant Chemical Species	2-7
2-2	Species Selected for Use in the TRW/NASA Nonequilibrium Performance Programs	2-9
2-3	Significant Species Considered in Each Propellant System	2-10
2-4	Chemical Reactions of Importance in Non-metallized Propellant Systems Containing Carbon, Hydrogen, Oxygen, Nitrogen, Fluorine and Chlorine Having Gaseous Combustion Products	2-14
2-5	Additional Chemical Reactions of Importance in Propellant Systems Containing Condensed Carbon as a Combustion Product	2-15
2-6	Additional Chemical Reactions of Importance in Aluminum Containing Propellant Systems	2-18
2-7	Additional Chemical Reactions of Importance in Berylium Containing Propellant Systems	2-23
2-8	Additional Chemical Reactions of Importance in Boron Containing Propellant Systems	2-25
2-9	Additional Chemical Reactions of Importance in Lithium Containing Propellant Systems	2-30
2-10	Chemical Reactions for Which Rate Constants Have Been Determined	2-32
7-1	Comparison of Measured and Calculated Gas-Particle Expansion Losses in Conical Nozzles	7-10

PRECEDING PAGE BLANK NOT FILMED.

NOMENCLATURE*

a	Reaction rate parameter, also nozzle area
b	Reaction rate parameter
c	Specifies mass fraction
C_{Di}	Particle drag coefficient
C_P	Heat capacity of gas phase at constant pressure
C_{ppi}	Heat capacity of particle at constant pressure
f	Derivative
f_{pi}	Drag coefficient ratio, $C_{Di}/(C_{Di})_{Stokes}$
g_{pi}	Heat transfer coefficient ratio, $Nu_i/(Nu_i)_{Stokes}$
h	Enthalpy, also integration increment
H	Total enthalpy
k	Reaction rate parameter, also variable increment
K	Equilibrium constant
m	Reaction rate ratio
$\overline{m}$	Molecular weight
m_{pi}	Particle bulk density
M	Mach number, also third body reaction term
n	Reaction rate parameter, also summation or iteration index
Nu_i	Particle Nusselt number
P	Pressure
Pr	Gas Prandtl number
r	Radial distance
r_{pi}	Particle radius

*The nomenclatures are different in Sections 2, 3 and 4. The symbols in those sections are either appropriately defined there or self explanatory. Also, symbols not defined in this list are defined as they appear.

NOMENCLATURE (Continued)

r^*	Nozzle throat radius
R	Gas constant
R^*	Nozzle wall radius of curvature at throat
T	Temperature
T_{pmi}	Particle melting temperature
u	Velocity in x-direction
v	Velocity in r-direction
V	Flow velocity
x	Axial distance
y	Dependent variable
z	Dependent variable
α_i	Partial derivative
$\beta_{i,j}$	Partial derivative
$\varphi_{i,j}$	Partial derivative
γ	Ratio of specific heats
ϵ	Nozzle expansion ratio
θ	Flow angle, also nozzle cone angle
μ	Gas viscosity
ρ	Density
ρ_{pi}	Particle density in gas phase
ψ_{pi}	Particle stream function
ω	Species mass production rate
ω_{pi}	Particle to gas mass flow ratio

Subscripts

i	Refers to ith species or equation
j	Refers to jth reaction or variable

NOMENCLATURE (Continued)

l	Refers to particle liquid state
pi	Refers to ith particle size group
s	Refers to particle solid state

<u>Superscripts</u>

*	Refers to throat condition or sonic condition

1. INTRODUCTION

This report contains a summary of the computer programs developed by TRW Systems Group for NASA/MSC under contract NAS 9-4358, Improvement of Analytical Predictions of Delivered Specific Impulse. The objective of this contract was to develop a family of our computer programs to calculate inviscid, one-dimensional and axisymmetric nonequilibrium nozzle flow fields accounting for the nonequilibrium effects of finite rate chemical reactions between gaseous combustion products and velocity and thermal lags between gaseous and condensed combustion products.

The four programs developed under this contract are:

- The One-Dimensional Reacting Gas Nonequilibrium Performance Program, which calculates the equilibrium, frozen and kinetic performance of propellant systems having gaseous exhaust products containing the elements carbon, hydrogen, oxygen, nitrogen, fluorine and chlorine.

- The One-Dimensional Two-Phase Reacting Gas Nonequilibrium Performance Program, which calculates the equilibrium, frozen and kinetic performance of systems having gaseous and condensed exhaust products containing the elements carbon, hydrogen, oxygen, nitrogen, fluorine, chlorine and one metal element, either aluminum, beryllium, boron or lithium.

- The Axisymmetric Reacting Gas Nonequilibrium Performance Program, which calculates the kinetic performance of propellant systems having gaseous exhaust products containing the elements carbon, hydrogen, oxygen, nitrogen, fluorine and chlorine. This program contains an option of considering either the expansion of a uniform mixture (the ideal engine case) or of a two-zoned mixture (the film cooled engine case).

- The Axisymmetric Two-Phase Perfect Gas Performance Program, which calculates the performance of propellant systems having both gaseous and condensed exhaust products. The program considers only the expansion of a uniform mixture (the ideal engine case) of constant specific heat ratio.

The first three programs differ in a number of ways from previous programs developed to calculate nonequilibrium nozzle expansions. In particular:

- The programs are completely self-contained requiring specification of only the propellant system (elemental composition and heat of formation), relaxation rates and nozzle geometry to run a case.

- The chemical species considered by the programs have been selected to allow accurate equilibrium, frozen and kinetic performance analyses of cryogenic, space storable, prepackaged, hybrid and solid propellant systems of current and projected operational use.

- All dissociation-recombination and binary exchange reactions between the gaseous species present in the exhaust are considered by the programs allowing complete kinetic expansion calculations.

- The programs utilize TRW Systems implicit integration method which allows rapid integration of the chemical and gas-particle relaxation equations from equilibrium chamber conditions.

- The axisymmetric program allows analysis of the performance loss associated with film cooling in propellant systems having all gaseous exhaust products.

- The one-dimensional two-phase program allows simultaneous consideration of both chemical and gas-particle relaxation losses in propellant systems having condensed exhaust products.

- The one-dimensional programs allow equilibrium, frozen, and kinetic performance calculations to be performed during a single machine run.

- The programs are written in machine independent language (FORTRAN IV) allowing their use on all standard computers.

The fourth program considers the velocity and thermal lags (for ten particle groups) between the gaseous and condensed combustion products (when they are present in the chamber), but it does not consider nonequilibrium effects of finite rate chemical reactions between gaseous and combustion products. This program utilizes standard explicit integration methods, and is an updated FORTRAN IV version of an earlier program.

In addition, the major components of an Axisymmetric Two-Phase Reacting Gas Nonequilibrium Performance Program were programmed. These components were not combined into a functioning program,

however, since the size of the resulting program would cause extremely long running time per case.

In Section 2 of this report, the results of the study to determine the chemical species and chemical reactions of importance in the propellant systems are summarized. Section 3 describes the implicit integration method used in the programs. Section 4 describes the transonic analyses which are used to construct the initial lines for the characteristics calculations in the axisymmetric programs. A general description of the functions and analysis of each of the computer programs is given in Section 5, and the general limitations of the programs are given in Section 6. Sample results using the programs are given in Section 7, and the concluding remarks are presented in Section 8.

2. CHEMICAL SPECIES AND CHEMICAL REACTIONS STUDY

The study performed to determine the significant chemical species and chemical reactions, which need to be considered in nonequilibrium performance calculations for typical propellant systems containing the elements of carbon, hydrogen, oxygen, nitrogen, fluorine and chlorine, and one metal element, either aluminum, beryllium, boron or lithium, has been described in a previous report by Gold and Weekley, "Chemical Species and Chemical Reactions of Importance in Nonequilibrium Performance Calculations."[1] The following description is taken from that report.

The significant chemical species were defined in the contract as those which must be considered to determine the equilibrium of the propellant systems under investigation to within 0.5 second of specific impulse at an area ratio of 40. The selection of the significant chemical species in typical propellant exhaust mixtures on the basis of equilibrium performance calculations does not, however, insure the validity of the selection for all nonequilibrium performance calculations. If the significant chemical species selection is valid for both equilibrium flow (infinite reaction rates) and frozen flow (zero reaction rates), however, the selection will also be valid for nonequilibrium flows having finite reaction rates. Thus, an additional restriction was imposed on the significant chemical species selection and the significant chemical species were defined as those which must be considered to determine both the equilibrium and frozen specific impulse of the propellant systems under investigation to within 0.5 second at an area ratio of 40.

After determining the significant species, all possible dissociation-recombination and binary exchange reactions between these species were studied. Those reactions having an energy barrier due to the fact that they cannot occur in the ground state (the so-called "spin forbidden" reactions) were identified, and those reactions, which while stoichiometrically possible were highly improbable due to structural or steric factors, were identified and eliminated from consideration. A literature

rate survey was performed to determine the status of rate data for the chemical reactions of interest.

These studies are described in the following sections.

2.1 CHEMICAL SPECIES STUDY

A number of propellant systems containing the elements: carbon, hydrogen, oxygen, nitrogen, fluorine and chlorine, and one metal element, either aluminum, beryllium, boron or lithium, were selected as representative of typical liquid rocket cryogenic, space storable and prepackaged storable propellant systems, hybrid and solid rocket propellants. The propellant systems selected for study are given in Table 2-1. These propellant systems are representative of current and projected operational propellant systems.

The number of chemical species in the exhaust mixtures of these propellants for which JANAF thermochemical data exists is over one hundred. The number of chemical reactions between these species which are stoichiometrically possible is naturally immense. It is clearly undesirable to attempt to account for all possible chemical species and chemical reactions in nonequilibrium performance calculations since it is known that relatively few of the total possible species and reactions are of engineering importance in nozzle and plume expansions.

The approach taken in this study to determine the minimum number of species which must be considered in nonequilibrium performance calculations was to consider equilibrium and frozen expansions as the limits of nonequilibrium expansions. Thus, by determining the significant species which must be considered to accurately calculate the equilibrium and frozen performance of these typical propellant systems, the significant species which must be considered in calculating the nonequilibrium performance of these and similar propellant systems can be determined. For the purpose of this study, the significant chemical species were defined as those which must be considered to determine both the equilibrium and frozen specific impulse of the propellant systems studied to within 0.5 second at an area ratio of 40.

Equilibrium and frozen performance calculations were performed for the propellant systems listed in Table 2-1, at two chamber pressures, 100 psia and 1000 psia, considering all species for which JANAF thermochemical data exist and are present in the exhaust mixtures. These calculations were used as the reference calculations for comparison with calculations performed considering fewer species. Those molecular species, appearing in only trace amounts (less than approximately 10^{-3} mole percent) in the reference calculations, were neglected and the calculations repeated to determine the effect of neglecting trace species on the calculated equilibrium and frozen performance of these propellant systems. After a series of such calculations considering different chemical species present in the various exhaust mixtures, it was determined that the significant species present in these exhaust mixtures are those given in Table 2-2. The significant species present in each propellant system studied are given in Table 2-3. Comparisons of the equilibrium and frozen performance calculated considering all species present and only the significant species present are given in Tables IV through XXXVII in Appendix A of Reference 1, for all propellant systems studied and are not repeated here.

From Tables IV through XXXVII, Appendix A of Reference 1, it can be seen that for the nonmetallized propellant systems the maximum performance difference between the calculations considering all species present and only the significant species present is 0.49 second of specific impulse at an area ratio of 40. This difference occurs in the frozen performance calculation of the Chlorine Trifluoride/86% Monomethyl Hydrazine +14% Hydrazine system at a mixture ratio of 3.2 and 100 psia chamber pressure. In the metallized systems, the maximum performance difference is 0.38 second of specific impulse at an area ratio of 40 which occurs in the frozen performance calculation of the double base-beryllium-ammonium perchlorate system for 100 psia chamber pressure. It is seen that the neglected chemical species have little effect on the calculated performance of the propellant systems studied. Thus, performance calculations performed considering only the significant chemical species given in Table 2-2 present in the exhaust mixture will allow the accurate determination of the equilibrium, frozen and non-equilibrium performance of these and similar propellant systems.

Although the significant chemical species given in Table 2-2 were determined from studying specific propellant systems, the utility of nonequilibrium performance programs based on this species selection is not limited to these specific propellant systems, but is equally valid for chemically similar propellant systems. In studying similar propellant systems, the applicability of the significant species selection can be simply established by comparing equilibrium and frozen performance calculations considering all species present and only the significant species present. For chemically nonsimilar systems, the above methods can be readily utilized to determine the significant chemical species in these systems.

2.2 CHEMICAL REACTION STUDY

Having identified the significant chemical species in the above propellant systems, all possible recombination-dissociation and binary exchange reactions between the significant species present in each propellant system were studied. Those reactions which, although stoichiometrically possible, were highly improbable on the basis of structural or steric factors were eliminated resulting in the identification of those reactions given in Tables 2-4 through 2-9 as those reactions of possible chemical significance in nonequilibrium expansions of the propellant systems studied.

Those reactions eliminated due to steric and structural arguments (listed in Table VII, Appendix B of Reference 1) involve the breaking and formation of a number of chemical bonds and molecular rearrangements which are highly improbable compared to other reactions which can occur between the same species.

Although arguments can be given that some of the reactions identified to be of possible chemical significance in the nonequilibrium expansion of the propellant systems studied can be of little significance due to concentration considerations or possible activation energy considerations, current lack of rate knowledge precludes their elimination at this time. This approach of retaining all possible chemical reactions in nonequilibrium calculations which cannot be eliminated due to steric consideration insures that future rate measurements which may change the relative

importance of various chemical reactions will not affect the nonequilibrium computer programs developed by TRW for NASA.

2.3 CHEMICAL REACTION RATE STUDY

A literature survey was performed to determine the status of rate data for the chemical reactions given in Tables 2-4 through 2-9. Those reactions for which rates have been reported are given in Table 2-10. In addition, those reactions having an energy barrier due to the fact that they cannot occur in the ground state (the so-called "spin forbidden" reactions) were identified and are listed in Table VIII, Appendix B of Reference 1.

Order of magnitude rate estimates can be obtained by statistical mechanics and kinetic theory for those reactions for which rate data are not reported. When rate constants are represented by an Arrhenius equation, $k = AT^n \exp(-E/RT)$, where T is the absolute temperature, R is the gas constant, A is the frequency factor, E is the activation energy, and n determines the pre-exponential temperature dependence, order of magnitude approximations can be made as follows:[2]

a) Exothermic, trimolecular reactions

$$B + C + M \rightleftarrows BC + M \quad , \quad k = 3\times10^{16}\, T^{-0.5}$$

b) Exothermic, bimolecular reactions with triatomic transition states

$$B + CD \rightleftarrows BC + D \quad , \quad k = 5\times10^{11}\, T^{0.5} \exp\left|- E/RT\right|$$

where E = 5.5% of the CD bond energy (Hirschfelder Rule)

c) Exothermic, bimolecular reactions with transition states of more than three atoms

$$BC + DE \rightleftarrows BCD + E \, , \quad k = 1\times10^{11}\, T^{0.5} \exp\left|- E/RT\right|$$

where E = 5.5% of the DE bond energy

d) <u>Exothermic</u>, bimolecular, binary exchange reactions

$$BC + DE \rightleftarrows BD + CE \quad , \quad k = 1 \times 10^{10}\, T^{0.5} \exp\left[- E/RT\right]$$

where E = 28% of the sum of the BC and DE bond energies

The reaction rates for the "spin forbidden" reactions can be similarly estimated if the rate constants are corrected by Boltzmann factors for the fact that these reactions do not occur in the ground state.

Table 2-1. Propellant Systems Studied at Chamber Pressures of 100 and 1000 psia to Identify Significant Chemical Species

	Oxidizer/Fuel	Mixture Ratios
1.	Oxygen/Hydrogen	MR = 2.0, 4.0, 5.0, 6.0, 10.0
2.	Fluorine/Hydrogen	MR = 3.0, 7.0, 10.0, 13.0, 20.0
3.	Oxygen/RP-1	MR = 1.0, 2.2, 2.6, 3.0, 5.0
4.	Nitrogen Tetroxide/Hydrazine	MR = 0.5, 0.9, 1.1, 1.3, 2.0
5.	Compound "A"/ Hydrazine	MR = 1.0, 2.3, 2.5, 2.7, 5.0
6.	Nitrogen Tetroxide/Monomethyl Hydrazine	MR = 0.5, 1.5, 1.8, 2.1, 3.5
7.	Oxygen Difluoride/Monomethyl Hydrazine	MR = 0.5, 1.5, 1.8, 2.1, 3.5
8.	Perchloryl Fluoride/Monomethyl Hydrazine	MR = 0.5, 1.5, 1.8, 2.1, 3.5
9.	Hydrazine/Diborane	MR = 1.15, 1.25, 1.35
10.	Oxygen Difluoride/Diborane	MR = 2.4, 3.2, 4.0
11.	Oxygen Difluoride/Lithium Hydride	MR = 2.5, 3.0, 3.5
12.	Chlorine Trifluoride/86% Monomethyl Hydrazine+14% Hydrazine	MR = 2.4, 2.8, 3.2
13.	Chlorine Trifluoride/49% Monomethyl Hydrazine+8% Hydrazine+ 43% Aluminum	MR = 2.5, 3.0, 3.5
14.	Chlorine Trifluoride/43% Monomethyl Hydrazine+7% Hydrazine+ 50% Boron	MR = 4.0, 5.0, 6.0
15.	Chlorine Trifluoride/43% Monomethyl Hydrazine+7% Hydrazine+ 50% Beryllium	MR = 3.5, 4.5, 5.5

Table 2-1. Propellant Systems Studied at Chamber Pressures of 100 and 1000 psia to Identify Significant Chemical Species (Continued)

Oxidizer/Fuel	Composition
16. Ammonium Perchlorate/PBAA— Aluminum	14 percent Organic Fuel 16 " Aluminum 70 " NH_4ClO_4
17. Ammonium Perchlorate/PBAA— Beryllium	16 " Organic Fuel 13 " Beryllium 71 " NH_4ClO_4
18. Ammonium Perchlorate/Double Base— Aluminum	69.4 " Double Base 19.8 " Aluminum 10.8 " NH_4ClO_4
19. Ammonium Perchlorate/Double Base— Beryllium	81 " Double Base 10 " Beryllium 9 " NH_4ClO_4

Table 2-2. Species Selected for Use in the TRW/NASA Nonequilibrium Performance Programs

Basic Species for C, H, N, O, Cl, and F Propellant Systems Having Gaseous Combustion Products

C	Cl	F	H	N	O
CO	Cl_2	F_2	H_2	N_2	O_2
CO_2	ClF		H_2O	NO	OH
			HF		
			HCl		

Additional Species for Propellant Systems Having Condensed Carbon as a Combustion Product	Additional Species for Propellant Systems Containing Aluminum	Additional Species for Propellant Systems Containing Boron	Additional Species for Propellant Systems Containing Beryllium	Additional Species for Propellant Systems Containing Lithium
C(S)	Al	B	Be	Li
C_2	AlO	B(L)	BeOH	LiH
CH	Al_2O	B(S)	BeO_2H_2	LiOH
CH_2	Al_2O_3(L)	BO	BeO	LiO
CH_3	Al_2O_3(S)	BO_2	BeO(L)	Li_2O
CH_4	AlOCl	BF	BeO(S)	LiCl
C_2H_2	AlOF	BF_2	Be_2O	LiF
CF	AlCl	BF_3	BeCl	Li_2F_2
C_2F_2	$AlCl_2$	BCl	$BeCl_2$	Li_2Cl_2
CN	$AlCl_3$	BCl_2	BeF	
ClCN	AlClF	BCl_3	BeF_2	
FCN	$AlClF_2$	BClF	BeClF	
HCN	$AlCl_2F$	BCl_2F		
	AlF	$BClF_2$		
	AlF_2	BOF		
	AlF_3	BOCl		
		BN		
		BN(S)		

Table 2-3. Significant Species Considered in Each Propellant System

Propellant System (Table 2-1)				
O_2/H_2	F_2/H_2	O_2/RP-1	N_2O_4/H_2H_4	A/N_2H_4
		Species		
H	H	C	H	Cl
H_2	H_2	C(S)	H_2	Cl_2
H_2O	HF	CO	H_2O	ClF
O	F	CO_2	N	F
O_2	F_2	C_2	N_2	F_2
OH		CH	NO	H
		CH_2	O	H_2
		CH_3	O_2	HF
		CH_4	OH	HCl
		C_2H		N
		H		N_2
		H_2		
		H_2O		
		O		
		O_2		
		OH		
Total Number of Species Considered In Each Case				
6	5	16	9	11

Table 2-3. Significant Species Considered in Each Propellant System (Continued)

N_2O_4/MMH	OF_2/MMH	ClO_3F/MMH	N_2H_4/B_2H_6	OF_2/B_2H_6
		Species		
C	C	C	B	B
C(S)	C(S)	C(S)	B(L)	B(L)
CO	CO	CO	B(S)	B(S)
CO_2	CO_2	CO_2	BN	BO
CN	CN	CN	BN(S)	BO_2
C_2	C_2	C_2	H	BF
CH	CH	CH	H_2	BF_2
CH_2	CH_2	CH_2	N	BF_3
CH_3	CH_3	CH_3	N_2	BOF
CH_4	CH_4	CH_4		F
C_2H_2	C_2H_2	C_2H_2		F_2
H	CF	CF		H
H_2	C_2F_2	C_2F_2		H_2
H_2O	F	Cl		H_2O
HCN	F_2	Cl_2		HF
N	FCN	ClCN		O
N_2	H	ClF		O_2
NO	H_2	F		OH
O	H_2O	F_2		
O_2	HF	FCN		
OH	HCN	H		
	N	H_2		
	N_2	H_2O		
	NO	HF		
	O	HCl		
	O_2	HCN		
	OH	N		
		N_2		
		NO		
		O		
		O_2		
		OH		
Total Number of Species Considered In Each System				
21	27	32	9	18

Table 2-3. Significant Species Considered in Each Propellant System (Continued)

OF_2/LiH	CTF/86% MMH + 14% N_2H_4	CTF/49% MMH + 8% N_2H_4 + 43% Al	CTF/43% MMH + 7% N_2H_4 + 50% B	CTF/43% MMH + 7% N_2H_4 + 50% Be
		Species		
F	C	C	C	C
F_2	C(S)	C(S)	C(S)	C(S)
H	C_2	C_2	C_2	C_2
H_2	CN	CN	CN	CN
H_2O	CH	CH	CH	CH
HF	CH_2	CH_2	CH_2	CH_2
Li	CH_3	CH_3	CH_3	CH_3
LiH	CH_4	CH_4	CH_4	CH_4
LiOH	C_2H_2	C_2H_2	C_2H_2	C_2H_2
LiO	CF	CF	CF	CF
Li_2O	C_2F_2	C_2F_2	C_2F_2	C_2F_2
LiF	Cl	Cl	Cl	Cl
Li_2F_2	Cl_2	Cl_2	Cl_2	Cl_2
O	ClCN	ClCN	ClCN	ClCN
O_2	ClF	ClF	ClF	ClF
OH	F	F	F	F
	F_2	F_2	F_2	F_2
	FCN	FCN	FCN	FCN
	H	H	H	H
	H_2	H_2	H_2	H_2
	HF	HF	HF	HF
	HCl	HCl	HCl	HCl
	HCN	HCN	HCN	HCN
	N	N	N	N
	N_2	N_2	N_2	N_2
		Al	B	Be
		AlCl	B(L)	BeCl
		$AlCl_2$	B(S)	$BeCl_2$
		AlF	BF	BeF
		AlF_2	BF_2	BeF_2
		AlF_3	BF_3	BeClF
		$AlCl_3$	BN	
		AlClF	BN(S)	
		$AlClF_2$	BCl	
		$AlCl_2F$	BCl_2	
			BCl_3	
			BClF	
			BCl_2F	
			$BClF_2$	
Total Number of Species Considered in Each System				
16	25	35	39	31

Table 2-3. Significant Species Considered in Each Propellant System (Continued)

AP/PBAA-Al	AP/PBAA-Be	AP/DB-Al	AP/DB-Be
	Species		
C	C	C	C
C(S)	C(S)	C(S)	C(S)
CO	CO	CO	CO
CO_2	CO_2	CO_2	CO_2
CN	CN	CN	CN
C_2	C_2	C_2	C_2
CH	CH	CH	CH
CH_2	CH_2	CH_2	CH_2
CH_3	CH_3	CH_3	CH_3
CH_4	CH_4	CH_4	CH_4
C_2H_2	C_2H_2	C_2H_2	C_2H_2
Cl	Cl	Cl	Cl
Cl_2	Cl_2	Cl_2	Cl_2
ClCN	ClCN	ClCN	ClCN
H	H	H	H
H_2	H_2	H_2	H_2
H_2O	H_2O	H_2O	H_2O
HCl	HCl	HCl	HCl
HCN	HCN	HCN	HCN
N	N	N	N
N_2	N_2	N_2	N_2
NO	NO	NO	NO
O	O	O	O
O_2	O_2	O_2	O_2
OH	OH	OH	OH
Al	Be	Al	Be
AlO	BeOH	AlO	BeOH
Al_2O	BeO_2H_2	Al_2O	BeO_2H_2
$Al_2O_3(L)$	BeO	$Al_2O_3(L)$	BeO
$Al_2O_3(S)$	BeO(L)	$Al_2O_3(S)$	BeO(L)
AlCl	BeO(S)	AlCl	BeO(S)
$AlCl_2$	BeCl	$AlCl_2$	BeCl
AlOCl	$BeCl_2$	AlOCl	$BeCl_2$
$AlCl_3$	Be_2O	$AlCl_3$	Be_2O
Total Number of Species Considered In Each System			
34	34	34	34

Table 2-4. Chemical Reactions of Importance in Nonmetallized Propellant Systems Containing Carbon, Hydrogen, Oxygen, Nitrogen, Fluorine and Chlorine Having Gaseous Combustion Products

Chemical Reaction	Chemical Reaction
$CO_2 + M \rightleftharpoons CO + O + M$	$HCl + HCl \rightleftharpoons H_2 + Cl_2$
$H_2O + M \rightleftharpoons OH + H + M$	$HCl + O \rightleftharpoons OH + Cl$
$CO + M \rightleftharpoons C + O + M$	$HF + Cl \rightleftharpoons HCl + F$
$Cl_2 + M \rightleftharpoons 2Cl + M$	$HF + F \rightleftharpoons H + F_2$
$F_2 + M \rightleftharpoons 2F + M$	$HF + H \rightleftharpoons H_2 + F$
$HCl + M \rightleftharpoons H + Cl + M$	$HF + HF \rightleftharpoons H_2 + F_2$
$HF + M \rightleftharpoons H + F + M$	$HF + O \rightleftharpoons OH + F$
$H_2 + M \rightleftharpoons 2H + M$	$HF + OH \rightleftharpoons H_2O + F$
$N_2 + M \rightleftharpoons 2H + M$	$H_2 + Cl \rightleftharpoons HCl + H$
$NO + M \rightleftharpoons N + O + M$	$H_2 + O \rightleftharpoons OH + H$
$OH + M \rightleftharpoons O + H + M$	$H_2 + O_2 \rightleftharpoons 2OH$
$O_2 + M \rightleftharpoons 2O + M$	$N_2 + O \rightleftharpoons NO + N$
$ClF + M \rightleftharpoons Cl + F + M$	$N_2 + O_2 \rightleftharpoons 2NO$
$CO_2 + H \rightleftharpoons CO + OH$	$NO + H \rightleftharpoons N + OH$
$CO_2 + O \rightleftharpoons CO + O_2$	$NO + O \rightleftharpoons N + O_2$
$H_2O + Cl \rightleftharpoons OH + HCl$	$O_2 + H \rightleftharpoons OH + O$
$H_2O + H \rightleftharpoons OH + H_2$	$Cl + ClF \rightleftharpoons Cl_2 + F$
$H_2O + O \rightleftharpoons 2OH$	$F + ClF \rightleftharpoons Cl + F_2$
$CO + CO \rightleftharpoons CO_2 + C$	$HF + Cl \rightleftharpoons ClF + H$
$CO + H \rightleftharpoons C + OH$	$HCl + F \rightleftharpoons ClF + H$
$CO + N \rightleftharpoons C + NO$	$HCl + HF \rightleftharpoons ClF + H_2$
$CO + NO \rightleftharpoons CO_2 + N$	$HF + ClF \rightleftharpoons F_2 + HCl$
$CO + O \rightleftharpoons C + O_2$	$HF + Cl_2 \rightleftharpoons ClF + HCl$
$HCl + Cl \rightleftharpoons H + Cl_2$	$ClF + ClF \rightleftharpoons F_2 + Cl_2$

Table 2-5. Additional Chemical Reactions of Importance in Propellant Systems Containing Condensed Carbon As a Combustion Product

Chemical Reaction	Chemical Reaction
$C_2 + M \rightleftharpoons C + C + M$	$CO + F \rightleftharpoons CF + O$
$CH + M \rightleftharpoons C + H + M$	$CO + H \rightleftharpoons CH + O$
$CH_2 + M \rightleftharpoons CH + H + M$	$CO + H_2 \rightleftharpoons CH + OH$
$CH_3 + M \rightleftharpoons CH_2 + H + M$	$CO + HF \rightleftharpoons CF + OH$
$CH_4 + M \rightleftharpoons CH_3 + H + M$	$CO + N \rightleftharpoons CN + O$
$C_2H_2 + M \rightleftharpoons CH + CH + M$	$CO + N_2 \rightleftharpoons CN + NO$
$CN + M \rightleftharpoons C + N + M$	$CO + OH \rightleftharpoons CH + O_2$
$HCN + M \rightleftharpoons CN + H + M$	$C + CO \rightleftharpoons C_2 + O$
$CNCl + M \rightleftharpoons CN + Cl + M$	$CO + CO \rightleftharpoons C_2 + O_2$
$CNF + M \rightleftharpoons F + CN + M$	$F + CNCl \rightleftharpoons CN + ClF$
$CF + M \rightleftharpoons C + F + M$	$HCl + CNF \rightleftharpoons HCN + ClF$
$C_2F_2 + M \rightleftharpoons CF + CF + M$	$HF + CNCl \rightleftharpoons HCN + ClF$
$HCN + M \rightleftharpoons CH + N + M$	$ClF + CNF \rightleftharpoons CNCl + F_2$
$CNF + M \rightleftharpoons CF + N + M$	$Cl_2 + CNF \rightleftharpoons CNCl + ClF$
$F + CF \rightleftharpoons F_2 + C$	$C + HCN \rightleftharpoons CH + CN$
$C + H_2 \rightleftharpoons CH + H$	$C + CNF \rightleftharpoons CF + CN$
$C + H_2O \rightleftharpoons CH + OH$	$C + CH_3 \rightleftharpoons CH + CH_2$
$C + HF \rightleftharpoons CH + F$	$C + CH_2 \rightleftharpoons CH + CH$
$C + HF \rightleftharpoons CF + H$	$CH + HCN \rightleftharpoons CN + CH_2$
$C + HCl \rightleftharpoons CH + Cl$	$HCN + CF \rightleftharpoons CNF + CH$
$C + N_2 \rightleftharpoons CN + N$	$CH_4 + C \rightleftharpoons CH_3 + CH$
$O + CN \rightleftharpoons NO + C$	$HCN + CH_2 \rightleftharpoons CH_3 + CN$
$C + OH \rightleftharpoons CH + O$	$HCN + CH_3 \rightleftharpoons CH_4 + CN$
$Cl + CF \rightleftharpoons ClF + C$	$CH_3 + CH \rightleftharpoons CH_2 + CH_2$

Table 2-5. Additional Chemical Reactions of Importance in Propellant Systems Containing Condensed Carbon As a Combustion Product (Continued)

$CH_4 + CH \rightleftharpoons CH_3 + CH_2$	$HF + CH_2 \rightleftharpoons CH_3 + F$
$CH_3 + CH_3 \rightleftharpoons CH_2 + CH_4$	$HF + CH_3 \rightleftharpoons CH_4 + F$
$Cl + HCN \rightleftharpoons CN + HCl$	$H_2 + C_2 \rightleftharpoons CH + CH$
$Cl + HCN \rightleftharpoons CNCl + H$	$H_2 + CF \rightleftharpoons CH + HF$
$Cl + CNF \rightleftharpoons CN + ClF$	$HF + HCN \rightleftharpoons CNF + H_2$
$Cl + CNCl \rightleftharpoons CN + Cl_2$	$HCl + HCN \rightleftharpoons CNCl + H_2$
$CF + CF \rightleftharpoons C_2 + F_2$	$H_2O + CH \rightleftharpoons CH_2 + OH$
$HF + CNF \rightleftharpoons HCN + F_2$	$OH + HCN \rightleftharpoons CN + H_2O$
$HCl + CNCl \rightleftharpoons HCN + Cl_2$	$H_2O + CH_2 \rightleftharpoons CH_3 + OH$
$H + C_2 \rightleftharpoons C + CH$	$H_2O + CH_3 \rightleftharpoons CH_4 + OH$
$H + CN \rightleftharpoons CH + N$	$HF + C_2 \rightleftharpoons CH + CF$
$H + CF \rightleftharpoons CH + F$	$HF + CF \rightleftharpoons CH + F_2$
$H + HCN \rightleftharpoons CN + H_2$	$HF + CNCl \rightleftharpoons CNF + HCl$
$HF + CN \rightleftharpoons CNF + H$	$HCl + CH \rightleftharpoons CH_2 + Cl$
$H + CNF \rightleftharpoons HCN + F$	$HCl + CF \rightleftharpoons CH + ClF$
$H + CNCl \rightleftharpoons CN + HCl$	$Cl + CH_3 \rightleftharpoons CH_2 + HCl$
$H_2 + CH \rightleftharpoons CH_2 + H$	$HCl + CH_3 \rightleftharpoons CH_4 + Cl$
$H + CH_3 \rightleftharpoons CH_2 + H_2$	$C + CN \rightleftharpoons C_2 + N$
$H_2 + CH_3 \rightleftharpoons CH_4 + H$	$N_2 + C_2 \rightleftharpoons CN + CN$
$H + C_2H_2 \rightleftharpoons CH + CH_2$	$CN + CO \rightleftharpoons C_2 + NO$
$F + C_2 \rightleftharpoons CF + C$	$OH + HCN \rightleftharpoons CH_2 + NO$
$F + CN \rightleftharpoons CF + N$	$N + CO \rightleftharpoons CN + O$
$HF + CN \rightleftharpoons HCN + F$	$O + HCN \rightleftharpoons CH + NO$
$F + CNF \rightleftharpoons CN + F_2$	$O + HCN \rightleftharpoons CN + OH$
$Cl + CNF \rightleftharpoons CNCl + F$	$O + CNF \rightleftharpoons CF + NO$
$HF + CH \rightleftharpoons CH_2 + F$	$OH + CH \rightleftharpoons CH_2 + O$

Table 2-5. Additional Chemical Reactions of Importance in Propellant Systems Containing Condensed Carbon As a Combustion Product (Continued)

$O + CH_3 \rightleftharpoons CH_2 + OH$

$OH + CH_3 \rightleftharpoons CH_4 + O$

$NO + CO \rightleftharpoons CN + O_2$

$CH + CO \rightleftharpoons C_2 + OH$

$OH + CN \rightleftharpoons CH + NO$

$OH + HCN \rightleftharpoons CH_2 + NO$

$H + HCN \rightleftharpoons CH_2 + N$

$N_2 + CH \rightleftharpoons HCN + N$

$N_2 + CF \rightleftharpoons CNF + N$

$N + C_2H_2 \rightleftharpoons CH + HCN$

$N + C_2F_2 \rightleftharpoons CF + CNF$

Table 2-6. Additional Chemical Reactions of Importance in Aluminum Containing Propellant Systems

Chemical Reaction	Chemical Reaction
$AlO + M \rightleftharpoons Al + O + M$	$Al + AlOCl \rightleftharpoons AlO + AlCl$
$Al_2O + M \rightleftharpoons Al + AlO + M$	$Al + AlOF \rightleftharpoons Al_2O + F$
$AlCl + M \rightleftharpoons Al + Cl + M$	$OH + AlF \rightleftharpoons HF + AlO$
$AlCl_2 + M \rightleftharpoons AlCl + Cl + M$	$O + AlF \rightleftharpoons F + AlO$
$AlCl_3 + M \rightleftharpoons AlCl_2 + Cl + M$	$AlO + H \rightleftharpoons Al + OH$
$AlF + M \rightleftharpoons Al + F + M$	$AlO + AlF \rightleftharpoons Al_2O + F$
$AlF_2 + M \rightleftharpoons AlF + F + M$	$AlOF + Al \rightleftharpoons AlF + AlO$
$AlF_3 + M \rightleftharpoons AlF_2 + F + M$	$Al_2O + Cl \rightleftharpoons AlO + AlCl$
$AlOCl + M \rightleftharpoons AlO + Cl + M$	$Al_2O + O \rightleftharpoons AlO + AlO$
$AlOF + M \rightleftharpoons AlO + F + M$	$AlCl + CO \rightleftharpoons AlOCl + C$
$AlClF + M \rightleftharpoons AlF + Cl + M$	$AlCl + HCl \rightleftharpoons AlCl_2 + H$
$AlCl_2F + M \rightleftharpoons AlCl_2 + F + M$	$AlCl + NO \rightleftharpoons AlOCl + N$
$AlClF_2 + M \rightleftharpoons AlF_2 + Cl + M$	$AlCl + OH \rightleftharpoons AlO + HCl$
$AlOCl + M \rightleftharpoons AlCl + O + M$	$AlCl + Cl \rightleftharpoons Al + Cl_2$
$AlOF + M \rightleftharpoons AlF + O + M$	$AlCl + H \rightleftharpoons Al + HCl$
$AlClF + M \rightleftharpoons AlCl + F + M$	$AlCl + O \rightleftharpoons AlO + Cl$
$AlCl_2F + M \rightleftharpoons AlClF + Cl + M$	$AlCl + AlCl \rightleftharpoons Al + AlCl_2$
$AlClF_2 + M \rightleftharpoons AlClF + F + M$	$AlCl + AlOCl \rightleftharpoons Al_2O + Cl_2$
$Al + CO_2 \rightleftharpoons AlO + CO$	$AlCl + AlOCl \rightleftharpoons AlO + AlCl_2$
$Al + CO \rightleftharpoons AlO + C$	$AlCl + AlOF \rightleftharpoons AlF + AlOCl$
$Al + NO \rightleftharpoons AlO + N$	$AlCl_2 + Cl \rightleftharpoons AlCl + Cl_2$
$Al + O_2 \rightleftharpoons AlO + O$	$AlOCl + CO \rightleftharpoons AlCl + CO_2$
$Al + AlOCl \rightleftharpoons Al_2O + Cl$	$AlOCl + HCl \rightleftharpoons AlCl_2 + OH$

Table 2-6. Additional Chemical Reactions of Importance in Aluminum Containing Propellant Systems (Continued)

$AlOCl + Cl \rightleftharpoons AlO + Cl_2$

$AlOCl + Cl \rightleftharpoons AlCl_2 + O$

$AlOCl + H \rightleftharpoons AlO + HCl$

$AlOCl + H \rightleftharpoons AlCl + OH$

$AlOCl + O \rightleftharpoons AlCl + O_2$

$AlF + AlF \rightleftharpoons Al + AlF_2$

$AlF + HCl \rightleftharpoons AlCl + HF$

$AlF + HF \rightleftharpoons AlF_2 + H$

$AlF + NO \rightleftharpoons AlOF + N$

$AlF + Cl \rightleftharpoons AlCl + F$

$AlF + F \rightleftharpoons Al + F_2$

$AlF + H \rightleftharpoons Al + HF$

$AlF + AlOF \rightleftharpoons AlO + AlF_2$

$AlF_2 + F \rightleftharpoons AlF + F_2$

$AlOF + HCl \rightleftharpoons AlOCl + HF$

$AlOF + HF \rightleftharpoons AlF_2 + OH$

$AlOF + Cl \rightleftharpoons AlOCl + F$

$AlOF + F \rightleftharpoons AlO + F_2$

$AlOF + F \rightleftharpoons AlF_2 + O$

$AlOF + H \rightleftharpoons AlO + HF$

$AlOF + H \rightleftharpoons AlF + OH$

$AlOF + O \rightleftharpoons AlF + O_2$

$Cl + AlF \rightleftharpoons ClF + Al$

$F + AlCl \rightleftharpoons ClF + Al$

$C + AlF \rightleftharpoons CF + Al$

$CN + AlF \rightleftharpoons CNF + Al$

$CN + AlCl \rightleftharpoons CNCl + Al$

$AlF_2 + AlF \rightleftharpoons AlF_3 + Al$

$AlClF + AlCl \rightleftharpoons AlCl_2F + Al$

$AlF + AlCl_2 \rightleftharpoons AlCl_2F + Al$

$AlF + AlClF \rightleftharpoons AlClF_2 + Al$

$Cl + AlOF \rightleftharpoons ClF + AlO$

$CO + AlF \rightleftharpoons CF + AlO$

$C + AlOF \rightleftharpoons CF + AlO$

$CN + AlOF \rightleftharpoons CNF + AlO$

$CN + AlOCl \rightleftharpoons CNCl + AlO$

$AlF_2 + AlOF \rightleftharpoons AlF_3 + AlO$

$AlOCl + AlCl_2 \rightleftharpoons AlCl_3 + AlO$

$AlOF + AlCl \rightleftharpoons AlClF + AlO$

$AlF + AlOCl \rightleftharpoons AlClF + AlO$

$AlOF + AlCl_2 \rightleftharpoons AlCl_2F + AlO$

$AlClF + AlOCl \rightleftharpoons AlCl_2F + AlO$

$AlCl_2 + AlOF \rightleftharpoons AlCl_2F + AlO$

$AlF_2 + AlOCl \rightleftharpoons AlClF_2 + AlO$

$AlClF + AlOF \rightleftharpoons AlClF_2 + AlO$

$AlOCl + AlF \rightleftharpoons ClF + Al_2O$

$AlCl + AlOF \rightleftharpoons ClF + Al_2O$

$ClF + AlF \rightleftharpoons F_2 + AlCl$

$F + AlClF \rightleftharpoons F_2 + AlCl$

$AlCl + HF \rightleftharpoons AlClF + H$

Table 2-6. Additional Chemical Reactions of Importance in Aluminum Containing Propellant Systems (Continued)

$Cl_2 + AlF \rightleftharpoons ClF + AlCl$	$Cl_2 + AlClF \rightleftharpoons ClF + AlCl_2$
$Cl + AlClF \rightleftharpoons ClF + AlCl$	$Cl + AlCl_2F \rightleftharpoons ClF + AlCl_2$
$C + AlClF \rightleftharpoons CF + AlCl$	$C + AlCl_2F \rightleftharpoons CF + AlCl_2$
$CNCl + AlF \rightleftharpoons CNF + AlCl$	$CN + AlCl_2F \rightleftharpoons CNF + AlCl_2$
$AlCl + CNF \rightleftharpoons AlClF + CN$	$CNCl + AlClF \rightleftharpoons CNF + AlCl_2$
$AlCl + AlCl_2 \rightleftharpoons AlCl_3 + Al$	$AlCl_2 + CNCl \rightleftharpoons AlCl_3 + CN$
$AlCl + AlF \rightleftharpoons Al + AlClF$	$AlCl_2F + AlF \rightleftharpoons AlF_2 + AlCl_2$
$AlClF + AlF \rightleftharpoons AlF_2 + AlCl$	$AlCl_2 + AlF_2 \rightleftharpoons AlClF + AlClF$
$AlCl + AlF_3 \rightleftharpoons AlF_2 + AlClF$	$AlCl_2 + AlOF \rightleftharpoons AlOCl + AlClF$
$AlCl + AlCl_3 \rightleftharpoons AlCl_2 + AlCl_2$	$AlCl_2 + AlF_3 \rightleftharpoons AlF_2 + AlCl_2F$
$AlF + AlCl_2 \rightleftharpoons AlClF + AlCl$	$AlCl_2 + AlF_3 \rightleftharpoons AlClF + AlClF_2$
$AlCl + AlCl_2F \rightleftharpoons AlCl_2 + AlClF$	$AlCl_3 + AlF \rightleftharpoons AlClF + AlCl_2$
$AlF + AlCl_3 \rightleftharpoons AlCl_2F + AlCl$	$AlCl_2 + AlCl_2F \rightleftharpoons AlCl_3 + AlClF$
$AlCl + AlClF_2 \rightleftharpoons AlCl_2 + AlF_2$	$AlCl_2 + AlClF_2 \rightleftharpoons AlF_2 + AlCl_3$
$AlCl_2F + AlF \rightleftharpoons AlClF_2 + AlCl$	$AlCl_2 + AlClF_2 \rightleftharpoons AlClF + AlCl_2F$
$AlCl + AlClF_2 \rightleftharpoons AlClF + AlClF$	$AlOCl + F \rightleftharpoons AlO + ClF$
$Cl + AlCl_3 \rightleftharpoons Cl_2 + AlCl_2$	$AlOCl + F \rightleftharpoons AlClF + O$
$AlCl_2 + F \rightleftharpoons AlCl + ClF$	$ClF + AlOF \rightleftharpoons F_2 + AlOCl$
$Cl + AlClF \rightleftharpoons F + AlCl_2$	$AlOCl + HF \rightleftharpoons AlClF + OH$
$F + AlCl_2F \rightleftharpoons F_2 + AlCl_2$	$Cl_2 + AlOF \rightleftharpoons ClF + AlOCl$
$Cl + AlClF_2 \rightleftharpoons F_2 + AlCl_2$	$CO + AlClF \rightleftharpoons CF + AlOCl$
$HCl + AlClF \rightleftharpoons HF + AlCl_2$	$AlClF + AlOF \rightleftharpoons AlF_2 + AlOCl$
$AlCl_2 + HF \rightleftharpoons AlCl_2F + H$	$AlClF_2 + AlOF \rightleftharpoons AlF_3 + AlOCl$
$AlCl_2 + HCl \rightleftharpoons AlCl_3 + H$	$AlCl_3 + AlOF \rightleftharpoons AlCl_2F + AlOCl$
$F + AlCl_3 \rightleftharpoons ClF + AlCl_2$	$AlCl_2F + AlOF \rightleftharpoons AlClF_2 + AlOCl$

Table 2-6. Additional Chemical Reactions of Importance in Aluminum Containing Propellant Systems (Continued)

$Cl + AlClF \rightleftharpoons Cl_2 + AlF$

$AlF + HCl \rightleftharpoons AlClF + H$

$Cl + AlF_2 \rightleftharpoons ClF + AlF$

$F + AlClF \rightleftharpoons ClF + AlF$

$CO + AlOF \rightleftharpoons CO_2 + AlF$

$AlF_2 + C \rightleftharpoons AlF + CF$

$AlF + CNF \rightleftharpoons AlF_2 + CN$

$CNCl + AlF \rightleftharpoons CN + AlClF$

$AlF + AlF_3 \rightleftharpoons AlF_2 + AlF_2$

$AlF + AlCl_2F \rightleftharpoons AlClF + AlClF$

$AlF + AlClF_2 \rightleftharpoons AlF_2 + AlClF$

$AlF_2 + Cl \rightleftharpoons AlClF + F$

$AlF_2 + Cl_2 \rightleftharpoons AlClF + ClF$

$F + AlCl_2F \rightleftharpoons Cl_2 + AlF_2$

$Cl + AlClF_2 \rightleftharpoons Cl_2 + AlF_2$

$F + AlF_3 \rightleftharpoons F_2 + AlF_2$

$H + AlF_3 \rightleftharpoons HF + AlF_2$

$AlF_2 + HCl \rightleftharpoons AlClF + HF$

$AlF_2 + HCl \rightleftharpoons AlClF_2 + H$

$F + AlClF_2 \rightleftharpoons ClF + AlF_2$

$C + AlF_3 \rightleftharpoons CF + AlF_2$

$CN + AlF_3 \rightleftharpoons CNF + AlF_2$

$AlF_2 + CNCl \rightleftharpoons AlClF_2 + CN$

$AlClF + AlCl_2F \rightleftharpoons AlCl_3 + AlF_2$

$AlF + AlClF_2 \rightleftharpoons AlClF + AlF_2$

$AlClF_2 + AlClF \rightleftharpoons AlCl_2F + AlF_2$

$AlF_3 + AlClF \rightleftharpoons AlClF_2 + AlF_2$

$AlOF + Cl \rightleftharpoons AlClF + O$

$AlOF + HCl \rightleftharpoons AlClF + OH$

$CO + AlF_2 \rightleftharpoons CF + AlOF$

$AlOF + CNCl \rightleftharpoons AlOCl + CNF$

$AlF_3 + Cl \rightleftharpoons AlF_2 + ClF$

$AlF_3 + Cl \rightleftharpoons AlClF_2 + F$

$AlF_3 + Cl_2 \rightleftharpoons AlClF_2 + ClF$

$AlF_3 + HCl \rightleftharpoons AlClF_2 + HF$

$AlF_3 + ClF \rightleftharpoons AlClF_2 + F_2$

$CNCl + AlF_3 \rightleftharpoons CNF + AlClF_2$

$AlF_3 + AlCl_3 \rightleftharpoons AlCl_2F + AlClF_2$

$AlClF_2 + AlClF_2 \rightleftharpoons AlCl_2F + AlF_3$

$Cl + AlCl_2F \rightleftharpoons F + AlCl_3$

$ClF + AlCl_2F \rightleftharpoons F_2 + AlCl_3$

$HCl + AlCl_2F \rightleftharpoons HF + AlCl_3$

$Cl_2 + AlCl_2F \rightleftharpoons ClF + AlCl_3$

$CNCl + AlCl_2F \rightleftharpoons CNF + AlCl_3$

$AlCl_3 + AlClF_2 \rightleftharpoons AlCl_2F + AlCl_2F$

$Cl + AlCl_2F \rightleftharpoons Cl_2 + AlClF$

$ClF + AlF_2 \rightleftharpoons F_2 + AlClF$

$F + AlClF_2 \rightleftharpoons F_2 + AlClF$

$H + AlClF_2 \rightleftharpoons HF + AlClF$

$AlClF + HCl \rightleftharpoons AlCl_2F + H$

Table 2-6. Additional Chemical Reactions of Importance in Aluminum Containing Propellant Systems (Continued)

$AlClF + ClF \rightleftharpoons AlCl_2 + F_2$

$F + AlCl_2F \rightleftharpoons ClF + AlClF$

$Cl + AlClF_2 \rightleftharpoons ClF + AlClF$

$C + AlClF_2 \rightleftharpoons CF + AlClF$

$CN + AlClF_2 \rightleftharpoons CNF + AlClF$

$CNCl + AlF_2 \rightleftharpoons CNF + AlClF$

$AlClF + CNCl \rightleftharpoons AlCl_2F + CN$

$AlClF_2 + Cl \rightleftharpoons AlCl_2F + F$

$AlClF_2 + Cl_2 \rightleftharpoons AlCl_2F + ClF$

$AlClF_2 + HCl \rightleftharpoons AlCl_2F + HF$

$AlClF_2 + ClF \rightleftharpoons AlCl_2F + F_2$

$AlClF_2 + CNCl \rightleftharpoons AlCl_2F + CNF$

$AlOCl + Cl_2 \rightleftharpoons AlCl_3 + O$

$O + AlClF_2 \rightleftharpoons F_2 + AlOCl$

$O + AlCl_2F \rightleftharpoons ClF + AlOCl$

$AlF + CO \rightleftharpoons AlOF + C$

Table 2-7. Additional Chemical Reactions of Importance in Berylium Containing Propellant Systems

Chemical Reactions	Chemical Reactions
$BeOH + M \rightleftharpoons Be + OH + M$	$Be_2O + HF \rightleftharpoons BeF + BeOH$
$BeOHOH + M \rightleftharpoons BeOH + OH + M$	$Be_2O + OH \rightleftharpoons BeO + BeOH$
$BeO + M \rightleftharpoons Be + O + M$	$Be_2O + Cl \rightleftharpoons BeO + BeCl$
$Be_2O + M \rightleftharpoons Be + BeO + M$	$Be_2O + H \rightleftharpoons Be + BeOH$
$BeCl + M \rightleftharpoons Be + Cl + M$	$Be_2O + O \rightleftharpoons BeO + BeO$
$BeCl_2 + M \rightleftharpoons BeCl + Cl + M$	$BeOHOH + Be \rightleftharpoons BeOH + BeOH$
$BeF + M \rightleftharpoons Be + F + M$	$BeOH + Cl \rightleftharpoons BeO + HCl$
$BeF_2 + M \rightleftharpoons BeF + F + M$	$BeOH + Cl \rightleftharpoons BeCl + OH$
$BeOH + M \rightleftharpoons BeO + H + M$	$H_2O + Be \rightleftharpoons H + BEOH$
$BeClF + M \rightleftharpoons BeCl + F + M$	$BeOH + H \rightleftharpoons BeO + H_2$
$BeClF + M \rightleftharpoons BeF + Cl + M$	$BeOH + O \rightleftharpoons BeO + OH$
$Be + BeF_2 \rightleftharpoons BeF + BeF$	$Be + BeCl_2 \rightleftharpoons BeCl + BeCl$
$BeO + H_2O \rightleftharpoons BeOH + OH$	$BeCl + H_2O \rightleftharpoons BeOH + HCl$
$CO_2 + Be \rightleftharpoons CO + BeO$	$H + BeCl_2 \rightleftharpoons HCl + BeCl$
$BeO + HCl \rightleftharpoons BeCl + OH$	$BeCl + Cl \rightleftharpoons Be + Cl_2$
$BeO + HF \rightleftharpoons BeOH + F$	$BeCl + H \rightleftharpoons Be + HCl$
$CO + Be \rightleftharpoons C + BeO$	$BeF + H_2O \rightleftharpoons BeOH + HF$
$BeO + Cl \rightleftharpoons BeCl + O$	$BeF + HCl \rightleftharpoons BeCl + HF$
$BeO + H \rightleftharpoons Be + OH$	$BeF + OH \rightleftharpoons BeO + HF$
$NO + Be \rightleftharpoons N + BeO$	$BeF + OH \rightleftharpoons BeOH + F$
$O_2 + Be \rightleftharpoons O + BeO$	$BeF + Cl \rightleftharpoons BeCl + F$
$BeO + BeF \rightleftharpoons Be_2O + F$	$BeF + F \rightleftharpoons Be + F_2$
$Be_2O + H_2O \rightleftharpoons BeOH + BeOH$	$BeF + H \rightleftharpoons Be + HF$
$Be_2O + HCl \rightleftharpoons BeCl + BeOH$	$BeF + O \rightleftharpoons BeO + F$

Table 2-7. Additional Chemical Reactions of Importance in Berylium Containing Propellant Systems (Continued)

$BeF_2 + H \rightleftharpoons BeF + HF$

$BeOHOH + H \rightleftharpoons BeOH + H_2O$

$Cl + BeF \rightleftharpoons ClF + Be$

$C + BeF \rightleftharpoons CF + Be$

$CN + BeF \rightleftharpoons CNF + Be$

$Be + CNCl \rightleftharpoons BeCl + CN$

$BeF + BeCl \rightleftharpoons BeClF + Be$

$F + BeClF \rightleftharpoons F_2 + BeCl$

$ClF + BeF \rightleftharpoons F_2 + BeCl$

$H + BeClF \rightleftharpoons HF + BeCl$

$Cl + BeClF \rightleftharpoons ClF + BeCl$

$Cl_2 + BeF \rightleftharpoons ClF + BeCl$

$C + BeClF \rightleftharpoons CF + BeCl$

$CNCl + BeF \rightleftharpoons CNF + BeCl$

$CN + BeCl_2 \rightleftharpoons CNCl + BeCl$

$BeCl + BeF_2 \rightleftharpoons BeClF + BeF$

$BeF + BeCl_2 \rightleftharpoons BeClF + BeCl$

$BeOH + C \rightleftharpoons BeO + CH$

$Cl + BeClF \rightleftharpoons F + BeCl_2$

$ClF + BeClF \rightleftharpoons F_2 + BeCl_2$

$BeCl_2 + HF \rightleftharpoons BeClF + HCl$

$Cl_2 + BeClF \rightleftharpoons ClF + BeCl_2$

$CNCl + BeClF \rightleftharpoons CNF + BeCl_2$

$BeCl_2 + BeF_2 \rightleftharpoons BeClF + BeClF$

$CO + BeF \rightleftharpoons CF + BeO$

$Cl + BeClF \rightleftharpoons Cl_2 + BeF$

$F + BeF_2 \rightleftharpoons F_2 + BeF$

$H + BeClF \rightleftharpoons HCl + BeF$

$Cl + BeF_2 \rightleftharpoons ClF + BeF$

$F + BeClF \rightleftharpoons ClF + BeF$

$C + BeF_2 \rightleftharpoons CF + BeF$

$CN + BeF_2 \rightleftharpoons CNF + BeF$

$BeF + CNCl \rightleftharpoons BeClF + CN$

$BeF_2 + Cl \rightleftharpoons BeClF + F$

$BeF_2 + Cl_2 \rightleftharpoons BeClF + ClF$

$BeF_2 + HCl \rightleftharpoons BeClF + HF$

$BeF_2 + ClF \rightleftharpoons BeClF + F_2$

$BeF_2 + CNCl \rightleftharpoons BeClF + CNF$

Table 2-8. Additional Chemical Reactions of Importance in Boron Containing Propellant Systems

Chemical Reaction	Chemical Reaction
$BN + M \rightleftharpoons B + N + M$	$BO + BO \rightleftharpoons B + BO_2$
$BO + M \rightleftharpoons B + O + M$	$CO + BO_2 \rightleftharpoons CO_2 + BO$
$BO_2 + M \rightleftharpoons BO + O + M$	$BO + CO \rightleftharpoons B + CO_2$
$BCl + M \rightleftharpoons B + Cl + M$	$BO + CO \rightleftharpoons BO_2 + C$
$BCl_2 + M \rightleftharpoons BCl + Cl + M$	$BO + HCl \rightleftharpoons BCl + OH$
$BCl_3 + M \rightleftharpoons BCl_2 + Cl + M$	$BO + HF \rightleftharpoons BF + OH$
$BF + M \rightleftharpoons B + F + M$	$BO + NO \rightleftharpoons BN + O_2$
$BF_2 + M \rightleftharpoons BF + F + M$	$BO + NO \rightleftharpoons BO_2 + N$
$BF_3 + M \rightleftharpoons BF_2 + F + M$	$CO + B \rightleftharpoons C + BO$
$BOCl + M \rightleftharpoons BCl + O + M$	$BO + Cl \rightleftharpoons BCl + O$
$BOF + M \rightleftharpoons BO + F + M$	$BO + F \rightleftharpoons BF + O$
$BClF + M \rightleftharpoons BF + Cl + M$	$BO + H \rightleftharpoons B + OH$
$BCl_2F + M \rightleftharpoons BCl_2 + F + M$	$BO + N \rightleftharpoons BN + O$
$BOF + M \rightleftharpoons BF + O + M$	$BO + O \rightleftharpoons B + O_2$
$BOCl + M \rightleftharpoons BO + Cl + M$	$BO + BCl \rightleftharpoons B + BOCl$
$BClF + M \rightleftharpoons BCl + F + M$	$BO + BOCl \rightleftharpoons BO_2 + BCl$
$BCl_2F + M \rightleftharpoons BClF + Cl + M$	$BO + BF \rightleftharpoons B + BOF$
$BClF_2 + M \rightleftharpoons BF_2 + Cl + M$	$BOF + BF_2 \rightleftharpoons BF_3 + BO$
$BClF_2 + M \rightleftharpoons BClF + F + M$	$BO + BOF \rightleftharpoons BF + BO_2$
$B + N_2 \rightleftharpoons BN + N$	$BO_2 + HF \rightleftharpoons BOF + OH$
$B + NO \rightleftharpoons BN + O$	$BO_2 + Cl \rightleftharpoons BOCl + O$
$N + BO \rightleftharpoons NO + B$	$BO_2 + H \rightleftharpoons BO + OH$
$N_2 + BO \rightleftharpoons NO + BN$	$BO_2 + O \rightleftharpoons BO + O_2$

Table 2-8. Additional Chemical Reactions of Importance in Boron Containing Propellant Systems (Continued)

Chemical Reaction	Chemical Reaction
$BCl + BCl \rightleftharpoons B + BCl_2$	$BF + BF_2 \rightleftharpoons B + BF_3$
$BCl + Cl \rightleftharpoons B + Cl_2$	$BF + BOF \rightleftharpoons BO + BF_2$
$BCl + H \rightleftharpoons B + HCl$	$BF_2 + F \rightleftharpoons BF + F_2$
$BCl + N \rightleftharpoons BN + Cl$	$BF_3 + F \rightleftharpoons BF_2 + F_2$
$BCl + BOF \rightleftharpoons BOCl + BF$	$BF_3 + H \rightleftharpoons BF_2 + HF$
$BCl_2 + Cl \rightleftharpoons BCl + Cl_2$	$BOF + BOF \rightleftharpoons BO_2 + BF_2$
$BCl_3 + Cl \rightleftharpoons BCl_2 + Cl_2$	$BOF + HCl \rightleftharpoons BOCl + HF$
$BOCl + HCl \rightleftharpoons BCl_2 + OH$	$BOF + HF \rightleftharpoons BF_2 + OH$
$HCl + BO_2 \rightleftharpoons OH + BOCl$	$BOF + Cl \rightleftharpoons BOCl + F$
$BOCl + Cl \rightleftharpoons BO + Cl_2$	$BOF + F \rightleftharpoons BO + F_2$
$BOCl + Cl \rightleftharpoons BCl_2 + O$	$BOF + F \rightleftharpoons BF_2 + O$
$BOCl + H \rightleftharpoons BO + HCl$	$BOF + H \rightleftharpoons BO + HF$
$BOCl + H \rightleftharpoons BCl + OH$	$BOF + H \rightleftharpoons BF + OH$
$BOCl + N \rightleftharpoons BCl + NO$	$BOF + O \rightleftharpoons BO_2 + F$
$BOCl + O \rightleftharpoons BCl + O_2$	$F + BCl \rightleftharpoons ClF + B$
$BF + BF \rightleftharpoons B + BF_2$	$B + CN \rightleftharpoons BN + C$
$CO + BOF \rightleftharpoons CO_2 + BF$	$C + BF \rightleftharpoons CF + B$
$BF + CO \rightleftharpoons BOF + C$	$B + HCN \rightleftharpoons BN + CH$
$BF + HCl \rightleftharpoons BCl + HF$	$CN + BF \rightleftharpoons CNF + B$
$BF + HF \rightleftharpoons BF_2 + H$	$B + CNF \rightleftharpoons BN + CF$
$BF + Cl \rightleftharpoons BCl + F$	$CN + BCl \rightleftharpoons CNCl + B$
$BF + F \rightleftharpoons B + F_2$	$BCl + BCl_2 \rightleftharpoons BCl_3 + B$
$BF + H \rightleftharpoons B + HF$	$BF + BCl \rightleftharpoons BCLF + B$
$BF + N \rightleftharpoons BN + F$	$BCl + BClF \rightleftharpoons BCl_2F + B$

Table 2-8. Additional Chemical Reactions of Importance in Boron Containing Propellant Systems (Continued)

Chemical Reaction	Chemical Reaction
$BF + BCl_2 \rightleftharpoons BCl_2F + B$	$C + BF_2 \rightleftharpoons CF + BF$
$BCl + BF_2 \rightleftharpoons BClF_2 + B$	$BF + CNF \rightleftharpoons BF_2 + CN$
$CN + BO \rightleftharpoons CO + BN$	$BF + CNCl \rightleftharpoons BCl + CNF$
$CN + BF \rightleftharpoons CF + BN$	$BF + CNCl \rightleftharpoons BClF + CN$
$F + BOCl \rightleftharpoons ClF + BO$	$BF + BCl_2 \rightleftharpoons BClF + BCl$
$CO + BF \rightleftharpoons CF + BO$	$BF + BCl_3 \rightleftharpoons BCl_2 + BClF$
$C + BOF \rightleftharpoons CF + BO$	$BF + BClF \rightleftharpoons BCl + BF_2$
$CN + BOCl \rightleftharpoons CNCl + BO$	$BF + BCl_2F \rightleftharpoons BCl + BClF_2$
$BCl + BOCl \rightleftharpoons BCl_2 + BO$	$BF + BCl_2F \rightleftharpoons BCl_2 + BF_2$
$BCl_2 + BOCl \rightleftharpoons BCl_3 + BO$	$BF + BCl_2F \rightleftharpoons BClF + BClF$
$BF + BOCl \rightleftharpoons BClF + BO$	$BF + BClF_2 \rightleftharpoons BCl + BF_3$
$BCl + BOF \rightleftharpoons BClF + BO$	$BF + BClF_2 \rightleftharpoons BClF + BF_2$
$BCl_2 + BOF \rightleftharpoons BCl_2F + BO$	$BF_2 + Cl \rightleftharpoons BClF + F$
$BClF + BOCl \rightleftharpoons BCl_2F + BO$	$BF_2 + Cl_2 \rightleftharpoons BClF + ClF$
$BO + BClF_2 \rightleftharpoons BOCl + BF_2$	$Cl + BClF_2 \rightleftharpoons Cl_2 + BF_2$
$BClF + BOF \rightleftharpoons BClF_2 + BO$	$BF_2 + HCl \rightleftharpoons BClF + HF$
$CO + BOF \rightleftharpoons CF + BO_2$	$BClF_2 + H \rightleftharpoons HCl + BF_2$
$BOCl + BOCl \rightleftharpoons BCl_2 + BO_2$	$Cl + BF_3 \rightleftharpoons ClF + BF_2$
$BOF + BOCl \rightleftharpoons BClF + BO_2$	$BF_2 + ClF \rightleftharpoons F_2 + BClF$
$BF + Cl_2 \rightleftharpoons BCl + ClF$	$F + BClF_2 \rightleftharpoons ClF + BF_2$
$Cl + BClF \rightleftharpoons Cl_2 + BF$	$CO + BF_2 \rightleftharpoons CF + BOF$
$BF + HCl \rightleftharpoons BClF + H$	$BF_2 + CNCl \rightleftharpoons BClF + CNF$
$F + BClF \rightleftharpoons ClF + BF$	$C + BF_3 \rightleftharpoons CF + BF_2$
$BF + ClF \rightleftharpoons BCl + F_2$	$CN + BF_3 \rightleftharpoons CNF + BF_2$

Table 2-8. Additional Chemical Reactions of Importance in Boron Containing Propellant Systems (Continued)

Chemical Reaction	Chemical Reaction
$CN + BClF_2 \rightleftarrows CNCl + BF_2$	$BOF + BCl_2 \rightleftarrows BOCl + BClF$
$BClF_2 + BCl \rightleftarrows BCl_2 + BF_2$	$BOF + BCl_3 \rightleftarrows BOCl + BCl_2F$
$BF_2 + BCl_2 \rightleftarrows BClF + BClF$	$BOF + BCl_2F \rightleftarrows BOCl + BClF_2$
$BClF_2 + BCl_2 \rightleftarrows BCl_3 + BF_2$	$F + BClF \rightleftarrows F_2 + BCl$
$BCl_2F + BClF \rightleftarrows BF_2 + BCl_3$	$BCl + HF \rightleftarrows BClF + H$
$BClF + BOF \rightleftarrows BOCl + BF_2$	$BCl + HCl \rightleftarrows BCl_2 + H$
$BF_3 + BCl \rightleftarrows BClF + BF_2$	$F + BCl_2 \rightleftarrows ClF + BCl$
$BF_3 + BCl_2 \rightleftarrows BCl_2F + BF_2$	$Cl + BClF \rightleftarrows ClF + BCl$
$BClF_2 + BClF \rightleftarrows BCl_2F + BF_2$	$CO + BOCl \rightleftarrows CO_2 + BCl$
$BF_3 + BClF \rightleftarrows BClF_2 + BF_2$	$C + BClF \rightleftarrows CF + BCl$
$BF_3 + Cl \rightleftarrows BClF_2 + F$	$BCl + CNF \rightleftarrows BClF + CN$
$BF_3 + Cl_2 \rightleftarrows BClF_2 + ClF$	$BCl + CNCl \rightleftarrows BCl_2 + CN$
$BF_3 + HCl \rightleftarrows BClF_2 + HF$	$BCl + BCl_3 \rightleftarrows BCl_2 + BCl_2$
$BF_3 + ClF \rightleftarrows BClF_2 + F_2$	$BCl + BCl_2F \rightleftarrows BCl_2 + BClF$
$BF_3 + CNCl \rightleftarrows BClF_2 + CNF$	$BCl + BClF_2 \rightleftarrows BClF + BClF$
$BF_3 + BCl_2 \rightleftarrows BClF + BClF_2$	$Cl + BClF \rightleftarrows F + BCl_2$
$BF_3 + BCl_3 \rightleftarrows BCl_2F + BClF_2$	$ClF + BClF \rightleftarrows F_2 + BCl_2$
$BClF_2 + BOF \rightleftarrows BOCl + BF_3$	$F + BCl_2F \rightleftarrows F_2 + BCl_2$
$BF_3 + BCl_2F \rightleftarrows BClF_2 + BClF_2$	$Cl + BClF_2 \rightleftarrows F_2 + BCl_2$
$BOF + Cl \rightleftarrows BClF + O$	$HCl + BClF \rightleftarrows HF + BCl_2$
$BOF + Cl_2 \rightleftarrows BOCl + ClF$	$H + BCl_2F \rightleftarrows HF + BCl_2$
$BOF + HCl \rightleftarrows BClF + OH$	$H + BCl_3 \rightleftarrows HCl + BCl_2$
$BOF + ClF \rightleftarrows BOCl + F_2$	$F + BCl_3 \rightleftarrows ClF + BCl_2$
$BOF + CNCl \rightleftarrows BOCl + CNF$	$Cl_2 + BClF \rightleftarrows ClF + BCl_2$

Table 2-8. Additional Chemical Reactions of Importance in Boron Containing Propellant Systems (Continued)

Chemical Reaction	Chemical Reaction
$Cl + BCl_2F \rightleftharpoons ClF + BCl_2$	$Cl + BCl_2F \rightleftharpoons Cl_2 + BClF$
$C + BCl_2F \rightleftharpoons CF + BCl_2$	$F + BClF_2 \rightleftharpoons F_2 + BClF$
$CNCl + BClF \rightleftharpoons CNF + BCl_2$	$H + BClF_2 \rightleftharpoons HF + BClF$
$CN + BCl_2F \rightleftharpoons CNF + BCl_2$	$H + BCl_2F \rightleftharpoons HCl + BClF$
$BCl_2 + CNCl \rightleftharpoons BCl_3 + CN$	$F + BCl_2F \rightleftharpoons ClF + BClF$
$BCl_2 + BClF_2 \rightleftharpoons BClF + BCl_2F$	$Cl + BClF_2 \rightleftharpoons ClF + BClF$
$Cl + BCl_2F \rightleftharpoons F + BCl_3$	$C + BClF_2 \rightleftharpoons CF + BClF$
$ClF + BCl_2F \rightleftharpoons F_2 + BCl_3$	$CN + BClF_2 \rightleftharpoons CNF + BClF$
$BCl_2 + BCl_2F \rightleftharpoons BCl_3 + BClF$	$CN + BCl_2F \rightleftharpoons CNCl + BClF$
$HCl + BCl_2F \rightleftharpoons HF + BCl_3$	$Cl + BClF_2 \rightleftharpoons F + BCl_2F$
$Cl_2 + BCl_2F \rightleftharpoons ClF + BCl_3$	$HCl + BClF_2 \rightleftharpoons HF + BCl_2F$
$CNCl + BCl_2F \rightleftharpoons CNF + BCl_3$	$Cl_2 + BClF_2 \rightleftharpoons ClF + BCl_2F$
$BCl_2F + BCl_2F \rightleftharpoons BClF_2 + BCl_3$	$CNCl + BClF_2 \rightleftharpoons CNF + BCl_2F$
$BOCl + F \rightleftharpoons BClF + O$	$ClF + BClF_2 \rightleftharpoons F_2 + BCl_2F$
$BOCl + HF \rightleftharpoons BClF + OH$	$BCl + CO \rightleftharpoons BOCl + C$
$CO + BClF \rightleftharpoons CF + BOCl$	

Table 2-9. Additional Chemical Reactions of Importance in Lithium Containing Propellant Systems

Chemical Reaction	Chemical Reaction
$LiH + M \rightleftarrows Li + H + M$	$LiO + OH \rightleftarrows LiH + O_2$
$LiOH + M \rightleftarrows Li + OH + M$	$NO + Li \rightleftarrows N + LiO$
$LiO + M \rightleftarrows Li + O + M$	$LiO + LiOH \rightleftarrows Li_2O + OH$
$Li_2O + M \rightleftarrows Li + LiO + M$	$LiO + LiF \rightleftarrows Li_2O + F$
$LiCl + M \rightleftarrows Li + Cl + M$	$LiOH + LiOH \rightleftarrows H_2O + Li_2O$
$Li_2Cl_2 + M \rightleftarrows LiCl + LiCl + M$	$LiF + LiOH \rightleftarrows HF + Li_2O$
$LiF + M \rightleftarrows Li + F + M$	$Li_2O + H_2 \rightleftarrows LiH + LiOH$
$Li_2F_2 + M \rightleftarrows LiF + LiF + M$	$Li_2O + H \rightleftarrows LiH + LiO$
$LiOH + M \rightleftarrows LiO + H + M$	$Li_2O + O \rightleftarrows LiO + LiO$
$Li + H_2O \rightleftarrows LiH + OH$	$H_2O + LiCl \rightleftarrows HCl + LiOH$
$Li + H_2O \rightleftarrows LiOH + H$	$LiOH + H_2 \rightleftarrows LiH + H_2O$
$Li + CO \rightleftarrows LiO + C$	$LiOH + OH \rightleftarrows LiO + H_2O$
$Li + HF \rightleftarrows LiH + F$	$OH + LiCl \rightleftarrows Cl + LiOH$
$Li + H_2 \rightleftarrows LiH + H$	$LiOH + H \rightleftarrows LiH + OH$
$Li + OH \rightleftarrows LiH + O$	$LiOH + H \rightleftarrows LiO + H_2$
$Li + OH \rightleftarrows LiO + H$	$LiOH + O \rightleftarrows LiO + OH$
$Li + O_2 \rightleftarrows LiO + O$	$LiOH + LiCl \rightleftarrows Li_2O + HCl$
$Li + LiOH \rightleftarrows LiH + LiO$	$LiF + H_2O \rightleftarrows LiOH + HF$
$Li + LiOH \rightleftarrows Li_2O + H$	$LiF + HF \rightleftarrows LiH + F_2$
$HCl + Li \rightleftarrows Cl + LiH$	$LiF + H_2 \rightleftarrows LiH + HF$
$CO_2 + Li \rightleftarrows CO + LiO$	$LiF + OH \rightleftarrows LiOH + F$
$Cl + LiOH \rightleftarrows HCl + LiO$	$LiF + OH \rightleftarrows LiO + HF$
$LiO + HF \rightleftarrows LiOH + F$	$LiF + Cl \rightleftarrows LiCl + F$
$LiO + H_2 \rightleftarrows LiH + OH$	$LiF + F \rightleftarrows Li + F_2$

Table 2-9. Additional Chemical Reactions of Importance in Lithium Containing Propellant Systems (Continued)

$LiF + H \rightleftharpoons Li + HF$

$LiF + H \rightleftharpoons LiH + F$

$LiF + O \rightleftharpoons LiO + F$

$LiCl + HCl \rightleftharpoons LiH + Cl_2$

$LiCl + HF \rightleftharpoons LiF + HCl$

$LiCl + H_2 \rightleftharpoons LiH + HCl$

$LiCl + OH \rightleftharpoons LiO + HCl$

$LiCl + Cl \rightleftharpoons Li + Cl_2$

$LiCl + H \rightleftharpoons Li + HCl$

$LiCl + H \rightleftharpoons LiH + Cl$

$LiCl + O \rightleftharpoons LiO + Cl$

$LiCl + LiO \rightleftharpoons Li_2O + Cl$

$F + LiCl \rightleftharpoons ClF + Li$

$Cl + LiF \rightleftharpoons ClF + Li$

$Li + CH \rightleftharpoons LiH + C$

$C + LiF \rightleftharpoons CF + Li$

$Li + HCN \rightleftharpoons LiH + CN$

$CN + LiF \rightleftharpoons CNF + Li$

$CN + LiCl \rightleftharpoons CNCl + Li$

$Li + CH_2 \rightleftharpoons LiH + CH$

$Li + CH_3 \rightleftharpoons LiH + CH_2$

$Li + CH_4 \rightleftharpoons LiH + CH_3$

$HF + LiCl \rightleftharpoons ClF + LiH$

$CO + LiF \rightleftharpoons CF + LiO$

$HCl + LiF \rightleftharpoons ClF + LiH$

$CH + LiF \rightleftharpoons CF + LiH$

$HCN + LiF \rightleftharpoons CNF + LiH$

$HCN + LiCl \rightleftharpoons CNCl + LiH$

$LiH + CO \rightleftharpoons LiO + CH$

$LiOH + C \rightleftharpoons LiO + CH$

$LiOH + CH \rightleftharpoons LiO + CH_2$

$LiOH + CN \rightleftharpoons LiO + HCN$

$LiOH + CH_2 \rightleftharpoons LiO + CH_3$

$LiOH + CH_3 \rightleftharpoons LiO + CH_4$

$LiF + Cl_2 \rightleftharpoons LiCl + ClF$

$LiF + ClF \rightleftharpoons LiCl + F_2$

$CNF + LiCl \rightleftharpoons CNCl + LiF$

Table 2-10. Chemical Reactions for Which Rate Constants Have Been Determined

Chemical Reaction	Exothermic Rate Constant*	Reference
$CO_2 + M \rightleftarrows CO + O + M$	$3 \times 10^{20} T^{-1.0} \exp - \left(\frac{11393}{T}\right)$	Avramenko, L.I. and Kolesnikova, R.V., Izvest. Akad. Navk. S.S.S.R., Otdel. Khim. Navk., 1562 (1959).
$H_2O + M \rightleftarrows OH + H + M$	$3 \times 10^{19} T^{-1.0}$	Mayer, S.W., Cook, E.A., Schieler, L., "Non-equilibrium Recombination in Nozzles," SSD-TDR-64-139, Aerospace Corporation, Los Angeles, California, 18 Sept. 1964.
$CO + M \rightleftarrows C + O + M$	$2 \times 10^{18} T^{-1.0}$	Wray, K.L., Avco Research Report 95 (1961).
$HF + M \rightleftarrows H + F + M$	$1 \times 10^{19} \times T^{-0.5}$	S.W. Mayer, E.A. Cook, and L. Schieler, "Nonequilibrium Recombination in Nozzles," SSD-TDR-64-139, Aerospace Corporation, Los Angeles, California, 19 Sept. 1964
$H_2 + M \rightleftarrows 2H + M$	$10^{19} T^{-1.0}$	W.E. Kaskan and W.G. Browne, "Kinetics of the $H_2/CO/O_2$ System," General Electric Document No. 63SD848, 14 February 1964.
$N_2 + M \rightleftarrows 2N + M$	$2 \times 10^{18} T^{-1.0}$	K.L. Wray, Avco Research Report 104 (1961).
$NO + M \rightleftarrows N + O + M$	$2 \times 10^{18} T^{-1.0}$	K.L. Wray, Avco Research Report 95 (1961).
$OH + M \rightleftarrows O + H + M$	$2 \times 10^{18} T^{-1.0}$	S.W. Mayer, E.A. Cook, and L. Schieler, "Nonequilibrium Recombination in Nozzles," SSD-TDR-64-139, Aerospace Corporation, Los Angeles, California, 19 Sept. 1964
$O_2 + M \rightleftarrows 2O + M$	$1 \times 10^{16} T^{-0.5}$	S.W. Mayer, E.A. Cook, and L. Schieler, "Nonequilibrium Recombination in Nozzles," SSD-TDR-64-139, Aerospace Corporation, Los Angeles, California, 19 Sept. 1964.
$CO_2 + H \rightleftarrows CO + OH$	$3.2 \times 10^{12} \exp - \left(\frac{6300}{RT}\right)$	W.E. Kaskan and W.G. Browne, "Kinetics of the $H_2/CO/O_2$ System," General Electric Document No. 63SD848, 14 Feb. 1964.
$CO_2 + O \rightleftarrows CO + O_2$	$3.58 \times 10^{15} T^{-1.0}$	L.I. Avramenko and R.V. Kilesnikova, Izvest. Akad. Navk. S.S.S.R., Otdel, Khim. Navk., 1562 (1959).
$H_2O + H \rightleftarrows OH + H_2$	$7 \times 10^{13} \exp - \left(\frac{6100}{RT}\right)$	S.W. Mayer, E.A. Cook, and L. Schieler, "Nonequilibrium Recombination in Nozzles," SSD-TDR-64-139, Aerospace Corporation, Los Angeles, California, 19 Sept. 1964.
$H_2O + O \rightleftarrows 2OH$	$2.5 \times 10^{14} \exp - \left(\frac{10000}{RT}\right)$	S.W. Mayer, E.A. Cook, and L. Schieler, "Nonequilibrium Recombination in Nozzles," SSD-TDR-64-139, Aerospace Corporation, Los Angeles, California, 19 Sept. 1964
$2CO \rightleftarrows CO_2 + C$	$2.11 \times 10^{16} T^{-1.0}$	L.I. Avramenko, R.V. Lorentso, Zhur. Fiz. Khim., 24, 207 (1950).

*Three body recombination rates have the units $cm^6/gmole^2$-sec.
Bimolecular reaction rates have the units $cm^3/gmole$-sec.

Table 2-10. Chemical Reactions for Which Rate Constants Have Been Determined (Continued)

Chemical Reaction	Exothermic Rate Constant	Reference
$CO + H \rightleftarrows C + OH$	$1 \times 10^{14} \exp - \left(\frac{13000}{T}\right)$	F. Kaufman and J.P. Kelso, J. Chem. Phys., 23, 1072 (1955).
$CO + N \rightleftarrows C + NO$	$1.44 \times 10^{16} T^{-1.0}$	L.I. Avramenki and R.V. Lorentso, Zhur. Fiz. Khim., 24, 207 (1950).
$CO + NO \rightleftarrows CO_2 + N$	$2.47 \times 10^{15} T^{-1.0}$	L.I. Avramenko and R.V. Kilesnikova, Izvest. Akad. Navk. S.S.S.R., Otdel. Khim. Navk., 1562 (1959).
$CO + O \rightleftarrows C + O_2$	$2.48 \times 10^{13} \exp - \left(\frac{990}{T}\right)$	L.I. Avramenko and R.V. Lorentso, Zhur, Fiz, Khim., 24, 207 (1950).
$HF + H \rightleftarrows H_2 + F$	$5 \times 10^{12} \exp - \left(\frac{5700}{RT}\right)$	S.W. Mayer, E.A. Cook, and L. Schieler, "Nonequilibrium Recombination in Nozzles," SSD-TDR-64-139, Aerospace Corporation, Los Angeles, California, 18 Sept. 1964
$HF + O \rightleftarrows OH + F$	$5 \times 10^{11} T^{0.5} \exp - \left(\frac{6000}{RT}\right)$	S.W. Mayer, E.A. Cook, and L. Schieler, "Nonequilibrium Recombination in Nozzles," SSD-TDR-64-139, Aerospace Corporation, Los Angeles, California, 18 Sept. 1964
$HF + OH \rightleftarrows H_2O + F$	$5 \times 10^{11} T^{0.5} \exp - \left(\frac{7000}{RT}\right)$	S.W. Mayer, E.A. Cook, and L. Schieler, "Nonequilibrium Recombination in Nozzles," SSD-TDR-64-139, Aerospace Corporation, Los Angeles, California, 18 Sept. 1964.
$H_2 + O \rightleftarrows OH + H$	$1.4 \times 10^{12} \exp - \left(\frac{5190}{RT}\right)$	W.E. Kaskan and W.G. Browne, "Kinetics of the $H_2/CO/O_2$ System," General Electric Document No. 63SD848, 14 February 1964.
$H_2 + O_2 \rightleftarrows 2OH$	$2.7 \times 10^{16} \exp - \left(\frac{53000}{T}\right)$	F. Kaufman and J.P. Kelso, J. Chem. Phys., 23, 1072 (1955).
$N_2 + O \rightleftarrows NO + N$	$1.5 \times 10^{16} T^{-1}$	L.E. Phillips and H.I. Schiff, J. Chem. Phys., 36, 1509 (1962).
$N_2 + O_2 \rightleftarrows 2NO$	$5 \times 10^{23} T^{-5.2} \exp - \left(\frac{43000}{T}\right)$	E. Freedman and J.W. Daiber, J. Chem. Phys., 34, 1271 (1961).
$NO + O \rightleftarrows N + O_2$	$1.011 \times 10^{11} T^{0.5} \exp - \left(\frac{3120}{T}\right)$	W.G. Vincenti, Stanford Univ. Dept. Aeronaut. Engr. Rept. 101 (1961).
$O_2 + H \rightleftarrows OH + O$	$3.2 \times 10^{11} T^{-0.47} \exp - \left(\frac{100}{RT}\right)$	W.E. Kaskan and W.G. Browne, "Kinetics of the $H_2/CO/O_2$ System," General Electric Document No. 63SD848, 14 Feb. 1964.

3. IMPLICIT INTEGRATION METHOD

In both of the one-dimensional programs developed under the contract, an implicit integration method has been used in solving the governing equations. This method is also used in solving the chemical and particle relaxation equations in the axisymmetric nonequilibrium programs as discussed in later sections of this report. The implicit integration method was developed by Tyson[3] and is described below.

It has been shown by Tyson[3] that in the numerical integration of relaxation equations in near equilibrium flow regions (such as the chember and nozzle inlet in rocket engines), explicit integration methods are unstable unless the integration step size is of the order of the characteristic relaxation distance of the relaxation equations. Since the characteristic relaxation distance is orders of magnitude smaller than the characteristic physical dimensions of the system of interest (such as the nozzle throat diameter and length) in near equilibrium flow regions, the use of explicit methods to integrate relaxation equations in these regions results in excessively long computation times. Implicit integration methods were shown to be inherently stable in integrating relaxation equations in all flow situations (whether near equilibrium or frozen) and can thus be used to integrate with step sizes of the order of the physical dimensions of the system of interest throughout the integration reducing the computation time per case several orders of magnitude. Since it has been demonstrated that there are significant advantages in using implicit rather than explicit integration methods for integrating relaxation equations, a second order implicit integration method has been chosen for use in the present program.

3.1 STABILITY CONSIDERATIONS

The numerical considerations leading to the above conclusions can be illustrated by considering the simple relaxation equation

$$\frac{dy}{dx} = -\frac{y - y_e}{\tau} \tag{3-1}$$

which represents the relaxation toward equilibrium of chemical reactions, gas particle lags, etc. In this equation, y_e is the equilibrium condition

and τ is the characteristic relaxation distance of the equation. In the equilibrium limit, τ is very small compared to the physical dimensions of the system of interest while in the frozen limit, τ, is very large compared to the physical dimensions of the system of interest. The mathematical behavior of solutions to the above equation can be found by considering the simple case where τ is constant and

$$y_e = y_{eo} + a(x - x_o) \tag{3-2}$$

which is equivalent to terminating the Taylor series for y_e after the first term. The exact solution of Equation (3-1) for this case can be shown to be

$$y(x_o + h) = y(x_o) + \left[y_{eo} - y(x_o) - a\tau\right]\left[1 - e^{-h/\tau}\right] + ah \tag{3-3}$$

where $y(x_o)$ is the initial value of y and h is the integration step.

It is seen that the solution consists of two parts, a term which varies slowly with x and a term which exponentially decays with a relaxation length of τ, the characteristic relaxation length of Equation (3-1). Thus after a few relaxation lengths

$$y(x) \simeq y_{eo} + ah, \quad h \gg \tau \tag{3-4}$$

which is independent of $y(x_o)$ the initial condition. Since explicit integration methods construct the solution of Equation (3-1) as a Taylor series about the initial condition $y(x_o)$, the above example indicates that explicit integration methods should be limited to step sizes of the order of a few relaxation lengths.

That this is indeed the case can be shown by explicitly integrating Equation (3-1) using Euler's method. The explicit finite difference form of Equation (3-1) is then

$$\frac{y(x_o + h) - y(x_o)}{h} = -\frac{y(x_o) - y_{eo}}{\tau} \tag{3-5}$$

which yields the truncated Taylor series

$$y(x_o + h) = y(x_o)\left(1 - \frac{h}{\tau}\right) + y_{eo}\frac{h}{\tau} \tag{3-6}$$

when solved for $y(x_o + h)$. After n integration steps, it is found that

$$y(x_o + nh) = y(x_o)\left[1 - \frac{h}{\tau}\right]^n + \sum_{i=1}^{n}\left[y_{eo} + (i-1)\,ah\right]\left[1 - \frac{h}{\tau}\right]^{-n-i}\frac{h}{\tau} \tag{3-7}$$

Examination of this equation shows that the dependence on the initial condition $y(x_o)$ will decay only if $|1 - h/\tau| < 1$, otherwise $y(x_o + nh)$ will oscillate with rapidly increasing amplitude. Hence the calculation will be stable only if $h/\tau < 2$. Similar results are obtained for other explicit integration methods. (The stable step size for Runge-Kutta integrations is $h/\tau < 5.6$.) Thus the stable step size for explicit integration of relaxation equations is of the order of the relaxation distance which explains the large computation times associated with explicit integration of relaxation equations in near equilibrium flow regions. As shown below, the use of implicit integration methods allows the integration of relaxation equations on a step size which is independent of the relaxation length.

Implicitly integrating Equation (3-1) using Euler's method, the finite difference form of Equation (3-1) is

$$\frac{y(x_o + h) - y(x_o)}{h} = -\frac{y(x_o + h) - y_{eo} - ah}{\tau} \tag{3-8}$$

which yields

$$y(x_o + h) = \frac{y(x_o) + (y_{eo} + ah)\frac{h}{\tau}}{1 + \frac{h}{\tau}} \tag{3-9}$$

when solved for $y(x_o + h)$. After n integration steps it is found that

$$y(x_o + nh) = \frac{y(x_o)}{\left[1 + \frac{h}{\tau}\right]^n} + \sum_{i=1}^{n} \frac{y_{eo} + iah}{\left[1 + \frac{h}{\tau}\right]^{n+1-i}} \frac{h}{\tau} \tag{3-10}$$

Examination of this equation shows that the dependence on the initial condition $y(x_o)$ always decays, regardless of the step size. Hence the implicit calculation will always be stable. As an extreme example, consider one integration step, $h = x - x_o$. From Equation (3-9), it is seen that

$$y(x) \simeq y_{eo} + ah \ , \ h \gg \tau \tag{3-11}$$

when the step size is large compared to the relaxation length and

$$y(x) = y(x_o)\left(1 - \frac{h}{\tau}\right) + y_{eo}\frac{h}{\tau} + \cdots, \ h \ll \tau \tag{3-12}$$

when the step size is small compared to the relaxation length.

It is seen that in the equilibrium limit (τ small, h/τ large) the exact solution and the implicit integration of the relaxation equation go to the same limit which is independent of the relaxation distance and depends only on the rate of change of the equilibrium condition. In the frozen case (τ large and h/τ small) the implicit and explicit methods are essentially the same (terminated Taylor series). Thus, implicit numerical integration methods can be used to integrate relaxation equations using step sizes of the order of the physical dimensions of the system of interest in all flow situations whether near equilibrium or near frozen. For a complete discussion of the numerical integration of relaxation equations, see Reference 2.

In choosing a numerical integration method, the primary items of concern are the stability, accuracy and simplicity of the method. As shown by Tyson[3] and discussed above, implicit methods are to be preferred for numerically integrating relaxation equations due to their

inherent stability. Having chosen the basic integration method for stability reasons, the order of the integration method is determined by accuracy and simplicity considerations. In general, the higher the order of the integration method, the more complex the method becomes requiring more information in the form of past values or past derivatives of the function being integrated. Second order methods (accurate to h^2 with error of order h^3) have the advantage of simplicity and flexibility since they require only one past value of the function while retaining sufficient accuracy to allow the use of reasonably economical step sizes. For these reasons, a second order implicit numerical integration method was chosen for use in the present program. A complete derivation of this numerical integration method is given in the following section.

3.2 DERIVATION OF NUMERICAL INTEGRATION METHOD

Consider the coupled set of first-order simultaneous differential equations.

$$\frac{dy_i}{dx} = f_i(x, y_1, \cdots, y_N) \quad , \quad i = 1, 2, \cdots, N \tag{3-13}$$

It will be assumed that the equations are not singular and that a solution exists which may be developed as a Taylor series about the forward point

$$k_{i,\,n+1} = \left.\frac{dy_i}{dx}\right|_{x_n+h} h - \left.\frac{d^2y_i}{dx^2}\right|_{x_n+h} \frac{h^2}{2} + \left.\frac{d^3y_i}{dx^3}\right|_{x_n+h} \frac{h^3}{6} - \left.\frac{d^4y_i}{dx^4}\right|_{x_n+h} \frac{h^4}{24} + \cdots \tag{3-14}$$

where $k_{i,\,n+1}$ is the increment in y_i and h is sufficiently small. For equal integration steps

$$k_{i,\,n+1} + k_{i,\,n} = 2\left.\frac{dy_i}{dx}\right|_{x_n+h} h - 4\left.\frac{d^2y_i}{dx^2}\right|_{x_n+h} \frac{h^2}{2} + 8\left.\frac{d^3y_i}{dx^3}\right|_{x_n+h} \frac{h^3}{6} - 16\left.\frac{d^4y_i}{dx^4}\right|_{x_n+h} \frac{h^4}{24} + \cdots \tag{3-15}$$

Solving these equations for the derivative at the forward point, it is found that

$$\left.\frac{dy_i}{dx}\right|_{x_n+h} = \frac{3k_{i,n+1} - k_{i,n}}{2h} + \left.\frac{d^3y_i}{dx^3}\right|_{x_n+h} \frac{h^2}{3} - \cdots \tag{3-16}$$

Expanding the function $f_i(x, y, \cdots, y_N)$ as a Taylor's series about the back point (x_n), it is found that

$$\left.\frac{dy_i}{dx}\right|_{x_n+h} = f_{i,n} + \alpha_{i,n}h + \sum_{j=1}^{N} \beta_{i,j,n}k_{j,n+1} + \left.\frac{d^3y}{dx^3}\right|_{x_n} \frac{h^2}{2} + \cdots \tag{3-17}$$

where

$$f_i = f_i(x, y, \cdots, y_N) \tag{3-18}$$

$$\alpha_i = \frac{\partial f_i}{\partial x} \tag{3-19}$$

$$\beta_{i,j} = \frac{\partial f_i}{\partial y_j} \tag{3-20}$$

and the subscript n refers to the functions f_i, α_i and $\beta_{i,j}$ evaluated at the point x_n. Since

$$\left.\frac{d^3y}{dx^3}\right|_{x_n} = \left.\frac{d^3y}{dx^3}\right|_{x_n+h} - \left.\frac{d^4y}{dx^4}\right|_{x_n+h} h + \cdots \tag{3-21}$$

and

$$\left.\frac{d^4y}{dx^4}\right|_{x_n} = \left.\frac{d^4y}{dx^4}\right|_{x_n+h} - \cdots, \tag{3-22}$$

Equation (3-17) can be rewritten as

$$\left.\frac{dy_i}{dx}\right|_{x_n+h} = f_{i,n} + \alpha_{i,n}h + \sum_{j=1}^{N} \beta_{i,j,n}k_{j,n+1} + \left.\frac{d^3y_i}{dx^3}\right|_{x_n+h} \frac{h^2}{2} - \cdots \tag{3-23}$$

Equating the two expressions for the derivative at the forward point [Equations (3-16) and (3-23)], it is found that

$$\frac{3k_{i,n+1} - k_{i,n}}{2h} = f_{i,n} + \alpha_{i,n}h + \sum_{j=1}^{N} \beta_{i,j,n}k_{j,n+1} + \left.\frac{d^3y_i}{dx^3}\right|_{x_n+h} \frac{h^2}{6} + \cdots \tag{3-24}$$

or

$$k_{i,n+1} = \frac{1}{3}\left[k_{i,n} + 2\left(f_{i,n} + \beta_{i,n}h + \sum_{j=1}^{N} \beta_{i,j,n}k_{j,n+1}\right)h\right] + \left.\frac{d^3y_i}{dx^3}\right|_{x_n+h} \frac{h^3}{9} + \cdots \tag{3-25}$$

Neglecting the third order derivative term and solving the set of N linear nonhomogeneous algebraic equations

$$\left(1 - \frac{2}{3}\beta_{i,i,n}h\right)k_{i,n+1} - \sum_{j=1}^{N}(1 - \delta_{i,j})\beta_{i,j,n}k_{j,n+1} = \frac{1}{3}\left[k_{i,n} + 2(f_{i,n} + \alpha_{i,n}h)h\right] \tag{3-26}$$

where $\delta_{i,j}$ is the Kronecker delta thus yields a second order implicit solution of the above set of coupled first order simultaneous differential equations.

For unequal step sizes, it can be similarly shown that solving the set of N linear nonhomogeneous algebraic equations

$$\left(1 - \frac{h_{n+1} + h_n}{2h_{n+1} + h_n} \beta_{i,i,n} h_{n+1}\right) k_{i,n+1} - \frac{h^2_{n+1}}{(2h_{n+1} + h_n) h_n} \sum_{j=1}^{N} (1 - \delta_{i,j}) \beta_{i,j,n} k_{j,n+1}$$

$$= \frac{h^2_{n+1}}{(2h_{n+1} + h_n) h_n} \left[k_{i,n} + (f_{i,n} + \alpha_{i,n} h_{n+1}) \frac{h_n}{h_{n+1}} (h_{n+1} + h_n) \right] \qquad (3\text{-}27)$$

yields a second order implicit solution of the above set of coupled first order simultaneous differential equations.

In Equation (3-24), the third derivative term was neglected which resulted in an integration error of

$$k_i - k_i^{(c)} = \left. \frac{d^3 y}{dx^3} \right|_{x_n + h} \frac{h^3}{3} + \cdots \qquad (3\text{-}28)$$

where $k_i^{(c)}$ is the correct (true) value of the increment k_i. Thus the ratio of the neglected third derivative term to the first derivation terms in Equation (3-24) can be used to determine the allowable integration step size. Since

$$\left. \frac{d^3 y}{dx^3} \right|_{x_n + h} = \frac{k_{i,n+1} - 2k_{i,n} + k_{i,n-1}}{h^3} + \frac{3}{2} \left. \frac{d^4 y}{dx^4} \right|_{x_n + h} h + \cdots \qquad (3\text{-}29)$$

the absolute value of the ratio of the neglected term to the remaining terms in Equation (3-24) is

$$\frac{1}{3}\left|\frac{k_{i,n+1} - 2k_{i,n} + k_{i,n-1}}{3k_{i,n+1} - k_{i,n}}\right|$$

Since this ratio varies as the step size squared, doubling or halving the step size will change this ratio by a factor of four. In order to maintain this ratio within prescribed limits without doubling or halving each step, the prescribed limits must differ by at least a factor of four. Thus in the programs, the integration step size is calculated from

$$h_{n+2} = 2h_{n+1}, \quad \left|\frac{k_{i,n+1} - 2k_{i,n} + k_{i,n-1}}{3k_{i,n+1} - k_{i,n}}\right| < \frac{\delta}{10} \tag{3-30}$$

$$h_{n+2} = \frac{1}{2}h_{n+1}, \quad \left|\frac{k_{i,n+1} - 2k_{i,n} + k_{i,n-1}}{3k_{i,n+1} - k_{i,n}}\right| > \delta \tag{3-31}$$

$$h_{n+2} = h_{n+1}, \quad \frac{\delta}{10} \leq \left|\frac{k_{i,n+1} - 2k_{i,n} + k_{i,n-1}}{3k_{i,n+1} - k_{i,n}}\right| \leq \delta \tag{3-32}$$

where δ is the maximum allowable ratio of the neglected term to the remaining terms in Equation (3-24).

4. TRANSONIC ANALYSES

Transonic analyses of uniform and two-zone expansions were developed to construct initial data lines for the characteristics calculations and are based on the assumptions pertaining to a perfect gas. Their application to the axisymmetric reacting programs is described in the program document reports and also in Sections 5.3 and 5.5 of this report. The transonic analyses have been described in detail in a report by Kliegel and Quan[4], and the analyses are summarized below.

4.1 UNIFORM EXPANSIONS

The equations governing the inviscid isentropic expansion of a perfect gas through a convergent-divergent nozzle are

$$\left(1 - u^2 - \frac{\gamma-1}{\gamma+1} v^2\right) \frac{\partial u}{\partial x} + \left(1 - v^2 - \frac{\gamma-1}{\gamma+1} u^2\right) \frac{\partial v}{\partial y} + \left[1 - \frac{\gamma-1}{\gamma+1} (u^2 + v^2)\right] \frac{\omega v}{y}$$

$$- \frac{4}{\gamma+1} uv \frac{\partial u}{\partial y} = 0 \qquad (4\text{-}1)$$

$$\frac{\partial v}{\partial x} - \frac{\partial u}{\partial y} = 0 \qquad (4\text{-}2)$$

where the velocities have been normalized with respect to the throat sonic velocity and ω equals 0 or 1 depending on whether the nozzle is planar or axisymmetric. In seeking solutions of the above equations, it is desirable to choose a set of non-dimensional coordinates such that the various velocity derivatives are independent of the nozzle scale. For large values of the normalized throat wall radius of curvature, the flow velocities asymptotically approach those obtained from the one-dimensional channel flow equations. It can be shown from the channel flow equations (see Appendix A of Reference 4) that for choked flows

$$u = 1 + \sqrt{\frac{\omega+1}{\gamma+1} \frac{1}{R}} \frac{x}{y^*} + \cdots \qquad (4\text{-}3)$$

at the nozzle throat, where x is the distance from the throat plane, y^* is the throat half height, and R is the normalized throat wall radius of curvature. Examination of this equation reveals that the axial nozzle coordinate x must be normalized with respect to the distance $\sqrt{R}\, y^*$ in order for the dimensionless axial velocity gradient to remain of order one at the nozzle throat independent of the nozzle scale. Since the nozzle scale perpendicular to the nozzle axis is set by the throat half height y^*, it is apparent that the perpendicular coordinate y should be normalized with respect to the distance y^*. Thus, solutions of the above equations should be sought in terms of the normalized coordinates

$$z = \sqrt{\frac{1}{R}}\,\frac{x}{y^*} \tag{4-4}$$

$$r = \frac{y}{y^*} \tag{4-5}$$

rather than in the x, y coordinate system for large values of the normalized throat wall radius of curvature.

The above axial coordinate choice differs from Hall's[5] by a factor $\sqrt{\frac{\omega+1}{\gamma+1}\,R}$, since the axial coordinate used by Hall is

$$z_H = \sqrt{\frac{\omega+1}{\gamma+1}\,R}\,\frac{x}{y^*} \tag{4-6}$$

As shown in Reference 4, the above choice results in the present solution being uniformly valid for all (subsonic, transonic and supersonic) nozzle flow regimes, while Hall's choice limits the validity of his solution to the transonic throat region.

In the r, z coordinate system, the above equations become

$$\sqrt{\frac{1}{R}}\left(1 - u^2 - \frac{\gamma-1}{\gamma+1}\,v^2\right)\frac{\partial u}{\partial z} + \left(1 - v^2 - \frac{\gamma-1}{\gamma+1}\,u^2\right)\frac{\partial v}{\partial r} + \left[1 - \frac{\gamma-1}{\gamma+1}\,(u^2+v^2)\right]\frac{\omega v}{r}$$

$$- \frac{4}{\gamma+1}\,uv\,\frac{\partial u}{\partial y} = 0 \tag{4-7}$$

$$\sqrt{\frac{1}{R}}\,\frac{\partial v}{\partial z} - \frac{\partial u}{\partial r} = 0 \tag{4-8}$$

The boundary conditions are

$$v(o, z) = 0 \tag{4-9}$$

and

$$\frac{v(r_w, z)}{u(r_w, z)} = \sqrt{\frac{1}{R}}\,\frac{dr_w}{dz} \tag{4-10}$$

At the nozzle throat,

$$\begin{aligned} r_w &= 1 + \frac{x^2}{2R} + \cdots \\ &= 1 + \frac{z^2}{2} + \cdots \end{aligned} \tag{4-11}$$

for all throat sections. Thus, both u and $\frac{dr_w}{dz}$ are 0(1) at the throat and v must be $0(R^{-1/2})$. This suggests that the velocity components can be expressed as expansions in inverse power of R, i.e.,

$$u = u_o(r, z) + \frac{u_1(r, z)}{R} + \frac{u_2(r, z)}{R^2} + \cdots \tag{4-12}$$

$$v = \sqrt{\frac{1}{R}}\left[v_o(r, z) + \frac{v_1(r, z)}{R} + \frac{v_2(r, z)}{R^2} + \cdots\right] \tag{4-13}$$

Substituting into Equations (4-7) and (4-8) and equating powers of R^{-1} separately yields two sets of equations:

$$\left(1 - u_o^2\right)\frac{\partial u_o}{\partial z} + \left(1 - \frac{\gamma-1}{\gamma+1}\,u_o^2\right)\left(\frac{\partial v_o}{\partial r} + \frac{\omega v_o}{r}\right) = 0 \tag{4-14}$$

$$\frac{\partial u_o}{\partial r} = 0 \tag{4-15}$$

$$\left(1 - u_o^2\right)\frac{\partial u_n}{\partial z} + \left(1 - \frac{\gamma-1}{\gamma+1} u_o^2\right)\left(\frac{\partial v_n}{\partial r} + \frac{\omega v_n}{r}\right) - \frac{4}{\gamma+1} u_o v_o \frac{\partial u_n}{\partial r} = \phi_n, \; n \geq 1 \quad (4\text{-}16)$$

$$\frac{\partial v_{n-1}}{\partial z} - \frac{\partial u_n}{\partial r} = 0 \quad (4\text{-}17)$$

where

$$\phi_1 = \left(2u_o u_1 + \frac{\gamma-1}{\gamma+1} v_o^2\right)\frac{\partial u_o}{\partial z} + \left(v_o^2 + 2\frac{\gamma-1}{\gamma+1} u_o u_1\right)\frac{\partial v_o}{\partial r}$$

$$+ \frac{\gamma-1}{\gamma+1}\left(2u_o u_1 + v_o^2\right)\frac{\omega v_o}{r} \quad (4\text{-}18)$$

$$\phi_2 = \left(2u_o u_2 + u_1^2 + 2\frac{\gamma-1}{\gamma+1} v_o v_1\right)\frac{\partial u_o}{\partial z} + \left[2v_o v_1 + \frac{\gamma-1}{\gamma+1}(2u_o u_2\right.$$

$$\left. + u_1^2)\right]\frac{\partial v_o}{\partial r} + \frac{\gamma-1}{\gamma+1}\left(2u_o u_2 + u_1^2 + 2v_o v_1\right)\frac{\omega v_o}{r}$$

$$+ \left(2u_o u_1 + \frac{\gamma-1}{\gamma+1} v_o^2\right)\frac{\partial u_1}{\partial z} + \left(v_o^2 + 2\frac{\gamma-1}{\gamma+1} u_o u_1\right)\frac{\partial v_1}{\partial r}$$

$$+ \frac{\gamma-1}{\gamma+1}\left(2u_o u_1 + v_o^2\right)\frac{\omega v_1}{r} + \frac{4}{\gamma+1}\left(u_o v_1 + u_1 v_o\right)\frac{\partial u_1}{\partial r} \quad (4\text{-}19)$$

....

From Equations (4-9), (4-10), (4-12) and (4-13), it is found that the boundary conditions are

$$v_n(o, z) = 0 \qquad n \geq 0 \quad (4\text{-}20)$$

and

$$v_n(r_w, z) = u_n(r_w, z) \frac{dr_w}{dz} \qquad n \geq 0 \tag{4-21}$$

Equation (4-15) shows that $u_o(r, z)$ is a function of z alone. Thus,

$$u_o(r, z) = a_o(z) \tag{4-22}$$

Equation (4-14) is satisfied if $v_o(r, z)$ is of the form,

$$v_o(r, z) = a_1(z)r + \omega a_3(z)r^{-1} + (1 - \omega)\, a_5(z) \tag{4-23}$$

From the axis and wall boundary conditions [Equations (4-20) and (4-21)], it is easily shown that

$$a_1 = \frac{a_o}{r_w} \frac{dr_w}{dz} \tag{4-24}$$

$$a_3 = 0 \tag{4-25}$$

$$a_5 = 0 \tag{4-26}$$

Substituting the above results into Equation (4-14) yields

$$\left(1 - a_o^2\right) \frac{da_o}{dz} + (\omega + 1) \left(1 - \frac{\gamma-1}{\gamma+1} a_o^2\right) \frac{a_o}{r_w} \frac{dr_w}{dz} = 0 \tag{4-27}$$

which is the one-dimensional channel flow equation. The solution of the above equations defines the one-dimensional velocity distribution (u_o and v_o) through the nozzle. Since the one-dimensional solution is valid for all (subsonic, transonic and supersonic) nozzle flow regimes, the present solution will also be valid for all nozzle flow regimes. The one-dimensional throat boundary conditions are that

$$a_o(0) = 1 \tag{4-28}$$

$$a_1(0) = 0 \tag{4-29}$$

for both planar and axisymmetric nozzle flows, since

$$\left.\frac{dr_w}{dz}\right|_o = 0 \tag{4-30}$$

at the nozzle throat.

The first order equations are

$$\left(1 - u_o^2\right)\frac{\partial u_1}{\partial z} + \left(1 - \frac{\gamma-1}{\gamma+1}u_o^2\right)\left(\frac{\partial v_1}{\partial r} + \frac{\omega v_1}{r}\right) - \frac{4}{\gamma+1}u_o v_o \frac{\partial u_1}{\partial r}$$

$$= \left(2u_o u_1 + \frac{\gamma-1}{\gamma+1}v_o^2\right)\frac{\partial u_o}{\partial z} + \left(v_o^2 + 2\frac{\gamma-1}{\gamma+1}u_o u_1\right)\frac{\partial v_o}{\partial r}$$

$$+ \frac{\gamma-1}{\gamma+1}\left(2u_o u_1 + v_o^2\right)\frac{\omega v_o}{r} \tag{4-31}$$

$$\frac{\partial v_o}{\partial z} - \frac{\partial u_1}{\partial r} = 0 \tag{4-32}$$

From Equations (4-23) and (4-32), it is easily shown that

$$u_1 = b_o(z) + b_2(z)r^2 \tag{4-33}$$

where

$$b_2 = \frac{1}{2}\frac{da_1}{dz} \tag{4-34}$$

From Equations (4-20), (4-31), and (4-33), it can be shown that

$$v_1 = b_1(z)r + b_3(z)r^3 \tag{4-35}$$

where

$$\left(1 - a_o^2\right)\frac{db_o}{dz} + (\omega + 1)\left(1 - \frac{\gamma-1}{\gamma+1} a_o^2\right) b_1 = 2a_o b_o\left[\frac{da_o}{dz} + \frac{\gamma-1}{\gamma+1}(\omega+1)a_1\right] \quad (4\text{-}36)$$

$$\left(1 - a_o^2\right)\frac{db_2}{dz} + (\omega + 3)\left(1 - \frac{\gamma-1}{\gamma+1} a_o^2\right) b_3 - \frac{8}{\gamma-1} a_o a_1 b_2$$

$$= 2a_o b_2 \left[\frac{da_o}{dz} + \frac{\gamma-1}{\gamma+1}(\omega + 1)a_1\right] + a_1^2\left[\frac{\gamma-1}{\gamma+1}\frac{da_o}{dz} + (1 + \frac{\gamma-1}{\gamma+1}\omega a_1\right] \quad (4\text{-}37)$$

From the wall boundary condition [Equation (4-21)], it can be shown that

$$b_1 = \left(b_o + b_2 r_w^2\right)\frac{1}{r_w}\frac{dr_w}{dz} - b_3 r_w^2 \quad (4\text{-}38)$$

The solution of the above equations defines the first order velocity components (u_1 and v_1) through the nozzle.

Examination of Equations (4-36) and (4-37) reveals that they are singular at the nozzle throat (where $a_o = 1$). Thus, the above equations are algebraic at the throat and can be solved directly for $b_o(0)$, $b_1(0)$ and $b_3(0)$, yielding

$$b_o(0) = -\frac{1}{4} \quad (4\text{-}39)$$

$$b_1(0) = -\frac{1}{4}\sqrt{\frac{\gamma+1}{2}} \quad (4\text{-}40)$$

$$b_3(0) = \frac{1}{4}\sqrt{\frac{\gamma+1}{2}} \quad (4\text{-}41)$$

for axisymmetric flows and

$$b_o(0) = -\frac{1}{6} \tag{4-42}$$

$$b_1(0) = -\frac{1}{6}\sqrt{\gamma+1} \tag{4-43}$$

$$b_3(0) = \frac{1}{6}\sqrt{\gamma+1} \tag{4-44}$$

for planar flows. From Equations (4-24) and (4-34) it can be shown that

$$b_2(0) = \frac{1}{2} \tag{4-45}$$

for both axisymmetric and planar flows.

The above first order throat conditions are identical to those obtained by Sauer[6] and Hall[5]. The two results differ away from the throat plane, however, due to the different functional dependence of the coefficients on the axial coordinate.

Examination of Equation (4-16) reveals that it is also singular at the nozzle throat (where $u_o = 1$). Thus, the boundary conditions for all orders are set at the nozzle throat, and the various order throat conditions can be determined directly. The fact that the boundary conditions are set at the throat for all orders is mathematical proof that the nozzle throat plane sets the choked flow through the nozzle.

Examination of Equations (4-24), (4-34) and (4-37) shows that b_2 depends on $\frac{d^2 r_w}{dz^2}$ and b_3 depends on $\frac{d^3 r_w}{dz^3}$. Thus, if $\frac{d^3 r_w}{dz^3}$ is discontinuous, the first order solution will be discontinuous. Thus, in general, if the wall derivative $\frac{d^{2n+1} r_w}{dz^{2n+1}}$ is nonanalytic, the nth order solution of the above equations will be discontinuous. The complete solution of the above equations will be analytic only if the wall is analytic.

The second order solutions can be similarly obtained and are given in Reference 4. A discussion of the second and higher order solutions and a comparison with other analyses are also contained in this reference.

4.2 TWO-ZONE EXPANSIONS

Since most rocket engines operate with a cool "barrier" zone near the wall to protect the thrust chamber from the hot "core" gases, the exhaust gas expansion through rocket engines can generally be represented as a two-zone expansion. In order to simplify the analysis, the barrier zone is assumed to be confined to an annular ring. Thus the flow is axisymmetric in both zones. (The analysis is also applicable to two-dimensional nozzle flows in which the outer zone is planar.)

The equations governing the inviscid isentropic expansion of two perfect gases through a nozzle are

$$\left(1 - u^2 - \frac{\gamma-1}{\gamma+1} v^2\right) \frac{\partial u}{\partial x} + \left(1 - v^2 - \frac{\gamma-1}{\gamma+1} u^2\right) \frac{\partial v}{\partial y} + \left[1 - \frac{\gamma-1}{\gamma+1} (u^2 + v^2)\right] \frac{\omega v}{y}$$

$$- \frac{4}{\gamma+1} uv \frac{\partial u}{\partial y} = 0 \tag{4-46}$$

$$\frac{\partial v}{\partial x} - \frac{\partial u}{\partial y} = 0 \tag{4-47}$$

in the inner zone and

$$\left(1 - \bar{u}^2 - \frac{\bar{\gamma}-1}{\bar{\gamma}+1} \bar{v}^2\right) \frac{\partial \bar{u}}{\partial x} + \left(1 - \bar{v}^2 - \frac{\bar{\gamma}-1}{\bar{\gamma}+1} \bar{u}^2\right) \frac{\partial \bar{v}}{\partial y} + \left[1 - \frac{\bar{\gamma}-1}{\bar{\gamma}+1} (\bar{u}^2 + \bar{v}^2)\right] \frac{\omega \bar{v}}{y}$$

$$- \frac{4}{\bar{\gamma}+1} \bar{u}\bar{v} \frac{\partial \bar{u}}{\partial y} = 0 \tag{4-48}$$

$$\frac{\partial \bar{v}}{\partial x} - \frac{\partial \bar{u}}{\partial y} = 0 \tag{4-49}$$

in the outer zone where the velocities have been normalized with respect to the appropriate throat sonic velocity and ω equals 0 or 1, depending on whether the nozzle is planar or axisymmetric. As in the previous analysis, we shall seek solutions of the above equations in nondimensional coordinates chosen from the channel flow solutions such that the various velocity derivatives are independent of the nozzle scale for large values of the normalized throat wall radius of curvature. It can be shown from the two-zone channel flow solutions (see Appendix A of Reference 4) that for choked flows

$$u = 1 + \sqrt{\frac{\omega+1}{\gamma+1}\frac{k}{R}}\,\frac{x}{y^*} + \cdots \tag{4-50}$$

$$\bar{u} = 1 + \frac{\gamma}{\bar{\gamma}}\sqrt{\frac{\omega+1}{\gamma+1}\frac{k}{R}}\,\frac{x}{y^*} + \cdots \tag{4-51}$$

at the nozzle throat where x is the distance from the throat plane, y^* is the throat half height, R is the normalized throat wall radius of curvature and k is a dimensionless constant of order one. Examination of these equations reveals that as in the previous analysis, the axial nozzle coordinate x must be normalized with respect to the distance $\sqrt{R}\ y^*$ in order for the dimensionless axial velocity gradients to remain of order one at the nozzle throat independent of the nozzle scale. Similarly, since the nozzle scale perpendicular to the nozzle axis is set by the throat half height y^*, the perpendicular coordinate y should be normalized with respect to the distance y^*. Thus, solutions to the above equations for large values of the normalized throat wall radius of curvature should again be sought in terms of the normalized coordinates

$$z = \sqrt{\frac{1}{R}}\,\frac{x}{y^*} \tag{4-52}$$

$$r = \frac{y}{y^*} \tag{4-53}$$

rather than in the x, y coordinate system.

In the r, z coordinate system, the above equations become

$$\sqrt{\frac{1}{R}}\left(1 - u^2 - \frac{\gamma-1}{\gamma+1} v^2\right)\frac{\partial u}{\partial z} + \left(1 - v^2 - \frac{\gamma-1}{\gamma+1} u^2\right)\frac{\partial v}{\partial r} + \left[1 - \frac{\gamma-1}{\gamma+1}(u^2+v^2)\right]\frac{\omega v}{r}$$

$$- \frac{4}{\gamma+1} uv \frac{\partial u}{\partial r} = 0 \qquad (4\text{-}54)$$

$$\sqrt{\frac{1}{R}}\frac{\partial v}{\partial z} - \frac{\partial u}{\partial r} = 0 \qquad (4\text{-}55)$$

in the inner zone and

$$\sqrt{\frac{1}{R}}\left(1 - \bar{u}^2 - \frac{\bar{\gamma}-1}{\bar{\gamma}+1} \bar{v}^2\right)\frac{\partial \bar{u}}{\partial z} + \left(1 - \bar{v}^2 - \frac{\bar{\gamma}-1}{\bar{\gamma}+1} \bar{u}^2\right)\frac{\partial \bar{v}}{\partial r} + \left[1 - \frac{\bar{\gamma}-1}{\bar{\gamma}+1}(\bar{u}^2 + \bar{v}^2)\right]\frac{\omega \bar{v}}{r}$$

$$- \frac{4}{\bar{\gamma}+1} \overline{uv} \frac{\partial \bar{u}}{\partial r} = 0 \qquad (4\text{-}56)$$

$$\sqrt{\frac{1}{R}}\frac{\partial \bar{v}}{\partial z} - \frac{\partial \bar{u}}{\partial r} = 0 \qquad (4\text{-}57)$$

in the outer zone.

The boundary conditions on the axis and at the wall are

$$v(o, z) = 0 \qquad (4\text{-}58)$$

$$\frac{\bar{v}(r_w, z)}{\bar{u}(r_w, z)} = \sqrt{\frac{1}{R}}\frac{dr_w}{dz} \qquad (4\text{-}59)$$

Since the flow angle and pressure match at the streamline dividing the two zones, the boundary conditions at the dividing streamline are

$$\frac{v(r_s, z)}{u(r_s, z)} = \frac{\bar{v}(r_s, z)}{\bar{u}(r_s, z)} = \sqrt{\frac{1}{R}}\,\frac{dr_s}{dz} \tag{4-60}$$

$$P^* \left\{ \frac{\gamma+1}{2} \left[1 - \frac{\gamma-1}{\gamma+1} \left(u(r_s, z)^2 + v(r_s, z)^2 \right) \right] \right\}^{\frac{\gamma}{\gamma-1}}$$

$$= \bar{P}^* \left\{ \frac{\bar{\gamma}+1}{2} \left[1 - \frac{\bar{\gamma}-1}{\bar{\gamma}+1} \left(\bar{u}(r_s, z)^2 + \bar{v}(r_s, z)^2 \right) \right] \right\}^{\frac{\bar{\gamma}}{\bar{\gamma}-1}} \tag{4-61}$$

where r_s is the radial position of the dividing streamline.

The sonic pressure is equal in both zones (see Appendix A of Reference 4) since this condition maximizes the mass flow through the nozzle and the throat plane then sets the flow through the nozzles. There are other families of solutions to the above equations for different pressure conditions (such as the total pressure in both zones being equal). In these solutions, the flow is not set at the throat plane but is set elsewhere in the flow system. These solutions (which correspond to nozzle flows with controlled external bleed such as occur in jet engines or ducted rockets) will not be considered.

Since u, $\bar{u}$, $\frac{dr_s}{dz}$ and $\frac{dr_w}{dz}$ are 0(1) at the throat, v and $\bar{v}$ must both be $0(R^{-1/2})$. This suggests that the velocity components in both zones can be expressed as expansions in inverse power of R for large values of the normalized throat wall radius of curvature. The procedure and the resulting system of equations are identical to those governing a uniform expansion. Thus, the solution for the inner zone is identical to the solution previously derived except that the dividing streamline boundary condition replaces the wall boundary condition. As was shown earlier [Equation (4-23)], the complete solution of the above equations for v_o is of the form

$$v_o(r, z) = a_1(z)r + \omega a_3(z)r^{-1} + (1 - \omega)\, a_5(z) \qquad (4\text{-}62)$$

where the functions $a_3(z)$ and $a_5(z)$ are identically zero in uniform expansions and in the inner zone. In the outer zone, however, $a_3(z)$ and $a_5(z)$ are not identically zero but are determined from the dividing streamline boundary conditions. Thus, the outer zone solutions contain additional terms dependent on $a_3(z)$ and $a_5(z)$ which do not appear in the inner zone solutions. Since planar two-zone expansions were not of primary interest in the study, only the axisymmetric solution has been obtained.

Be expanding the position of the dividing streamline r_s in inverse powers of R, i.e.,

$$r_s(z) = r_{so}(z) + \frac{r_{s1}(z)}{R} + \frac{r_{s2}(z)}{R^2} + \cdots \qquad (4\text{-}63)$$

expanding the velocity components about r_{so} using Taylor series, substituting the resulting expansions into Equations (4-60) and (4-61) and equating inverse powers of R, one obtains the dividing streamline boundary conditions for the various order solutions. The various order axis and wall boundary conditions are the same as in the uniform expansion case. The dividing streamline throat boundary condition is related to the ratio of mass flows through the two zones.

The one-dimensional, first-order, and second-order solutions are obtained in a manner similar to the uniform expansion case. They are shown in detail in Reference 4. Due to the lengthy expressions for the solutions, they are not repeated here.

5. PROGRAM ANALYSES

A documentation report containing a complete engineering and programming description has been published separately for each of the programs developed under the contract. A summary of the analysis for each of the programs is given below.

5.1 ONE-DIMENSIONAL REACTING GAS PROGRAM[7]

This program calculates the inviscid one-dimensional equilibrium, frozen and nonequilibrium nozzle expansion of gaseous propellant exhaust mixtures containing the six elements: carbon, hydrogen, oxygen, nitrogen, fluorine and chlorine. The computer program considers the 19 significant gaseous species (listed in Table 2-2) present in the exhaust mixtures of propellants (listed in Table 2-1) containing these elements and the 48 chemical reactions (13 dissociation-recombination reactions and 35 binary exchange reactions as listed in Table 2-4) which can occur between the exhaust products. In order to reduce computation time per case to a minimum, the program utilizes a second-order implicit integration method (described in Section 3). Typical run time is 3 minutes per case for this program on an IBM 7094 Mod II computer. The program analysis is given below.

In this program, the solutions for frozen and equilibrium flows are obtained by solving the simultaneous set of algebraic equations of continuity, energy, state, and entropy. For nonequilibrium expansions, the conservation equations governing the inviscid one-dimensional flow of reacting gas mixtures have been given by Hirshfelder, Curtiss and Byrd,[8] Penner[9] and others. The basic assumptions made in the derivation of these equations are:

- There are no mass or energy losses from the system.
- The gas is inviscid.
- Each component of the gas is a perfect gas.
- The internal degrees of freedom (translational, rotational and vibrational) of each component of the gas are in equilibrium.

The conservation equations are presented here in the form used in the present analysis. These equations are integrated using the second-order implicit method described in Section 3.

For each component of the gas the continuity equation is

$$\frac{d}{dx}(\rho_i Va) = \omega_i r^* a \tag{5-1}$$

where the axial coordinate (x) has been normalized with the throat radius. Summing over all components of the mixture, the overall continuity equation is obtained

$$\frac{d}{dx}(\rho Va) = 0 \tag{5-2}$$

By use of the above equation, Equation (5-1) can be rewritten as

$$\frac{dc_i}{dx} = \frac{\omega_i r^*}{\rho V} \tag{5-3}$$

The momentum equation is

$$\rho V \frac{dV}{dx} + \frac{dP}{dx} = 0 \tag{5-4}$$

The energy equation is

$$h + \frac{1}{2} V^2 = H_c \tag{5-5}$$

where

$$h = \sum_{i=1} c_i h_i \tag{5-6}$$

and

$$h_i = \int_o^T C_{pi} dT + h_{io} \tag{5-7}$$

For each component of the gas, the equation of state is

$$P_i = \rho_i R_i T \tag{5-8}$$

Summing over all components of the mixture, the overall equation of state is obtained

$$P = \rho R T \tag{5-9}$$

where

$$R = \sum_{i=1} c_i R_i \tag{5-10}$$

Since the expansion through a nozzle can be specified either by the expansion process or by the nozzle geometry, two forms of the above equations are of interest.

If the expansion process is specified and the pressure is known as a function of distance through the nozzle, the above equations become

$$\frac{dc_i}{dx} = \frac{\omega_i r^*}{\rho V} \tag{5-11}$$

$$\frac{dV}{dx} = -\frac{1}{\rho V}\frac{dP}{dx} \tag{5-12}$$

$$\frac{d\rho}{dx} = \left[\frac{1}{\gamma P}\frac{dP}{dx} - A\right]\rho \tag{5-13}$$

$$\frac{dT}{dx} = \left[\frac{\gamma-1}{\gamma}\frac{1}{P}\frac{dP}{dx} - B\right] T \tag{5-14}$$

while if the nozzle geometry is specified, the above equations become

$$\frac{dc_i}{dx} = \frac{\omega_i r^*}{\rho V} \tag{5-15}$$

$$\frac{dV}{dx} = \left[\frac{1}{a}\frac{da}{dx} - A\right]\frac{V}{M^2 - 1} \tag{5-16}$$

$$\frac{d\rho}{dx} = -\left\{\left[\frac{1}{a}\frac{da}{dx} - A\right]\frac{M^2}{M^2 - 1} + A\right\}\rho \tag{5-17}$$

$$\frac{dT}{dx} = -\left\{\left[\frac{1}{a}\frac{da}{dx} - A\right]\frac{(\gamma - 1)M^2}{M^2 - 1} + B\right\}T \tag{5-18}$$

$$P = \rho RT \tag{5-19}$$

where

$$A = \frac{r^*}{PV}\left[\sum_{i=1} \omega_i R_i T - \frac{\gamma - 1}{\gamma}\sum_{i=1} \omega_i h_i\right] \tag{5-20}$$

$$B = \frac{\gamma - 1}{\gamma}\frac{r^*}{PV}\sum_{i=1} \omega_i h_i \tag{5-21}$$

$$M = \frac{V}{\sqrt{\gamma RT}} \tag{5-22}$$

$$\gamma = \frac{C_p}{C_p - R} \tag{5-23}$$

and

$$C_p = \sum_{i=1} c_i C_{pi} \tag{5-24}$$

The first set of equations is completely specified at the sonic point while the second set of equations is singular. Thus, if the expansion through the nozzle is specified by the pressure distribution, the equations

governing the expansion can be directly integrated through the sonic point without mathematical difficulty. The expansion from the chamber through the sonic point is specified by the pressure distribution in the present program in order to eliminate numerical difficulties at the sonic point. In the expansion section downstream of the sonic point, however, the area variation is specified and the second set of equations is integrated through the supersonic expansion section.

In specifying the nozzle pressure distribution from the chamber through the sonic point, rather than the known area distribution, a question naturally arises regarding how accurately the calculation represents the flow through a specified nozzle geometry. It has been shown by Bray[10] and others that the pressure distribution through a nozzle is essentially identical with the equilibrium pressure distribution up to the freeze point which generally occurs downstream of the throat (or sonic point). Thus, the difference in the expansion and predicted performance caused by utilizing the equilibrium pressure distribution rather than the nozzle geometry to specify the expansion from the chamber to the sonic point is negligible. If a case does arise in which the equilibrium pressure distribution is not an adequate representation of the expansion, the pressure distribution can be iterated to obtain the correct pressure distribution. Experience has shown that this is rarely if ever required, however.

The net species production rate, ω_i, for each species considered by the program is calculated from

$$\omega_i = \overline{m}_i \rho^2 \sum_{j=1} (\nu'_{ij} - \nu_{ij}) X_j \tag{5-25}$$

where the net production rate for each reaction (X_j) considered by the program is calculated from

$$X_j = \left[K_j \prod_{i=1} c_i^{\nu_{ij}} - \rho \prod_{i=1} c_i^{\nu'_{ij}} \right] M_j k_{Rj} \tag{5-26}$$

for the dissociation-recombination reactions and

$$X_j = \left[K_j \prod_{i=1} c_i^{\nu_{ij}} - \prod_{i=1} c_i^{\nu'_{ij}} \right] k_{Rj} \tag{5-27}$$

for the binary exchange reactions.

The stoichiometric coefficients (ν_{ij} and ν'_{ij}) appearing in the above equations are defined by the generalized chemical reaction equation

$$\sum_{i=1} \nu_{ij} \overline{M}_i \rightleftarrows \sum_{i=1} \nu'_{ij} \overline{M}_i \tag{5-28}$$

where $\overline{M}_i$ represents the ith chemical species.

Since each dissociation-recombination reaction has a distinct reaction rate associated with each third body, the net production rate for each dissociation-recombination reaction should be calculated from

$$X_j = \sum_{k=1} \left[K_j \prod_{i=1} c_i^{\nu_{ij}} - \rho \prod_{i=1} c_i^{\nu'_{ij}} \right] c_k \, k_{Rkj} \tag{5-29}$$

rather than Equation (5-26). Benson and Fueno[11] have shown theoretically that the temperature dependence of recombination rates is approximately independent of the third body. Available experimental recombination rate data also indicates that the temperature dependence of recombination rates is independent of the third body within the experimental accuracy of the measurements. Assuming that the temperature dependence of recombination rates is independent of the third body, the recombination rate associated with the kth species (third body) can be represented as

$$k_{Rkj} = a_{kj} T^{-n_j} e^{-k_j/T} \tag{5-30}$$

where only the constant a_{kj} is different from different species (third bodies). From Equation (5-29) it can be shown that

$$X_j = \left[K_j \prod_{i=1} c_i^{\nu_{ij}} - \rho \prod_{i=1} c_i^{\nu'_{ij}} \right] \sum_{k=1} a_{kj} c_k T^{-n_j} e^{-k_j/T}$$

$$= \left[K_j \prod_{i=1} c_i^{\nu_{ij}} - \rho \prod_{i=1} c_i^{\nu'_{ij}} \right] \left[\sum_{i=1} \frac{a_{ij}}{a_{kj}} c_i \right] a_{kj} T^{-n_j} e^{-k_j/T} \qquad (5\text{-}31)$$

Thus the recombination rates associated with each third body can be considered as in Equation (5-26) by calculating the general third body term (M_j) as

$$M_j = \sum_{i=1} m_{j,i} c_i \qquad (5\text{-}32)$$

where $m_{j,i}$ is the ratio (a_{ij}/a_{kj}) of the recombination rate associated with the ith species (third body) to the recombination rate associated with the kth species (third body) which is the reference species (third body) whose rate [in the form of Equation (5-30)] is specified in the program input.

The computer program subroutines which include the computation of performance parameters such as specific impulse, characteristic velocity, etc. are given in detail in Reference 7.

5.2 ONE-DIMENSIONAL TWO-PHASE REACTING GAS PROGRAM[12]

This program calculates the inviscid one-dimensional two-phase equilibrium, frozen and nonequilibrium nozzle expansion of propellant exhaust mixtures containing the six elements: carbon, hydrogen, oxygen, nitrogen, fluorine, and chlorine and one metal element, either aluminum, beryllium, boron or lithium. The computer program considers the 79 significant gaseous species and eight significant condensed species, liquid or solid (listed in Table 2-2), present in the exhaust mixtures of propellants (listed in Table 2-1) containing these elements. The program considers the 763 gas phase chemical reactions (84 dissociation-recombination reactions and 679 binary exchange reactions as listed in Tables 2-4 through 2-9) which can occur between the exhaust products. The program

also considers the velocity and thermal lags (for up to five particle groups) between the gaseous and condensed combustion products (when they are present in the chamber). The program does not consider mass transfer (only momentum and energy transfer) between gaseous and condensed combustion products, except in the equilibrium option.

In order to reduce computation time per case to a minimum, the program utilizes a second-order implicit integration method (described in Section 3). The machine run time depends to a large extent on the number of chemical reactions involved and on whether or not condensed phase exists in the case. Typical run time varies between 5 and 30 minutes per case on an IBM 7094 Mod II computer. The program analysis is given below.

In this program, the solution for frozen and equilibrium flows are obtained by solving the simultaneous set of algebraic equations of continuity, energy, state, and entropy. For nonequilibrium expansions, the conservation equations governing the inviscid one-dimensional flow of a two-phase reacting gas mixture can be simply derived utilizing the following assumptions:

- There are no mass or energy losses from the system.
- The gas is inviscid except for its interactions with the condensed particles.
- Each component of the gas is a perfect gas.
- The internal degrees of freedom (rotational and vibrational) of each component of the gas are in equilibrium.
- The volume occupied by the condensed particles is negligible.
- The thermal (Brownian) motion of the condensed particles is negligible.
- The condensed particles do not interact.
- The condensed particle size distribution may be approximated by groups of different size spheres.
- The internal temperature of the condensed particles is uniform.
- Energy exchange between the gas and the condensed particles occurs only by convection.

- The only forces on the condensed particles are viscous drag forces.
- There is no mass transfer from the gas to the condensed phase during the nozzle expansion.

These assumptions have been previously used in all studies of reacting gas[8] and gas-particle[13] nozzle flows.

The conservation equations are presented here in the form used in the present analysis. These equations are integrated using the second-order implicit method described in Section 3.

For each component of the gas the continuity equation is

$$\frac{d}{dx}(\rho_i Va) = \omega_i r^* a \tag{5-33}$$

where the axial coordinate (x) has been normalized with the throat radius. Summing over all components of the mixture, the overall continuity equation for the gas is obtained

$$\frac{d}{dx}(\rho Va) = 0 \tag{5-34}$$

By use of the above equation, Equation (5-33) can be rewritten as

$$\frac{dc_i}{dx} = \frac{\omega_i r^*}{\rho V} \tag{5-35}$$

For each particle size group the continuity equation is

$$\frac{d}{dx}(\rho_{pi} V_{pi} a) = 0 \tag{5-36}$$

since there is no mass transfer from the gas to the condensed phase.

The overall momentum equation for the mixture is

$$\frac{d}{dx}(\rho VaV) + \frac{d}{dx}\left(\sum_{i=1} \rho_{pi} V_{pi} a V_{pi}\right) + a\frac{dP}{dx} = 0 \tag{5-37}$$

which becomes

$$\rho V \frac{dV}{dx} + \sum_{i=1} \rho_{pi} V_{pi} \frac{dV_{pi}}{dx} + \frac{dP}{dx} = 0 \tag{5-38}$$

through use of the continuity equations.

Similarly, the overall energy equation for the mixture is

$$\rho V \left(\frac{dh}{dx} + \frac{V dV}{dx} \right) + \sum_{i=1} \rho_{pi} V_{pi} \left(\frac{dh_{pi}}{dx} + V_{pi} \frac{dV_{pi}}{dx} \right) = 0 \tag{5-39}$$

where for the gas phase

$$h = \sum_{i=1} c_i h_i \tag{5-40}$$

and

$$h_i = \int_o^T C_{pi} dT + h_{io} \tag{5-41}$$

while for each particle group

$$h_{pi} = \int_o^{T_{pi}} C_{ppi}\, dT + h_{pio}\,, \quad T_{pi} < T_{pmi} \tag{5-42}$$

and

$$h_{pi} = \int_o^{T_{pi}} C_{ppi}\, dT + h_{pio} + \Delta H_{pi}\,, \quad T_{pi} > T_{pmi} \tag{5-43}$$

For each component of the gas, the equation of state is

$$P_i = \rho_i R_i T \tag{5-44}$$

Summing over all components of the mixture, the overall equation of state for the gas is obtained

$$P = \rho R T \tag{5-45}$$

where

$$R = \sum_{i=1} c_i R_i \tag{5-46}$$

The particle drag equation is

$$V_{pi} \frac{dV_{pi}}{dx} = \frac{9}{2} \frac{\mu f_{pi} r^*}{m_{pi} r_{pi}^2} (V - V_{pi}) \tag{5-47}$$

and the particle heat transfer equation is

$$V_{pi} \frac{dh_{pi}}{dx} = - \frac{3\mu g_{pi} r^*}{m_{pi} r_{pi}^2} \frac{C_P}{Pr} (T_{pi} - T) \tag{5-48}$$

for each particle group.

Since the expansion through a nozzle can be specified either by the expansion process or by the nozzle geometry, two forms of the above equations are of interest.

If the expansion process is specified and the pressure is known as a function of distance through the nozzle, the above equations become

$$\frac{dc_i}{dx} = \frac{\omega_i r^*}{\rho V} \tag{5-49}$$

$$\frac{d\rho_{pi}}{dx} = \left[\frac{1}{\gamma P} \frac{M^2 - 1}{M^2} \frac{dP}{dx} - D_i\right] \rho_{pi} \tag{5-50}$$

$$\frac{dV}{dx} = - \frac{1}{\rho V} \left[\frac{dP}{dx} + C\right] \tag{5-51}$$

$$\frac{d\rho}{dx} = \left[\frac{1}{\gamma P} \frac{dP}{dx} - A\right] \rho \tag{5-52}$$

$$\frac{dT}{dx} = \left[\frac{\gamma - 1}{\gamma} \frac{1}{P} \frac{dP}{dx} - B\right] T \tag{5-53}$$

while if the nozzle geometry is specified, the above equations become

$$\frac{dc_i}{dx} = \frac{\omega_i r^*}{\rho V} \tag{5-54}$$

$$\frac{d\rho_{pi}}{dx} = -\left[\frac{1}{a}\frac{da}{dx} - F_i\right]\rho_{pi} \tag{5-55}$$

$$\frac{dV}{dx} = \left[\frac{1}{a}\frac{da}{dx} - E\right]\frac{V}{M^2 - 1} - V(E - A) \tag{5-56}$$

$$\frac{d\rho}{dx} = -\left\{\left[\frac{1}{a}\frac{da}{dx} - E\right]\frac{M^2}{M^2 - 1} + A\right\}\rho \tag{5-57}$$

$$\frac{dT}{dx} = -\left\{\left[\frac{1}{a}\frac{da}{dx} - E\right]\frac{(\gamma - 1)M^2}{M^2 - 1} + B\right\}T \tag{5-58}$$

$$P = \rho R T \tag{5-59}$$

where

$$B = \frac{\gamma - 1}{\gamma}\frac{r^*}{PV}\left\{\sum_{i=1}\omega_i h_i - \sum_{i=1}\rho_{pi}\left[\frac{9}{2}\frac{\mu f_{pi}}{m_{pi} r_{pi}^2}\left(V - V_{pi}\right)^2 + \frac{3\mu g_{pi}}{m_{pi} r_{pi}^2}\frac{C_{Pg}}{P_r}\left(T_{pi} - T\right)\right]\right\} \tag{5-60}$$

$$A = \frac{r^*}{PV}\sum_{i=1}\omega_i R_i T - B \tag{5-61}$$

$$C = \sum_{i=1}\rho_{pi}\frac{9}{2}\frac{\mu f_{pi} r^*}{m_{pi} r_{pi}^2}(V - V_{pi}) \tag{5-62}$$

$$E = A + \frac{C}{\rho V^2} \tag{5-63}$$

$$F_i = -\frac{9}{2}\frac{\mu f_{pi} r^*}{m_{pi} r_{pi}^2}\frac{(V - V_{pi})}{V_{pi}} \tag{5-64}$$

$$D_i = E - F_i \tag{5-65}$$

$$M = \frac{V}{\sqrt{\gamma RT}} \tag{5-66}$$

$$\gamma = \frac{C_p}{C_p - R} \tag{5-67}$$

and

$$C_p = \sum_{i=1} c_i C_{pi} \tag{5-68}$$

The first set of equations is completely specified at the sonic point while the second set of equations is singular. Thus, if the expansion through the nozzle is specified by the pressure distribution, the equations governing the expansion can be directly integrated through the sonic point without mathematical difficulty. The expansion from the chamber through the sonic point is specified by the pressure distribution in the present program in order to eliminate numerical difficulties at the sonic point. In the expansion section downstream of the sonic point, however, the area variation is specified and the second set of equations is integrated through the supersonic expansion section.

In specifying the nozzle pressure distribution from the chamber through the sonic point, rather than the known area distribution, a question naturally arises regarding how accurately the calculation represents the flow through a specified nozzle geometry. Experience has shown that by iterating on the inlet pressure distribution, the difference in the expansion and predicted performance caused by utilizing the inlet pressure distribution to specify the inlet expansion process rather than the inlet nozzle geometry is negligible.

The net species production rate ω_i for each species considered in the program is governed by the same equations as those for one-dimensional reacting gas case (see pages 5-5 to 5-7).

The computer program subroutines, which indicate the computation of performance parameters such as specific impulse, characteristic velocity, etc., are given in detail in Reference 12.

5.3 AXISYMMETRIC REACTING GAS PROGRAM[14]

This program calculates the inviscid axisymmetric nonequilibrium nozzle expansion of gaseous propellant exhaust mixtures containing the six elements carbon, hydrogen, oxygen, nitrogen, fluorine and chlorine. The computer program considers the 19 significant gaseous species (listed in Table 2-2) present in the exhaust mixtures of propellants (listed in Table 2-1) containing these elements and the 48 chemical reactions (13 dissociation-recombination reactions and 35 binary exchange reactions as listed in Table 2-4) which can occur between the exhaust products. On option, this program calculates either the expansion of a uniform mixture (the ideal engine case) or of a two-zone mixture (the film-cooled engine case).

The initial data line required to start the characteristic calculations is obtained from the transonic analyses described in Section 4. The characteristic equations governing the fluid dynamic variables are integrated using a second-order (modified Euler) explicit integration method while the chemical relaxation equations are integrated using a first-order implicit integration method to insure numerical stability in near equilibrium flows. Typical machine run time for this computer program is 10 minutes for a uniform expansion case and about 12 to 15 minutes for a two-zone case. The program analysis is given below.

The conservation equations governing the axisymmetric inviscid flow of reacting gas mixtures have been given by Hirshfelder, Curtiss and Bird,[8] Penner[9] and others. The basic assumptions made in the derivation of these equations are:

- There are no mass or energy losses from the system
- The gas is inviscid
- Each component of the gas is a perfect gas
- The internal degrees of freedom (translational, rotational, and vibrational) of each component of the gas are in equilibrium.

The conservation equations are presented here in the form used in the present analysis.

For each component of the gas, the continuity equation is

$$\left(\rho_i u\right)_x + \frac{1}{r}\left(r\rho_i v\right)_r = \omega_i r^* \tag{5-69}$$

where the coordinates (r, x) have been normalized with the throat radius. Summing over all components of the mixture, the overall continuity equation is obtained

$$(\rho u)_x + \frac{1}{r}(r\rho v)_r = 0 \tag{5-70}$$

By use of the above equation, Equation (5-69) can be rewritten as

$$u\left(c_i\right)_x + v\left(c_i\right)_r = \frac{\omega_i r^*}{\rho} \tag{5-71}$$

The momentum equations are

$$\rho(uu_x + vu_r) + P_x = 0 \tag{5-72}$$

$$\rho(uv_x + vv_r) + P_r = 0 \tag{5-73}$$

The energy equation is

$$h + \frac{1}{2}(u^2 + v^2) = H_c \tag{5-74}$$

where

$$h = \sum_{i=1} c_i h_i \tag{5-75}$$

and

$$h_i = \int_o^T C_{pi}\, dT + h_{io} \tag{5-76}$$

For each component of the gas, the equation of state is

$$P_i = \rho_i R_i T \tag{5-77}$$

Summing over all components of the mixture, the overall equation of state is obtained

$$P = \rho R T \tag{5-78}$$

where

$$R = \sum_{i=1} c_i R_i \tag{5-79}$$

By standard methods,[15] the characteristic relationships for the conservation equations can be shown to be

$$\frac{dr}{dx} = \tan \theta \tag{5-80}$$

$$d \frac{V^2}{2} + \frac{dP}{\rho} = 0 \tag{5-81}$$

$$\frac{dP}{\gamma P} - \frac{d\rho}{\rho} = \frac{A}{\cos \theta} dx \tag{5-82}$$

$$\frac{\gamma - 1}{\gamma} \frac{dP}{P} - \frac{dT}{T} = \frac{B\, dx}{\cos \theta} \tag{5-83}$$

$$dc_i = \frac{\omega_i r^*}{\rho V \cos \theta} dx \tag{5-84}$$

along streamlines,

$$\frac{dx}{dr} = \cot (\theta + \alpha) \tag{5-85}$$

$$\frac{dP}{P} = G \left[\left(A - \frac{\sin \theta}{r} \right) F\, dr - d\theta \right] \tag{5-86}$$

along left running characteristics, and

$$\frac{dr}{dx} = \tan(\theta - \alpha) \tag{5-87}$$

$$\frac{dP}{P} = -G\left[\left(A - \frac{\sin\theta}{r}\right)H\,dx - d\theta\right] \tag{5-88}$$

along right running characteristics, where

$$A = \frac{r^*}{PV}\left(\sum_{i=1} \omega_i R_i T - \frac{\gamma - 1}{\gamma}\sum_{i=1} \omega_i h_i\right) \tag{5-89}$$

$$B = \frac{r^*}{PV}\,\frac{\gamma - 1}{\gamma}\sum_{i=1} \omega_i h_i \tag{5-90}$$

$$V = \left(u^2 + v^2\right)^{1/2} \tag{5-91}$$

$$\theta = \tan^{-1}\left(\frac{v}{u}\right) \tag{5-92}$$

$$\alpha = \sin^{-1}\left(\frac{1}{M}\right) \tag{5-93}$$

$$M = \frac{V}{(\gamma R T)^{1/2}} \tag{5-94}$$

$$\gamma = \frac{C_p}{C_p - R} \tag{5-95}$$

$$C_p = \sum_{i=1} c_i C_{pi} \tag{5-96}$$

$$F = \cos\theta - \sin\theta\cot(\theta + \alpha) \tag{5-97}$$

$$G = \frac{\gamma}{\sin\alpha\cos\alpha} \tag{5-98}$$

$$H = \cos\theta\tan(\theta - \alpha) - \sin\theta \tag{5-99}$$

The above form of the characteristic relationships remains determinant when the stream line is horizontal, when the left running characteristic is vertical, or when the right running characteristic is horizontal. Rarely (if ever) will the inverse of the three situations occur in nozzle flow field calculations.

The net species production rate ω_i for each species considered in the program is governed by the same equations as those for the one-dimensional reacting gas case (see pages 5-5 to 5-7).

To solve the preceding equations, one can, in principle, use perturbation methods to obtain asympotic expansions for the subsonic and transonic flow fields as has been done for nonreacting gas flows.[4] Such solutions are extremely complex for nonequilibrium flows however, and it is doubtful if more than one term of the expansion can be determined.

An alternate method of constructing nonequilibrium initial lines for characteristic calculations is to determine the effect of nozzle curvature on the gas flow field using an average expansion coefficient to approximate the nonequilibrium expansion process through the throat region and to then calculate the effect of the altered gas flow field on the relaxation processes. This method (which is the equivalent to the first step of a relaxation process) has been successfully used by Kliegel and Nickerson[16] in two-phase flow nozzle studies to predict nozzle inlet angle and throat curvature effects. It was chosen for use in this program because of its relative simplicity and proven accuracy. The calculations performed in constructing the nonequilibrium initial lines used as starting lines for the characteristic calculations are summarized below.

For uniform expansions, a one-dimensional calculation is performed from the chamber to the throat for the propellant system and nozzle geometry of interest using the One-Dimensional Reacting Gas Program[7] and tables of flow properties (ρ, V, T) and species concentrations (c_i) are constructed as a function of pressure starting at the throat. An average expansion coefficient in the throat region is calculated from

$$\overline{\gamma} = \frac{\ln (P_{20}/P_1)}{\ln (\rho_{20}/\rho_1)} \qquad (5\text{-}100)$$

where the subscripts 1 and 20 refer to the first and last table entries. An axisymmetric uniform expansion transonic flow field is constructed for the nozzle of interest using this average expansion coefficient and the second order analysis of Kliegel and Quan (Reference 4 and Section 4). The pressure, location and flow angle variation along the constant pressure line originating at the throat wall are determined. The remaining flow properties (ρ, V, T) and species concentrations (c_i) along the constant pressure line are determined by interpolation on pressure from the tables previously constructed with the One-Dimensional Reacting Gas Program.

For two-zone expansions, a one-dimensional calculation is performed from the chamber to the throat for the propellant system and nozzle geometry of interest for the inner zone using the One-Dimensional Reacting Gas Program and tables of flow properties (ρ, V, T) and species concentrations (c_i) are constructed for the inner zone as a function of pressure starting at the throat. An average expansion coefficient in the throat region is calculated for the inner zone from

$$\overline{\gamma} = \frac{\ln (P_{20}/P_1)}{\ln (\rho_{20}/\rho_1)} \tag{5-101}$$

where the subscripts 1 and 20 refer to the first and last inner zone table entries. A one-dimensional calculation is performed from the chamber to the throat for the propellant system and nozzle geometry of interest for the outer zone using the One-Dimensional Reacting Gas Nonequilibrium Performance Program. The stagnation pressure of the outer zone is adjusted by the ratio of the outer and inner zone throat pressures and another one-dimensional calculation is performed from the chamber to the throat for the outer zone and tables of flow properties (ρ, V, T) and species concentrations (c_i) are constructed for the outer zone as a function of pressure starting at the throat. An average expansion coefficient in the throat region is calculated for the outer zone from

$$\overline{\gamma} = \frac{\ln (P_{20}/P_1)}{\ln (\rho_{20}/\rho_1)} \tag{5-102}$$

where the subscripts 1 and 20 refer to the first and last outer zone table entries. An axisymmetric two-zone transonic flow field is constructed for the nozzle of interest using these average expansion coefficients for each zone and the second-order analysis of Kliegel and Quan. The pressure, location and flow angle variation along the constant pressure line originating at the throat wall are determined. The remaining flow properties (ρ, V, T) and species concentrations (c_i) along the constant pressure line in each zone are determined by interpolation on pressure from the tables previously constructed for each zone with the One-Dimensional Reacting Gas Program.

The above method of constructing initial lines for nonequilibrium characteristic calculations accounts for the dominant curvature effects through second order and ignores the curvature effects which would cause a constant pressure line, chosen as the initial starting line, not to be a constant property line. By comparing the above method of constructing nonequilibrium initial lines with a rigorous expansion method, it can be shown that the two methods are equivalent through first order (the effect of curvature causing departure from constant property lines being of order $R^{-3/2}$). The great advantage of the current method is its simplicity in accounting for the dominant curvature effects and the fact that the flow field varies smoothly across the initial line (i.e., there are no sudden energy release changes or flow field adjustments downstream of the initial line caused by incompatibilities between the gas and chemical properties along the initial line). Thus inaccuracies in the initial line construction used in the present program do not cause physically unreal expansions, compressions or shocks in the characteristic calculations. This later advantage is extremely important since experience has shown that even small incompatibilities between the gas and chemical properties along the initial line can cause very large, physically unreal, flow field adjustments downstream of the initial line.

After constructing the initial data line, the reacting gas characteristic relationships [Equations (5-80) through (5-88)] are integrated. Characteristic equations are generally integrated using second-order explicit methods. It has been shown in Section 3, however, that implicit integration methods are superior to explicit methods for integrating chemical relaxation equations. Thus, in the present program, the fluid

dynamic equations are integrated using an explicit modified Euler method while the chemical relaxation equations are integrated using a first-order implicit integration method.

In numerically calculating flow fields using the method of characteristics, only two (previously calculated) known points are directly usable in calculating a forward point. In perfect gas flows, only two known points are required to calculate a forward point and the calculation is straightforward and unambiguous. In nonequilibrium flows, however, more than two known points are required to calculate a forward point so that a choice must be made as to which points in the flow field will be used directly and which will be interpolated. Since even small interpolation errors in species concentrations are known to cause serious stability and accuracy problems in the numerical integration of the chemical relaxation equations, the back streamline point and one characteristic point were chosen as the known points. This choice avoids interpolation for the species concentrations in that only fluid dynamic properties (velocity, pressure, etc.) and the total entropy production term due to all nonequilibrium effects need be interpolated at one of the back characteristic points. Since these quantities are all slowly varying across the characteristics mesh, they can be interpolated quite accurately. Experience has shown that this choice of numerical integration methods and known data points is optimum for reacting gas characteristics calculations. A complete derivation of the numerical integration methods used in the program are given below.

Consider the flow field shown in Figure 5-1.

The fluid dynamic equations are integrated as follows. Between points 3 and 4 the streamline characteristics relationships are integrated as

$$r_3 = r_4 + \tan\left[\frac{1}{2}(\theta_4 + \theta_3)\right](x_3 - x_4) \tag{5-103}$$

$$V_3 = \left\{V_4^2 + \frac{2N}{N-1}\frac{P_4}{\rho_4}\left[1 - \left(\frac{P_3}{P_4}\right)^{\frac{N-1}{N}}\right]\right\}^{1/2} \tag{5-104}$$

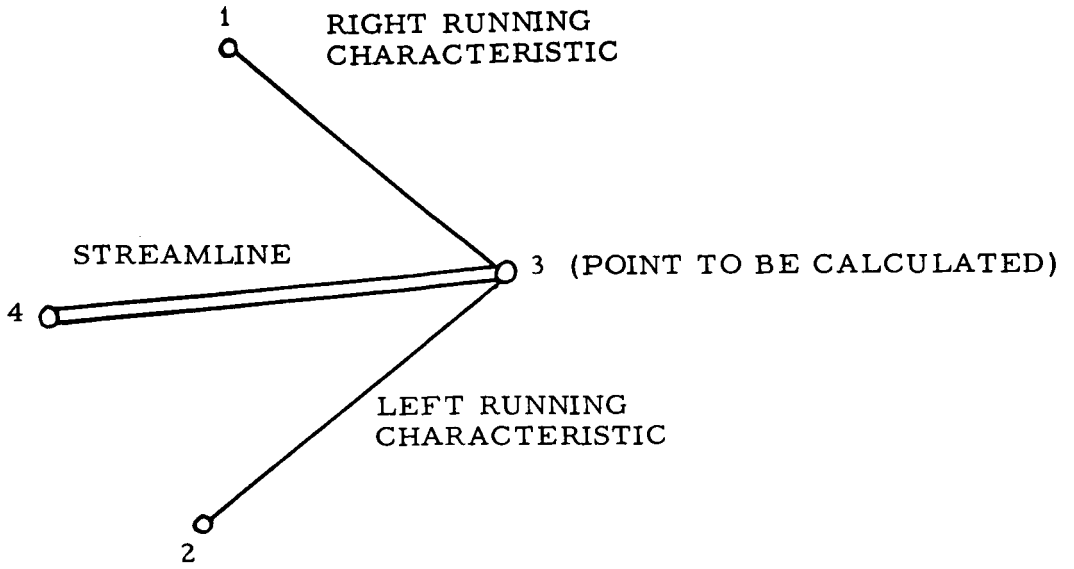

Figure 5-1. Flow Field Calculation

$$\rho_3 = \rho_4 \left(\frac{P_4}{P_4}\right)^{\frac{1}{2}\left(\frac{1}{\gamma_4}+\frac{1}{\gamma_3}\right)} \exp\left[-\frac{1}{2}\left(\frac{A_4}{\cos\theta_4}+\frac{A_3}{\cos\theta_3}\right)(x_3 - x_4)\right] \tag{5-105}$$

$$T_3 = T_4 \left(\frac{P_3}{P_4}\right)^{\frac{1}{2}\left(\frac{\gamma_4-1}{\gamma_4}+\frac{\gamma_3-1}{\gamma_3}\right)} \exp\left[-\frac{1}{2}\left(\frac{B_4}{\cos\theta_4}+\frac{B_3}{\cos\theta_3}\right)(x_3 - x_4)\right] \tag{5-106}$$

where

$$N = \frac{\ln\left(\frac{P_3}{P_4}\right)}{\ln\left(\frac{\rho_3}{\rho_4}\right)} \tag{5-107}$$

The integration formula (5-103) relating the coordinates of points 3 and 4 was chosen because it is exact if the streamline is a circular arc between points 3 and 4. This is an excellent approximation over one

one mesh step. In integrating the momentum equation to obtain Equation (5-104) it was assumed that P varies as ρ^N along the streamline. In integrating the energy equation and the perfect gas relationship to obtain Equations (5-105) and (5-106), the coefficients [γ^{-1}, A/cos θ, $(\gamma - 1)/\gamma$, and B/cos θ] appearing in these equations were assumed to be equal to their average value between points 3 and 4. The streamline integration formulas (5-104), (5-105), and (5-106) are exact for nonreacting, constant gamma flows, (note that in this case N equals γ and that A and B are zero). Since much of the supersonic portion of the flow fields is nonreacting (frozen) and approximately a constant gamma flow, these integration formulas are believed to be the best choice for supersonic reacting gas flow field calculations.

Between points 1 and 3 the right running characteristics relationships are integrated as

$$r_3 = r_1 + \tan\left[\frac{1}{2}(\theta_1 + \theta_3 - \alpha_1 - \alpha_3)\right](x_3 - x_1) \qquad (5\text{-}108)$$

$$P_3 = P_1 \exp - \left[\frac{1}{2}(A_1G_1H_1 + A_3G_3H_3)(x_3 - x_1) - \frac{1}{2}\left(\frac{G_1H_1 \sin\theta_1}{r_1} + \frac{G_3H_3 \sin\theta_3}{r_3}\right)(x_3 - x_1) - \frac{1}{2}(G_1 + G_3)(\theta_3 - \theta_1)\right] \qquad (5\text{-}109)$$

The integration formula (5-108) relating the coordinates of points 1 and 3 was chosen because it is exact if the right running characteristic is a circular arc between points 1 and 3. This is an excellent approximation over one mesh step. In integrating the right running characteristic relationship to obtain Equation (5-109) the coefficients (AGH, GH sin θ/r, and G) appearing in Equation (5-88) were assumed to equal their average value between points 1 and 3. This is an excellent approximation over one mesh step. If point 3 is an axis point then r_3 and θ_3 are zero and the indeterminate quantity sin θ_3/r_3 appearing in Equation (5-109) is approximated by

$$\frac{\sin \theta_3}{r_3} = \frac{\tan \theta_1}{r_1 + (x_3 - x_1) \tan \theta_1} \tag{5-110}$$

Equation (5-110) is obtained by extrapolating for the ratio $\sin \theta / r$ on the axis, assuming that the flow near the axis is a source flow.

Between points 2 and 3 the left running characteristics relationships are integrated as

$$x_3 = x_2 + \cot \left[\frac{1}{2}(\theta_2 + \theta_3 + \alpha_2 + \alpha_3)\right](r_3 - r_2) \tag{5-111}$$

$$P_3 = P_2 \exp \left[\frac{1}{2}(A_2 G_2 F_2 + A_3 G_3 F_3)(r_3 - r_2) - \frac{1}{2}\left(\frac{G_2 F_2 \sin \theta_2}{r_2} + \frac{G_3 F_3 \sin \theta_3}{r_3}\right)(r_3 - r_2) - \frac{1}{2}(G_2 + G_3)(\theta_3 - \theta_2)\right] \tag{5-112}$$

The integration formula (5-111) relating the coordinates of points 2 and 3 was chosen because it is exact if the left running characteristic is a circular arc between points 2 and 3. This is an excellent approximation over one mesh step. In integrating the left running characteristic relationship to obtain Equation (5-112), the coefficients (AGE, GF $\sin \theta / r$, and G) appearing in Equation (5-86) were assumed to equal their average value between points 2 and 3. This is an excellent approximation over one mesh step. If point 2 is an axis point, then r_2 and θ_2 are zero and the indeterminate quantity $\sin \theta_2 / r_2$ appearing in Equation (5-112) is that quantity previously calculated for the axis point using Equation (5-110).

Equations (5-109) and (5-112) can be combined to yield

$$\theta_3 = \frac{1}{G_3 + \frac{1}{2}(G_1 + G_2)} \left[\ln\left(\frac{P_2}{P_1}\right) + \frac{1}{2}(G_1 + G_3)\theta_1 + \frac{1}{2}(G_2 + G_3)\theta_2 \right.$$

$$+ \frac{1}{2}(A_2G_2F_2 + A_3G_3F_3)(r_3 - r_2)$$

$$- \frac{1}{2}\left(\frac{G_2F_2 \sin\theta_2}{r_2} + \frac{G_3F_3 \sin\theta_3}{r_3}\right)(r_3 - r_2)$$

$$+ \frac{1}{2}(A_1G_1H_1 + A_3G_3H_3)(x_3 - x_1)$$

$$\left. - \frac{1}{2}\left(\frac{G_1H_1 \sin\theta_1}{r_1} + \frac{G_3H_3 \sin\theta_3}{r_3}\right)(x_3 - x_1) \right] \quad (5\text{-}113)$$

In the calculations for the various points in the flow field, Equation (5-113) is solved for θ_3 and either Equation (5-109) or (5-112) is solved for P_3, depending on whether or not point 1 or 2 is the known data point. Experience has shown that the above choice of integration equations is optimum for reacting gas characteristic calculations.

It can be verified that use of these integration equations results in an error or order h^3 where h is the integration increment (mesh size). Since these integration equations involve the flow properties at the unknown point (point 3), they must be solved by iteration. The modified Euler iteration method is used to solve these equations, and various point calculations are described in detail in Section 5.3 of Reference 14.

In integrating the chemical relaxation equations, it is advantageous to employ an implicit method as discussed in Section 3. A first-order implicit integration method was chosen for use in the present program to integrate the chemical relaxation equations. The derivation of the integration formula is described below.

The chemical relaxation equations are a coupled set of first order simultaneous differential equations of the form

$$\frac{dc_i}{dx} = f_i(c_1, c_2, \cdots, c_N, y_1, y_2, y_3, y_4) \quad i = 1, 2, \cdots, N \tag{5-114}$$

along the streamline where y_1, y_2, y_3, and y_4 refer to the fluid dynamic variables V, ρ, T, and θ, respectively. Assuming that the equations are not singular and that a solution exists which may be developed as a Taylor series about the forward point, one obtains

$$k_i = \left.\frac{dc_i}{dx}\right|_{x_{n+h}} h \tag{5-115}$$

where k_i is the increment in c_i and h is sufficiently small. The first coefficient of the Taylor series may be calculated as

$$\frac{dc_i}{dx} = f_i(c_1, c_2, \cdots, c_N, y_1, y_2, y_3, y_4) \tag{5-116}$$

Expanding them as a Taylor series about the point x_n, it is found that

$$\left.\frac{dc_i}{dx}\right|_{x_{n+h}} = f_{i,n} + \sum_{j=1}^{N} \beta_{i,j,n} k_j + \sum_{j=1}^{4} \phi_{i,j,n} \Delta y_j + 0\left[h^2\right] \tag{5-117}$$

where

$$\beta_{i,j} = \frac{\partial f_i}{\partial c_j} \tag{5-118}$$

$$\phi_{i,j} = \frac{\partial f_i}{\partial y_j} \tag{5-119}$$

and the subscript n refers to the functions f_i, $\beta_{i,j}$ and $\phi_{i,j}$ evaluated at the point x_n.

Substituting the above derivative into Equation (5-115) and neglecting the second-order error and derivative terms yields the integration formula for the increment k_i

$$k_i = \left[f_{i,n} + \sum_{j=1}^{N} \beta_{i,j,n} \, k_j + \sum_{j=1}^{4} \phi_{i,j,n} \, \Delta y_j \right] h \qquad (5\text{-}120)$$

The computer program subroutines which include the computation of performance parameters, i.e., specific impulse, characteristic velocity, etc., are given in detail in Reference 14.

5.4 AXISYMMETRIC TWO-PHASE PERFECT GAS PROGRAM[17]

This program calculates the inviscid axisymmetric nozzle expansion of propellant systems having both gaseous and condensed exhaust products. The program considers the velocity and thermal lags (for up to ten particle groups) between the gaseous and condensed combustion products (when they are present in the chamber). It does not consider mass transfer (only momentum and energy transfer) between gaseous and condensed combustion products. It also does not consider nonequilibrium effects of finite rate chemical reactions between gaseous and combustion products. This program utilizes standard explicit integration methods. Typical computer run time is 5 minutes per case. This program is an updated FORTRAN IV version of an earlier program. The original analysis has been published previously,[16] and is summarized below.

The conservation equations governing the inviscid axisymmetric flow of two-phase mixtures have been previously derived utilizing the following assumptions:[13]

- There are no mass or energy losses from the system.
- The gas is inviscid except for its interactions with the condensed particles.
- The gas is a perfect gas of constant specific heat ratio.
- The volume occupied by the condensed particles is negligible.
- The thermal (Brownian) motion of the condensed particles is negligible.
- The condensed particles do not interact.
- The condensed particle size distribution may be approximated by groups of different size spheres.

- The internal temperature of the condensed particles is uniform.
- Energy exchange between the gas and the condensed particles occurs only by convection.
- The only forces on the condensed particles are viscous drag forces.
- There is no mass transfer from the gas to the condensed phase during the nozzle expansion.

The resulting conservation equations are:

Gas Continuity Equation

$$(\rho u)_x + \frac{1}{r}(r\rho v)_r = 0 \tag{5-121}$$

Particle Continuity Equation

$$(\rho_{pi} u_{pi})_x + \frac{1}{r}(r\rho_{pi} v_{pi})_r = 0 \tag{5-122}$$

Momentum Equations

$$\rho(uv_x + vu_r) + \sum_{i=1} \frac{9}{2} \frac{\mu \rho_{pi} f_{pi} r^*}{m_p r_{pi}^2} (u - u_{pi}) + P_x = 0 \tag{5-123}$$

$$\rho(uv_x + vv_r) + \sum_{i=1} \frac{9}{2} \frac{\mu \rho_{pi} f_{pi} r^*}{m_p r_{pi}^2} (v - v_{pi}) + P_r = 0 \tag{5-124}$$

Energy Equation

$$uP_x + vP_r - \gamma RT(u\rho_x + v\rho_r) - \sum_{i=1} \frac{9}{2} \frac{\mu_g \rho_{pi} f_{pi} r^*}{m_p r_{pi}^2} (\gamma-1) \left[(u-u_{pi})^2 \right.$$

$$\left. + (v-v_{pi})^2 + \frac{2}{3} \frac{g_{pi}}{f_{pi}} \frac{C_P}{Pr} (T_{pi} - T) \right] = 0 \tag{5-125}$$

Perfect Gas Law

$$P = \rho RT \tag{5-126}$$

Particle Drag Equations

$$u_{pi} (u_{pi})_x + v_{pi} (u_{pi})_r = \frac{9}{2} \frac{\mu f_{pi} r^*}{m_p r_{pi}^2} (u - u_{pi}) \tag{5-127}$$

$$u_{pi} (v_{pi})_x + v_{pi} (v_{pi})_r = \frac{9}{2} \frac{\mu f_{pi} r^*}{m_p r_{pi}^2} (v - v_{pi}) \tag{5-128}$$

Particle Heat Transfer Equation

$$u_{pi} (h_{pi})_x + v_{pi} (h_{pi})_r = -3 \frac{\mu g_{pi} r^*}{m_p r_{pi}^2} \frac{C_P}{Pr} (T_{pi} - T) \tag{5-129}$$

where

$$T_{pi} = T_{pm} + \frac{h_{pi} - h_{p\ell}}{C_{P\ell}} \qquad h_{pi} \geq h_{p\ell} \tag{5-130}$$

$$T_{pi} = T_{pm} \qquad h_{p\ell} > h_{pi} \geq h_{ps} \tag{5-131}$$

$$T_{pi} = \frac{h_{pi}}{C_{Ps}} \qquad h_{ps} > h_{pi} \tag{5-132}$$

By standard methods,[14] the characteristic relationships for the above conservation equations can be shown to be

$$\frac{dr}{dx} = \frac{v}{u} \tag{5-133}$$

$$\rho\,(u\,du + v\,dv) + dP = -\sum_{i=1} \frac{9}{2}\,\frac{\mu\,\rho_{pi} f_{pi} r^*}{m_p r_{pi}^2}\left[(u - u_{pi})\,dx + (v - v_{pi})\,dr\right] \quad (5\text{-}134)$$

$$\frac{dP}{P} - \gamma\,\frac{d\rho}{\rho} = -\sum \frac{9}{2}\,\frac{\mu\,\rho_{pi} f_{pi} r^*}{m_p r_{pi}^2}\,\frac{(\gamma-1)}{P\,u}\left[(u - u_{pi})^2 + (v - v_{pi})^2\right.$$

$$\left. + \frac{2}{3}\,\frac{g_{pi}}{f_{pi}}\,\frac{C_P}{Pr}\,(T_{pi} - T)\right] dx \quad (5\text{-}135)$$

along gas streamlines,

$$\frac{dr}{dx} = \frac{u\,v \pm \gamma\,RT\,\sqrt{M^2 - 1}}{u^2 - \gamma\,RT} \quad (5\text{-}136)$$

$$(u\,\frac{dr}{dx} - v)\left\{\sum_{i=1} \frac{9}{2}\,\frac{\mu\,\rho_{pi}\,f_{pi}\,r^*}{m_p r_{pi}^2}\,(\gamma-1)\left[(u - u_{pi})^2 + (v - v_{pi})^2\right.\right.$$

$$\left.\left. + \frac{2}{3}\,\frac{g_{pi}}{f_{pi}}\,\frac{C_P}{Pr}\,(T_{pi} - T)\right] dx - u\,dP\right\}$$

$$+ \gamma\,RT\left\{\sum_{i=1} \frac{9}{2}\,\frac{\mu\,\rho_{pi}\,f_{pi}\,r^*}{m_p r_{pi}^2}\left[(u - u_{pi})\,dr - (v - v_{pi})\,dx\right]\right.$$

$$\left. + \rho\left[v\,du - u\,dv - \frac{v}{r}\,(u\,dr - v\,dx)\right] + dP\,\frac{dr}{dx}\right\} = 0 \quad (5\text{-}137)$$

along gas Mach lines,

$$\left.\frac{dr}{dz}\right|_i = \frac{v_{pi}}{u_{pi}} \tag{5-138}$$

$$u_{pi}\, du_{pi} = \frac{9}{2} \frac{\mu f_{pi} r^*}{m_p r_{pi}^2} (u - u_{pi})\, dx \tag{5-139}$$

$$v_{pi}\, dv_{pi} = \frac{9}{2} \frac{\mu f_{pi} r^*}{m_p r_{pi}^2} (v - v_{pi})\, dr \tag{5-140}$$

$$u_{pi}\, dh_{pi} = -3 \frac{\mu g_{pi} r^*}{m_p r_{pi}^2} \frac{C_P}{Pr} (T_{pi} - T)\, dx \tag{5-141}$$

$$d\psi_{pi} = 0 \tag{5-142}$$

along particle streamlines where the particle stream function ψ_{pi} is defined by

$$(\psi_{pi})_r = r\rho_{pi} u_{pi}\,, \quad (\psi_{pi})_x = -r\rho_{pi} v_{pi} \tag{5-143}$$

It is seen that all the characteristics of the equations governing the flow of a gas-particle system are real if the flow is supersonic ($M > 1$). Using Equations (5-133) to (5-143), the supersonic flow of a gas-particle mixture may be computed using the method of characteristics.

It is interesting to note that one of the characteristic directions of Equations (5-133) to (5-143) is identical with the gas Mach lines and is independent of the presence of the particles. This result is similar to the situation found in reacting gas mixtures[18] in which one of the

characteristic directions is also identical with the gas Mach lines and is independent of chemical reactions occurring in the flow.

To solve the equations governing the transonic flow of a gas-particle mixture is an extremely formidable task. For perfect gas flows, approximate transonic solutions can be obtained by taking perturbations about the sonic velocity[6]. This method is applicable for perfect gas flows because the throat conditions are essentially determined by the nozzle geometry in the immediate neighborhood of the throat and are quite insensitive to the nozzle inlet geometry. This is not true for gas-particle flows, because the throat conditions are determined by the nozzle inlet geometry[19]. Thus to obtain initial conditions to start a characteristic calculation for a gas-particle system, the equations for the complete subsonic and transonic flow field in the nozzle inlet and throat regions must be solved.

It is evident that only approximate solutions to the equations governing the transonic flow of a gas-particle system can be obtained. In order to reduce the complexity of the calculations, the nozzle inlet and throat geometry considered in this study consisted of a conical inlet section joined smoothly to a constant radius of curvature throat section. It is believed that this simplified geometry adequately represents the inlet and throat geometry for nozzle configurations of interest.

The following method was used to obtain approximate initial conditions for the characteristic calculations. In the conical inlet section, the flow was assumed to be a one-dimensional sink flow. The equations governing the one-dimensional flow of a gas-particle system were solved to obtain the flow properties on the sink line. The gas properties in the throat region were approximated by the perfect gas relationships similar to those developed for the nonequilibrium programs. The particle trajectories were calculated through the throat region to determine the particle properties along the initial line. An average expansion coefficient was used which approximated the gas-particle expansion, including the effects of gas-particle nonequilibrium[19].

The initial conditions thus determined were self-consistent as was evidenced by the fact that the characteristic calculations proceeded smoothly away from the initial line. Comparison of the nozzle weight flows obtained by the above method with those obtained by one-dimensional

calculations shows that the two-dimensional weight flows are slightly less than the one-dimensional weight flows. This agrees with the results obtained[20] for perfect gases. In addition, the above method of obtaining the gas-particle flow properties along the initial line is exact for the case of gas-particle equilibrium. It is concluded that the gas-particle flow properties determined along the initial line by the above method are an adequate representation of the true flow properties for nozzle calculations.

The gas-particle characteristic relationships [Equations (5-133) through (5-143)] are integrated using standard second-order explicit methods. In numerically calculating flow fields using the method of characteristics, only two (previously calculated) known points are directly usable in calculating a forward point. In perfect gas flows, only two known points are required to calculate a forward point and the calculation is straightforward and unambiguous. In nonequilibrium flows, however, more than two known points are required to calculate a forward point so that a choice must be made as to which points in the flow field will be used directly and which will be interpolated. In the present program, both characteristic points are chosen as the known points and the required gas and particle properties at the back streamline points were determined by interpolation as shown in Figure 5-2. Experience has shown that the above integration method yields accurate results.

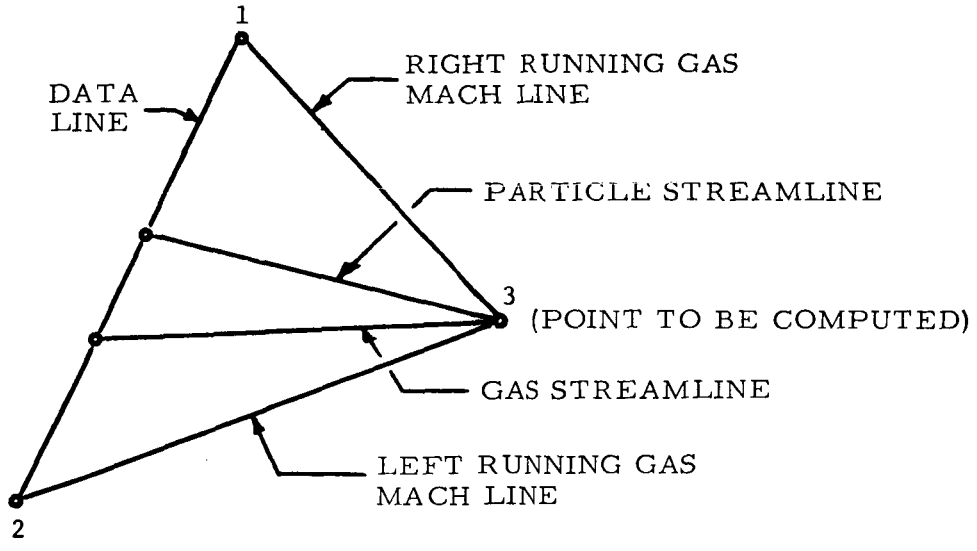

Figure 5-2. Two-Phase Mesh Calculation

The computer program subroutines which include the computation of performance parameters, i.e., specific impulse, characteristic velocity, etc., are given in detail in Reference 17.

5.5 AXISYMMETRIC TWO-PHASE REACTING GAS ANALYSIS[21]

The study described in this section was performed to initiate the development of an additional computer program. The program consists of three major parts: the one-dimensional two-phase reacting gas part which is the One-dimensional Two-Phase Reacting Gas Program[12], the axisymmetric two-phase transonic part, and the axisymmetric two-phase characteristics part. These parts have been programmed, but have not been combined into a functioning program since the large size of the complete program necessitates an excessive number of overlays during program execution causing extremely long computer time per case.

A program based on the present effort may be put into operational form when larger computers become available. Upon completion, this program will calculate the inviscid axisymmetric nonequilibrium nozzle expansion of propellant exhaust mixtures containing the six elements: carbon, hydrogen, oxygen, nitrogen, fluorine, and chlorine and one metal element, either aluminum, beryllium, boron or lithuim. The computer program will consider 79 significant gaseous species and eight significant condensed species (listed in Table 2-2) present in the exhaust mixtures of propellants (listed in Table 2-1) containing these elements and the 763 gas phase chemical reactions (listed in Tables 2-4 through 2-9) which can occur between the exhaust products. The program will also consider the velocity and thermal lags (for five particle groups) between the gaseous and condensed combustion products (when they are present in the chamber). The program will not consider mass transfer (only momentum and energy transfer) between gaseous and condensed combustion products. The program will calculate only the expansion of uniform mixtures (the ideal engine case).

In the program, the initial data line required to start the characteristic calculations is obtained from an appropriate transonic analysis which utilizes the results of the one-dimensional two-phase reacting gas program. The characteristic equations governing the fluid dynamic variables

are integrated using a second order (modified Euler) explicit integration method while the chemical and particle relaxation equations are integrated using a first order implicit integration method to insure numerical stability in near equilibrium flows. The program analysis is given below.

The conservation equations governing the inviscid axisymmetric flow of a two-phase reacting gas mixture can be simply derived utilizing the following assumptions:

- There are no mass or energy losses from the system.
- The gas is inviscid except for its interactions with the condensed particles.
- Each component of the gas is a perfect gas.
- The internal degrees of freedom (rotational and vibrational) of each component of the gas are in equilibrium.
- The volume occupied by the condensed particles is negligible.
- The thermal (Brownian) motion of the condensed particles is negligible.
- The condensed particles do not interact.
- The condensed particle size distribution may be approximated by groups of different size spheres.
- The internal temperature of the condensed particles is uniform.
- Energy exchange between the gas and the condensed particles occurs only in convection.
- The only forces on the condensed particles are viscous drag forces.
- There is no mass transfer from the gas to the condensed phase during the nozzle expansion.

These assumptions have been previously used in all studies of reacting gas[8] and gas-particle[13] nozzle flows.

The conservation equations are derived here in the form used in the present analysis.

For each component of the gas the continuity equation is

$$(\rho_i u)_x + \frac{1}{r}(r\rho_i v)_r = \omega_i r^* \tag{5-144}$$

where the axial coordinates (r, x) have been normalized with the throat radius. Summing over all components of the mixture, the overall continuity equation for the gas is obtained

$$(\rho u)_x + \frac{1}{r}(r\rho v)_r = 0 \tag{5-145}$$

By use of the above equation, Equation (5-144 can be rewritten as

$$u(c_i)_x + v(c_i)_r = \frac{\omega_i r^*}{\rho} \qquad 5\text{-}146$$

For each particle size group the continuity equation is

$$(\rho_{pi}\, u_{pi})_x + \frac{1}{r}(r\rho_{pi}\, v_{pi})_r = 0 \tag{5-147}$$

since there is no mass transfer from the gas to the condensed phase.

The overall momentum equations for the mixture are

$$\rho(uu_x + vu_r) + \sum_{i=1} \rho_{pi}\left[u_{pi}(u_{pi})_x + v_{pi}(u_{pi})_r\right] + P_x = 0 \tag{5-148}$$

$$\rho(uv_x + vv_r) + \sum_{i=1} \rho_{pi}\left[u_{pi}(v_{pi})_x + v_{pi}(v_{pi})_r\right] + P_r = 0 \tag{5-149}$$

The overall energy equation for the mixture is

$$\rho\left[uh_x + vh_r + u(uu_x + vu_r) + v(uv_x + vv_r)\right]$$
$$+ \sum_{i=1} \rho_{pi}\Big\{ u_{pi}(h_{pi})_x + v_{pi}(h_{pi})_r + u_{pi}\left[u_{pi}(u_{pi})_x + v_{pi}(u_{pi})_r\right]$$
$$+ v_{pi}\left[u_{pi}(v_{pi})_x + v_{pi}(v_{pi})_r\right]\Big\} = 0 \qquad (5\text{-}150)$$

where for the gas phase

$$h = \sum_{i=0} c_i h_i \qquad (5\text{-}151)$$

and

$$h_i = \int_o^T C_{pi} dT + h_{io} \qquad (5\text{-}152)$$

while for each particle group

$$h_{pi} = \int_o^{T_{pi}} C_{ppi} dT + h_{io} \quad , \quad T_{pi} < T_{pmi} \qquad (5\text{-}153)$$

and

$$h_{pi} = \int_o^{T_{pi}} C_{ppi} dT + h_{io} + \Delta H_{pi}, \quad T_{pi} > T_{pmi} \qquad (5\text{-}154)$$

For each component of the gas, the equation of state is

$$P_i = \rho_i R_i T \qquad (5\text{-}155)$$

Summing over all components of the mixture, the overall equation of state for the gas is obtained

$$P = \rho R T \qquad (5\text{-}156)$$

where

$$R = \sum_{i=1} c_i R_i \qquad (5\text{-}157)$$

The particle drag equations are

$$u_{pi}(u_{pi})_x + v_{pi}(u_{pi})_r = \frac{9}{2}\frac{\mu f_{pi} r^*}{m_{pi} r_{pi}^2}(u - u_{pi}) \tag{5-158}$$

$$u_{pi}(v_{pi})_x + v_{pi}(v_{pi})_r = \frac{9}{2}\frac{\mu f_{pi} r^*}{m_{pi} r_{pi}^2}(v - v_{pi}) \tag{5-159}$$

and the particle heat transfer equation is

$$u_{pi}(h_{pi})_x + v_{pi}(h_{pi})_r = -\frac{3\,\mu g_{pi} r^*}{m_{pi} r_{pi}^2}\frac{C_p}{Pr}(T_{pi} - T) \tag{5-160}$$

By standard methods, [15] the characteristic relationships for the conservation equations can be shown to be

$$\frac{dr}{dx} = \tan\theta \tag{5-161}$$

$$d\frac{V^2}{2} + \frac{dP}{\rho} = \frac{C}{\cos\theta}\,dx \tag{5-162}$$

$$\frac{dP}{\gamma P} - \frac{d\rho}{\rho} = \frac{A}{\cos\theta}\,dx \tag{5-163}$$

$$\frac{\gamma-1}{\gamma}\frac{dP}{P} - \frac{dT}{T} = \frac{B}{\cos\theta}\,dx \tag{5-164}$$

$$dc_i = \frac{\omega_i r^*}{\rho V\cos\theta}\,dx \tag{5-165}$$

along streamlines,

$$\frac{dx}{dr} = \cot(\theta + \alpha) \tag{5-166}$$

$$\frac{dP}{P} = G\left[\left(D - \frac{\sin\theta}{r}\right)F\,dr - d\theta\right] \tag{5-167}$$

along left running characteristics,

$$\frac{dr}{dx} = \tan(\theta - \alpha) \tag{5-168}$$

$$\frac{dP}{P} = -G\left[\left(E - \frac{\sin\theta}{r}\right) H\, dx - d\theta\right] \tag{5-169}$$

along right running characteristics,

$$\frac{dr_{pi}}{dx_{pi}} = \tan\theta_{pi} \tag{5-170}$$

$$u_{pi}\, du_{pi} = \frac{9}{2}\frac{\mu f_{pi} r^*}{m_{pi} r_{pi}^2}(V\cos\theta - u_{pi})\, dx_{pi} \tag{5-171}$$

$$v_{pi}\, dv_{pi} = \frac{9}{2}\frac{\mu f_{pi} r^*}{m_{pi} r_{pi}^2}(V\sin\theta - v_{pi})\, dr_{pi} \tag{5-172}$$

$$u_{pi}\, dh_{pi} = -\frac{3\mu g_{pi} r^*}{m_{pi} r_{pi}^2}\frac{Cp}{Pr}(T_{pi} - T)\, dx_{pi} \tag{5-173}$$

$$d\psi_{pi} = 0 \tag{5-174}$$

along particle streamlines, where

$$V = (u^2 + v^2)^{1/2} \tag{5-175}$$

$$\theta = \tan^{-1}\left(\frac{v}{u}\right) \tag{5-176}$$

$$\alpha = \sin^{-1}\left(\frac{1}{M}\right) \tag{5-177}$$

$$M = \frac{V}{(\gamma R T)^{1/2}} \tag{5-178}$$

$$\gamma = \frac{Cp}{C_p - R} \tag{5-179}$$

$$C_p = \sum_{i=1} c_i C_{pi} \tag{5-180}$$

$$F = \cos\theta - \sin\theta\cot(\theta+\alpha) \tag{5-181}$$

$$G = \frac{\gamma}{\sin\alpha\cos\alpha} \tag{5-182}$$

$$H = \cos\theta \tan(\theta - \alpha) - \sin\theta \tag{5-183}$$

$$V_{pi} = (u_{pi}^2 + v_{pi}^2)^{1/2} \tag{5-184}$$

$$\theta_{pi} = \tan^{-1}\left(\frac{v_{pi}}{u_{pi}}\right) \tag{5-185}$$

$$K_{pi} = V_{pi}\,(\cos\theta_{pi}\cos\theta + \sin\theta_{pi}\sin\theta) \tag{5-186}$$

$$A = \frac{r^*}{PV}\sum_{i=1}\omega_i R_i T - B \tag{5-187}$$

$$B = \frac{\gamma-1}{\gamma}\frac{r^*}{PV}\left\{\sum_{i=1}\omega_i h_i - \sum_{i=1}\rho_{pi}\left[\frac{9}{2}\frac{\mu f_{pi}}{m_{pi} r_{pi}^2}(V^2 + V_{pi}^2 - 2VK_{pi}) + \frac{3\mu g_{pi}}{m_{pi} r_{pi}^2}\frac{C_p}{Pr}(T_{pi} - T)\right]\right\} \tag{5-188}$$

$$C = -\frac{r^*}{\rho}\sum_{i=1}\rho_{pi}\frac{\mu f_{pi}}{m_{pi} r_{pi}^2}(V - K_{pi}) \tag{5-189}$$

$$D = A + \frac{r^*}{\rho V}\sum_{i=1}\rho_{pi}\frac{9}{2}\frac{\mu f_{pi}}{m_{pi} r_{pi}^2}\left\{1 - \frac{V_{pi}}{VF}\left[\cos\theta_{pi} - \sin\theta_{pi}\cot(\theta+\gamma)\right]\right\} \tag{5-190}$$

$$E = A + \frac{r^*}{\rho V}\sum_{i=1}\rho_{pi}\frac{9}{2}\frac{\mu f_{pi}}{m_{pi} r_{pi}^2}\left\{1 - \frac{V_{pi}}{VH}\left[\cos\theta_{pi}\tan(\theta-\gamma) - \sin\theta_{pi}\right]\right\} \tag{5-191}$$

and where the particle stream function ψ_{pi} is defined by

$$(\psi_{pi})_{r_{pi}} = r_{pi}\rho_{pi}u_{pi}, \quad (\psi_{pi})_{x_{pi}} = r_{pi}\rho_{pi}V_{pi} \tag{5-192}$$

The above form of the characteristic relationship remains determinate when the streamline is horizontal, when the left running characteristic is vertical, or when the right running characteristic is horizontal. Rarely (if ever) will the inverse of the three situations occur in nozzle flow field calculations.

The net species production rate ω_i for each species considered in the program is governed by the same equation as those for the one-dimensional reacting gas case (see pages 5-5 to 5-7).

To solve the preceeding equations, one can, in principle, use perturbation methods to obtain asympotic expansions for the subsonic and transonic flow fields as has been done for nonreacting gas flows.[4] Such solutions are extremely complex for nonequilibrium flows however, and it is doubtful if more than one term of the expansion can be determined.

An alternate method of constructing nonequilibrium initial lines for characteristic calculations is to determine the effect of nozzle curvature on the gas flow field using an average expansion coefficient to approximate the nonequilibrium expansion process through the throat region and to then calculate the effect of the altered gas flow field on the relaxation processes. This method (which is the equivalent to the first step of a relaxation process) has been successfully used by Kliegel and Nickerson[16] in two-phase flow nozzle studies to predict nozzle inlet angle and throat curvature effects. It was chosen for use in this program because of its relative simplicity and proven accuracy. The calculations performed in constructing the nonequilibrium initial lines used as starting lines for the characteristic calculations are summarized below.

For the gas flow field, a one-dimensional calculation is performed from the chamber to the throat for the propellant system and nozzle geometry of interest using the One-Dimensional Two-Phase Reacting Gas Program[12] and tables of flow properties (θ, V, T), species concentrations (c_i) and particle properties (V_{pi}, T_{pi}) are constructed as a function of pressure starting at the throat. An average expansion coefficient in the throat region is calculated from

$$\bar{\gamma} = \frac{\ln (P_{20}/P_1)}{\ln (\rho_{20}/\rho_1)} \qquad (5\text{-}193)$$

where the subscripts 1 and 20 refer to the first and last table entries. An axisymmetric uniform expansion transonic flow field is constructed for the nozzle of interest using this average expansion coefficient and the second order analysis of Kliegel and Quan (Reference 4 and Section 4). The pressure, location and gas flow angle variation along the constant pressure line originating at a specified wall point are determined. The remaining gas flow properties (ρ, V, T) and species concentrations (c_i) along the constant pressure line are determined by interpolation on pressure from the tables previously constructed with the One-Dimensional Two-Phase Reacting Gas Program.

For the particle flow field, the particle flow angle variation along the above constant pressure line is calculated from the constant fraction lag relationship

$$\frac{du}{dx}\left(\frac{dv}{dx}\right)^{-1}\left[\frac{\sqrt{1+\frac{8}{9}\frac{m_{pi}r_{pi}^2}{u\,f_{pi}r^*}\cot\theta_{pi}\frac{dv}{dx}}-1}{\sqrt{1+\frac{8}{9}\frac{m_{pi}r_{pi}^2}{u\,f_{pi}r^*}\frac{du}{dx}}-1}\right]\tan\theta = 1 \quad (5\text{-}194)$$

where $\frac{du}{dx}$ and $\frac{dv}{dx}$ are the gas velocity derivatives along the particle streamlines. These derivatives are calculated from

$$\frac{du}{dx} = V^*\left\{\frac{1}{\sqrt{R}}\left[\frac{da_o}{dz}+\frac{1}{R}\left(\frac{db_o}{dz}+\frac{db_2}{dz}r^2\right)+\frac{1}{R^2}\left(\frac{dc_o}{dz}+\frac{dc_2}{dz}r^2+\frac{dc_4}{dz}r^4\right)\right]+\frac{1}{R}\left[2b_2r+\frac{1}{R}\left(2c_2r+4c_4r^3\right)\right]\tan\theta_{pi}\right\} \quad (5\text{-}195)$$

$$\frac{dv}{dx} = V^*\left\{\frac{1}{R}\left[\frac{da_1}{dz} r + \frac{1}{R}\left(\frac{db_1}{dz} r + \frac{db_3}{dz} r^3\right) + \frac{1}{R^2}\left(\frac{dc_1}{dz} r + \frac{dc_3}{dz} r^3 + \frac{dc_5}{dz} r^5\right)\right] + \frac{1}{\sqrt{R}}\left[a_1 + \frac{1}{R}(b_1 + 3b_3 r^2) + \frac{1}{R^2}(c_1 + 3c_3 r^2 + 5c_5 r^4)\right]\right\} \tan \theta_{pi} \tag{5-196}$$

where the coefficients a_i, b_i, and c_i are those derived by Kliegel and Quan.[4]

The particle velocities and temperature along the constant pressure line are calculated from

$$u_{pi} = V_{pi}(0) \cos \theta_{pi} \tag{5-197}$$

$$v_{pi} = V_{pi}(0) \sin \theta_{pi} \tag{5-198}$$

$$T_{pi} = T_{pi}(0) \tag{5-199}$$

where the values on the initial line axis $\left[V_{pi}(0) \text{ and } T_{pi}(0)\right]$ are determined by interpolation on pressure from the tables previously constructed with the One-Dimensional Two-Phase Reacting Gas Program.

The axis particle density $\rho_{pi}(0)$ is evaluated by integrating the particle continuity and drag equations along the axis using Kliegel and Quan's second order analysis for the gas velocity and relating the axial particle velocity to the gas axial velocity through the constant fractional lag relationships. The particle densities along the constant pressure line are then calculated from

$$\rho_{pi} = \rho_{pi}(0) \tag{5-200}$$

The constant pressure line is then integrated to determine the gas mass flow $\dot{m}$ where

$$\dot{m} = 2\pi \int_{\text{axis}}^{\text{wall}} r\rho V(\cos\theta dr - \sin\theta dx) \qquad (5\text{-}201)$$

and the particle limiting streamline location is determined from the particle continuity relationship across the initial line

$$\dot{m}\, W_{pi} = 2\pi \int_{\text{axis}}^{\text{limiting streamline}} r\, \rho_{pi}(u_{pi}dr - v_{pi}dx) \qquad (5\text{-}202)$$

where W_{pi} is particle to gas mass flow ratio for the ith particle size group.

The above method of constructing initial lines for nonequilibrium characteristic calculations accounts for the dominant curvature effects on the gas and particle flow fields through second order and ignores the curvature effects which would cause a constant pressure line, chosen as the initial starting line, not to be a constant property line. By comparing the above method of constructing nonequilibrium initial lines with a rigorous expansion method, it can be shown that the two methods are equivalent through the first order (the effect of curvature causing departure from constant property lines being of order $R^{-3/2}$). The great advantage of the current method is its simplicity in accounting for the dominant curvature effects and the fact that the flow field varies smoothly across the initial line (i.e., there are no sudden energy release changes or flow field adjustments downstream of the initial line caused by incompatibilities between the gas and chemical properties along the initial line). Thus inaccuracies in the initial line construction used in the present program do not cause physically unreal expansions, compressions or shocks in the characteristic calculations. This later advantage is extremely important since experience has shown that even small incompatibilities between the gas and chemical properties along the initial line can cause very large, physically unreal, flow field adjustments downstream of the initial line. The present method also

conserves energy across the initial line which is only approximately conserved in other methods.

The above method of constructing the particle properties makes use of the constant fractional lag relationships to relate the gas and particle flow fields. These relationships can be simply derived from the particle drag equations along particle streamlines.

$$u_{pi} \frac{du_{pi}}{dx} = \frac{9}{2} \frac{\mu f_{pi} r^*}{m_{pi} r_{pi}^2} (u - u_{pi}) \tag{5-203}$$

$$u_{pi} \frac{dv_{pi}}{dx} = \frac{9}{2} \frac{\mu f_{pi} r^*}{m_{pi} r_{pi}^2} (v - v_{pi}) \tag{5-204}$$

These equations can be rewritten as

$$K_i^2 \frac{du}{dx} + K_i u \frac{dK_i}{dx} = \frac{9}{2} \frac{\mu f_{pi} r^*}{m_{pi} r_{pi}^2} (1 - K_i) \tag{5-205}$$

$$L_i \frac{dv}{dx} + \frac{dL_i}{dx} = \frac{9}{2} \frac{\mu f_{pi} r^*}{m_{pi} r_{pi}^2} \frac{1 - L_i}{K_i} \tan \theta \tag{5-206}$$

where

$$K_i = \frac{u_{pi}}{u} \tag{5-207}$$

$$L_i = \frac{v_{pi}}{v} \tag{5-208}$$

In the throat region of a nozzle, the terms $\frac{u \, d K_i}{dx}$ and $\frac{v \, d L_i}{dx}$ are negligible compared to the other terms. Neglecting these terms the above equations can be solved for K_i and L_i where

$$K_i = \frac{9}{4} \frac{\mu f_{pi} r^*}{m_{pi} r_{pi}^2} \left(\frac{du}{dx}\right)^{-1} \left[\sqrt{1 + \frac{8}{9} \frac{m_{pi} r_{pi}^2}{u f_{pi} r^*} \frac{du}{dx}} - 1\right] \tag{5-209}$$

$$L_i = \frac{9}{4} \frac{\mu f_{pi} r^*}{m_{pi} r_{pi}^2} \tan \theta_{pi} \left(\frac{dv}{dx}\right)^{-1} \left[\sqrt{1 + \frac{8}{9} \frac{m_{pi} r_{pi}^2}{\mu f_{pi} r^*} \cot \theta_{pi} \frac{dv}{dx}} - 1\right] \tag{5-210}$$

Since

$$\tan \theta_{pi} = \frac{L_i}{K_i} \tan \theta \tag{5-211}$$

one obtains by use of the above relationships

$$\frac{du}{dx} \left(\frac{dv}{dx}\right)^{-1} \left[\frac{\sqrt{1 + \frac{8}{9} \frac{m_{pi} r_{pi}^2}{\mu f_{pi} r^*} \cot \theta_{pi} \frac{dv}{dx}} - 1}{\sqrt{1 + \frac{8}{9} \frac{m_{pi} r_{pi}^2}{\mu f_{pi} r^*} \frac{du}{dx}} - 1}\right] \tan \theta = 1 \tag{5-212}$$

which is Equation (5-194)

After constructing the initial data line, the reacting gas characteristic relationships (Equations (5-161) through (5-174)) are integrated. Characteristic equations are generally integrated using second-order explicit methods which are generally simpler than implicit methods. It has been shown in Section 3, however, that implicit integration methods are superior to explicit methods for integrating chemical relaxation equations. The particle properties are also governed by equations of the relaxation type. Thus, in the present program, the fluid dynamic equations are integrated using an explicit modified Euler method while the particle and chemical relaxation equations are integrated using a first order implicit integration method.

In perfect gas flows, the flow is isentropic along streamlines and the streamline relationships can be integrated in close form. Thus, in calculating supersonic perfect gas flow fields using the methods of characteristics, only the Mach line relationships need be numerically integrated to construct the flow field. In the calculation of supersonic reacting-gas flow fields, the flow is nonisentropic along streamlines and the streamline relationships must be numerically integrated as well as the Mach line relationships. In two-phase flows, the condensed phase does not follow the gas streamlines due to particle inertia and the

calculation becomes even more complicated since a separate particle streamline must be considered for each particle present in the flow.

In numerical calculating flow fields using the method of characteristics only two (previously calculated) known points are directly usable in calculating a forward point. In nonequilibrium flows, however, more than two known points are required to calculate a forward point so that a choice must be made as to which points in the flow field will be used directly and which will be interpolated. In the reacting gas program,[14] the back streamline point and one characteristic point were chosen as the known points since even small interpolation errors in species concentrations will cause serious stability and accuracy problems in the numerical integration of the chemical relaxation equations. This choice avoids interpolation for the species concentrations in that only the fluid dynamic properties (velocity, temperature, etc.) and the total entropy production term due to all nonequilibrium effects need to be interpolated at one of the back characteristic points. Since these quantities are all slowly varying across the characteristic mesh, they can be interpolated quite accurately. In the present two phase reacting gas nonequilibrium program, the same basic numerical methods are used by choosing as known points the gas streamline point and one characteristic point and interpolating for the other characteristic point and the particle streamline points. A complete derivation of the numerical methods used in the program are given below.

Consider the flow field shown in Figure 5-3.

The fluid dynamic equations are integrated as follows. Between points 3 and 4, the gas streamline characteristic relationships are integrated as

$$r_3 = r_4 + \tan\left[\frac{1}{2}(\theta_4 + \theta_3)\right](x_3 - x_4) \tag{5-213}$$

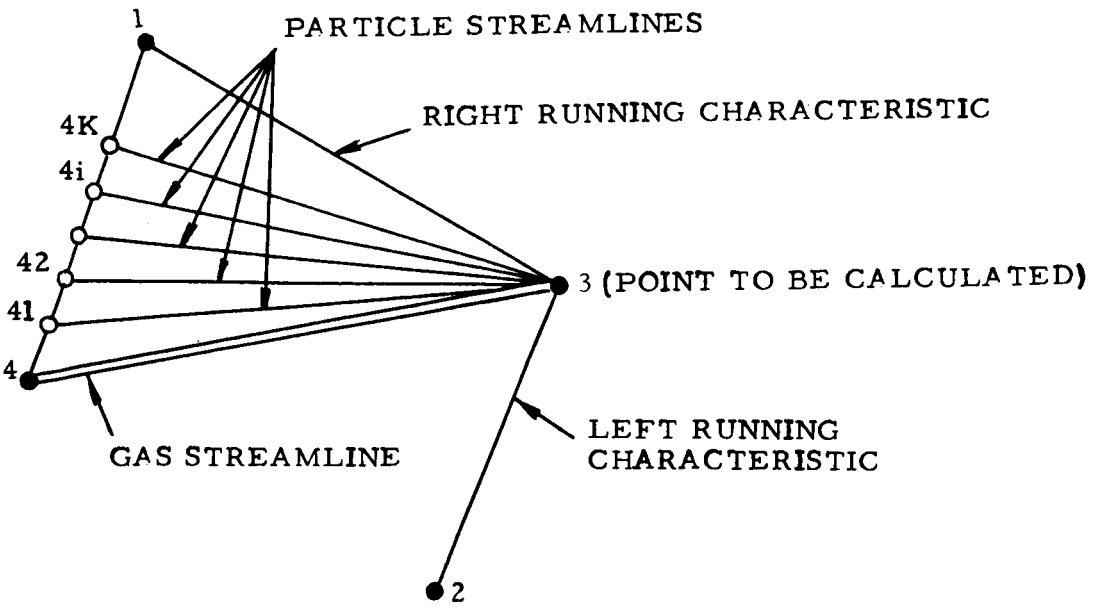

Figure 5-3. Flow Field Calculation

$$V_3 = \left\{V_4^{\,2} + \frac{2N}{N-1}\,\frac{P_4}{\rho_4}\left[1 - \left(\frac{P_3}{P_4}\right)^{\frac{N-1}{N}}\right] + \left(\frac{C_4}{\cos\theta_4} + \frac{C_3}{\cos\theta_3}\right)(x_3 - x_4)\right\}^{\frac{1}{2}} \tag{5-214}$$

$$\rho_3 = \rho_4\left(\frac{P_4}{P_4}\right)^{\frac{1}{2}\left(\frac{1}{\gamma_4} + \frac{1}{\gamma_3}\right)} \exp\left[-\frac{1}{2}\left(\frac{A_4}{\cos\theta_4} + \frac{A_3}{\cos\theta_3}\right)(x_3 - x_4)\right] \tag{5-215}$$

$$T_3 = T_4\left(\frac{P_3}{P_4}\right)^{\frac{1}{2}\left(\frac{\gamma_4 - 1}{\gamma_4} + \frac{\gamma_3 - 1}{\gamma_3}\right)} \exp\left[-\frac{1}{2}\left(\frac{B_4}{\cos\theta_4} + \frac{B_3}{\cos\theta_3}\right)(x_3 - x_4)\right] \tag{5-216}$$

where

$$N = \frac{\ln\left(\frac{P_3}{P_4}\right)}{\ln\left(\frac{\rho_3}{\rho_4}\right)} \tag{5-217}$$

The integration formula (5-213) relating the coordinates of points 3 and 4 was chosen since it is exact if the streamline is a circular arc between points 3 and 4. This is an excellent approximation over one mesh step. In integrating the momentum equation to obtain Equation (5-214), it was assumed that P varies as ρ^N along the streamline. Equations (5-215) and (5-216) are obtained by using the energy equation and the equation of state. In obtaining formulas (5-214), (5-215), and (5-216), the coefficients $\left[\gamma^{-1}, (\gamma-1)/\gamma, A/\cos\theta, B/\cos\theta, \text{ and } C/\cos\theta\right]$ appearing in these equations were assumed to be equal to their average value between points 3 and 4. These integration formulas are exact for nonreacting, one-phase, constant-gamma flows (note that in this case N equals γ and A, B, and C are zero).

Between points 1 and 3 the right running characteristic relationships are integrated as

$$r_3 = r_1 + \tan\left[\frac{1}{2}(\theta_1 + \theta_3 - \alpha_1 - \alpha_3)\right](x_3 - x_1) \tag{5-218}$$

$$P_3 = P_1 \exp - \left[\frac{1}{2}(E_1G_1H_1 + E_3G_3H_3)(x_3 - x_1) - \frac{1}{2}\left(\frac{G_1H_1 \sin\theta_1}{r_1} + \frac{G_3H_3 \sin\theta_3}{r_3}\right)(x_3 - x_1) - \frac{1}{2}(G_1 + G_3)(\theta_3 - \theta_1)\right] \tag{5-219}$$

The integration formula (5-218) relating the coordinates of points 1 and 3 was chosen since it is exact if the right running characteristic is a circular arc between points 1 and 3. This is an excellent approximation over one mesh step. In integrating the right running characteristic relationship to obtain Equation (5-219) the coefficients (EGH, GH $\sin\theta/r$, and G) appearing in Equation (5-169) were assumed to equal their average value between points 1 and 3. This is an excellent approximation over one mesh step. If point 3 is an axis point then r_3 and $\sin\theta_3$ are zero and the indeterminate quantity $\sin\theta_3/r_3$ appearing in Equation (5-219) is approximated by

$$\frac{\sin \theta_3}{r_3} = \frac{\tan \theta_1}{r_1 + (x_3 - x_1) \tan \theta_1} \tag{5-220}$$

Equation (5-220) is obtained by extrapolating for the ratio $\sin \theta / r$ on the axis, assuming that the flow near the axis is a source flow.

Between points 2 and 3, the left running characteristic relationships are integrated as

$$x_3 = x_2 + \cot \left[\frac{1}{2}(\theta_2 + \theta_3 + \alpha_2 + \alpha_3)\right](r_3 - r_2) \tag{5-221}$$

$$\begin{aligned} P_3 = P_2 \exp \Bigg[& \frac{1}{2}(D_2 G_2 F_2 + D_3 G_3 F_3)(r_3 - r_2) \\ & - \frac{1}{2}\left(\frac{G_2 F_2 \sin \theta_2}{r_2} + \frac{G_3 F_3 \sin \theta_3}{r_3}\right)(r_3 - r_2) \\ & - \frac{1}{2}(G_2 + G_3)(\theta_3 - \theta_2) \Bigg] \end{aligned} \tag{5-222}$$

The integration formula (5-221) relating the coordinates of points 2 and 3 was chosen because it is exact if the left running characteristic is a circular arc between points 2 and 3. This is an excellent approximation over one mesh step. In integrating the left running characteristic relationship to obtain Equation (5-222), the coefficients (DGF, GF $\sin \theta / r$, and G) appearing in Equation (5-167) were assumed to equal their average value between points 2 and 3. This is an excellent approximation over one mesh step. If point 2 is an axis point, then r_2 and θ_2 are zero and the indeterminate quantity $\sin \theta_2 / r_2$ appearing in Equation (5-222) is that quantity previously calculated for the axis point using Equation (5-220).

Equations (5-219) and (5-222) can be combined to yield

$$\theta_3 = \frac{1}{G_3 + \frac{1}{2}(G_1 + G_2)} \left[\ln\left(\frac{P_2}{P_1}\right) + \frac{1}{2}(G_1 + G_3)\theta_1 + \frac{1}{2}(G_2 + G_3)\theta_2 \right.$$

$$+ \frac{1}{2}(D_2G_2F_2 + D_3G_3F_3)(r_3 - r_2)$$

$$- \frac{1}{2}\left(\frac{G_2F_2 \sin\theta_2}{r_2} + \frac{G_3F_3 \sin\theta_3}{r_3}\right)(r_3 - r_2)$$

$$+ \frac{1}{2}(E_1G_1H_1 + E_3G_3H_3)(x_3 - x_1)$$

$$\left. - \frac{1}{2}\left(\frac{G_1H_1 \sin\theta_1}{r_1} + \frac{G_3H_3 \sin\theta_3}{r_3}\right)(x_3 - x_1) \right] \quad (5\text{-}223)$$

In the various point calculations, Equation (5-223) is solved for θ_3 and either Equation (5-219) or (5-222) is solved for P_3, depending on whether point 1 or point 2 is the known data point.

It can be shown that use of these integration equations results in an error of order h^3 where h is the integration increment (mesh size). Since these integration equations involve the flow properties at the unknown point (point 3), they must be solved by iteration. The modified Euler iteration method is used to solve these equations, and the various point calculations are similar to those described in Section 5.3 of Reference 14.

In integrating the chemical relaxation equations, it is advantageous to employ an implicit method as discussed in Section 3. A first order implicit integration method was chosen for use in the present program to integrate the chemical relaxation equations. The derivation is identical to that shown on page 5-26, with Equation (5-120) being the resulting integration formula.

To integrate the particle flow equations, the following procedure is used. The equation relating the coordinates of an ith particle streamline [Equation (5-170)] can be integrated using second order explicit method. The integration formula is

$$r_3 = r_{4i} + \tan\left[\frac{1}{2}\left(\theta_{pi_{4i}} + \theta_{pi_{3i}}\right)\right](x_3 - x_{4i}) \tag{5-224}$$

which relates point 4i to point 3 (see Figure 5-3).

In calculating the particle density ρ_{pi} from Equations (5-174) and (5-192), it is convenient to use an integration formula obtained by making a mass balance between mesh points. By equating the mass flow between points 4i and 2 to the mass flow between points 3 and 2 (there is no mass flow of ith particles between points 4i and 3 since these points are the ith particle streamline points), one obtains an integration formula for the density of the ith particle group at point 3.

$$\begin{aligned}\rho_{pi_3} = &\left[u_{pi_3}(r_3^2 - r_2^2) - v_{pi_3}(x_3 - x_2)(r_3 + r_2)\right]^{-1} \\ &\Big\{\rho_{pi_{4i}}\left[u_{pi_{4i}}(r_{4i}^2 - r_2^2) - v_{pi_{4i}}(x_{4i} - x_2)(r_{4i} + r_2)\right] \\ &+ \rho_{pi_2}\Big[u_{pi_2}(r_{4i}^2 - r_3^2) - v_{pi_2}(x_{4i} + x_2)(r_{4i} + r_2) + \\ &\qquad v_{pi_2}(x_3 - x_2)(r_3 + r_2)\Big]\Big\}\end{aligned} \tag{5-225}$$

For the particle velocities u_{pi} and v_{pi} and the particle enthalpies h_{pi}, the governing equations [Equations (5-171) to (5-173)] are of the relaxation type. Hence the implicit method employed in integrating for the chemical species is also used in integrating for u_{pi}, v_{pi}, and h_{pi}. Letting

$$\bar{f}_i = \frac{9}{2} \frac{\mu f_{pi} r^*}{m_{pi} r_{pi}^2 u_{pi}} \tag{5-226}$$

$$\bar{g}_i \doteq - \frac{3\mu g_{pi} r^*}{m_{pi} r_{pi}^2 u_{pi}} \frac{C_p}{c_{ppi} P_r} \tag{5-227}$$

and using a formula parallel to Equation (5-115), one obtains

$$\Delta u_{pi} = \left[\bar{f}_i (u - u_{pi})\right]_{x_{pi} + \Delta x_{pi}} \Delta x_{pi} \tag{5-228}$$

$$\Delta v_{pi} = \left[\bar{f}_i (v - v_{pi})\right]_{x_{pi} + \Delta x_{pi}} \Delta x_{pi} \tag{5-229}$$

$$\Delta T_{pi} = \left[\bar{g}_i (T_{pi} - T)\right]_{x_{pi} + \Delta x_{pi}} \Delta x_{pi}, \quad T_{pi} \neq T_{pmi} \tag{5-230}$$

$$\Delta h_{pi} = \left[C_{ppi} \bar{g}_i (T_{pmi} - T)\right]_{x_{pi} + \Delta x_{pi}} \Delta x_{pi}, \quad T_{pi} = T_{pmi} \tag{5-231}$$

Equation (5-230) is used when the particle temperature is changing, and Equation (5-231) is used when the particle is in the state of solidification.

6. PROGRAM LIMITATIONS

To operate any of the four computer programs developed, one should be thoroughly familiar with the Program User's Manual which is written as a separate section in the documentation report for the program. The general limitations of the programs are summarized below.

- The species and reactions considered in the programs have been verified only for the propellant systems and mixture ratios listed in Table 2-1. For other propellant systems, one should verify that the significant chemical species and reactions are included in those considered by the program.

- To run a nonequilibrium case, one must first determine (either by making an equilibrium run or from some other source) whether condensed phase (liquid or solid) exists at the initial point between the chamber and the throat. In the one-dimensional two-phase program, the amount of condensed phase is internally determined by the program and is equal to the equilibrium value at the initial point. In the axisymmetric two-phase program, the amount of condensed phase must be input.

- In the one-dimensional two-phase program, only one metal element can be considered in a propellant system.

- In the axisymmetric two-phase program, the gas is a perfect gas of constant specific heat ratio.

- If one runs extreme physical cases (such as extremely large on small particles or physically unreal kinetic rates), the program integration step size and mesh control parameters may have to be adjusted from nominal values to insure accurate calculations.

- Accurate chemical reaction rate inputs are required for the non-equilibrium runs. The thermochemical data are semi-permanent, i.e., they have already been input, and are taken from the December 1966 revision of the JANAF Tables. These data should be updated when better information becomes available.

- The nozzle walls should be smooth and not have discontinuities.

- The nozzle inlet geometry needs to satisfy the relation $\sqrt{EC} < 1 + (R^* + RI)(1 - \cos \theta I)$ where EC is the contraction ratio, R^* is the normalized throat wall radius of curvature, RI is the normalized inlet wall radius of curvature, and θI is the inlet angle.

- In the axisymmetric programs, the normalized throat wall radius of curvature R which is used to generate the transonic initial data line should have a value not less than 2.0, since the transonic solution becomes inaccurate for smaller values of R.

- The proper integration step size depends on the nozzle geometry and propellant system. In general, an optimum initial integration step size is about 0.025 and the fractional incremental error input should be of order 0.001.

7. ILLUSTRATIONS OF RESULTS

The results of the four programs developed are illustrated in Figures 7-1 through 7-14 and Table 7-1.

Figures 7-1 through 7-6 compare the equilibrium, frozen, and kinetic results using the One-Dimensional Reacting Gas Program.[7] The case corresponds to the propellant system of N_2O_4/A50 at a mixture ratio of 2.0 and to a nozzle of typical geometry. It is seen that the kinetic results fall between the equilibrium and frozen solutions in general.

Figures 7-7 through 7-10 illustrate the results obtained from the One-Dimensional Two-Phase Reacting Gas Program.[12] The case corresponds to a propellant system with liquid Al_2O_3 particles in the chamber. It may be noted from Figure 7-10 that the kinetic performance is below the frozen performance calculated for gas-particle equilibrium; this is due to the performance loss caused by particle lag.

Figure 7-11 illustrates the two-zone results of the Axisymmetric Reacting Gas Program.[14] The case corresponds to the propellant system of N_2O_4/A50 at an overall mixture ratio of 1.6. It is seen that the performance varies significantly with the outer-zone stagnation temperature, which is a function of the outer-zone mixture ratio, and with the fraction of mass flow in the outer zone.

Figures 7-12 to 7-14 and Table 7-1 pertain to the Axisymmetric Two-Phase Perfect Gas Program[17] and are taken from Reference 13. Table 7-1 is a summary of the measured and calculated nozzle efficiencies of six conical nozzles. In Figures 7-12 to 7-14, I_{spe} is the ideal specific impulse. Figure 7-12 shows a comparison of the experimental and calculated effect of changes in nozzle throat geometry. For Figure 7-12, the nozzles consisted only of a convergent section; the nozzle inlet geometry was fixed and the wall radius of curvature upstream of the throat was varied. Figure 7-13 shows a comparison of the experimental and calculated effect of changing the nozzle inlet angle. For this figure, the nozzles had identical throat and exit cone geometries and the wall inlet angle from the chamber wall was varied. Figure 7-14 compares the experimental and calculated effects of nozzle contouring. For this figure, the nozzle inlet and throat

section were identical; the exit cones were the same length and had the same expansion ratio but different wall contours. From these figures and Table 7-1, it is seen that the calculated, heat, friction, and expansion losses reasonably account for the observed efficiency losses.

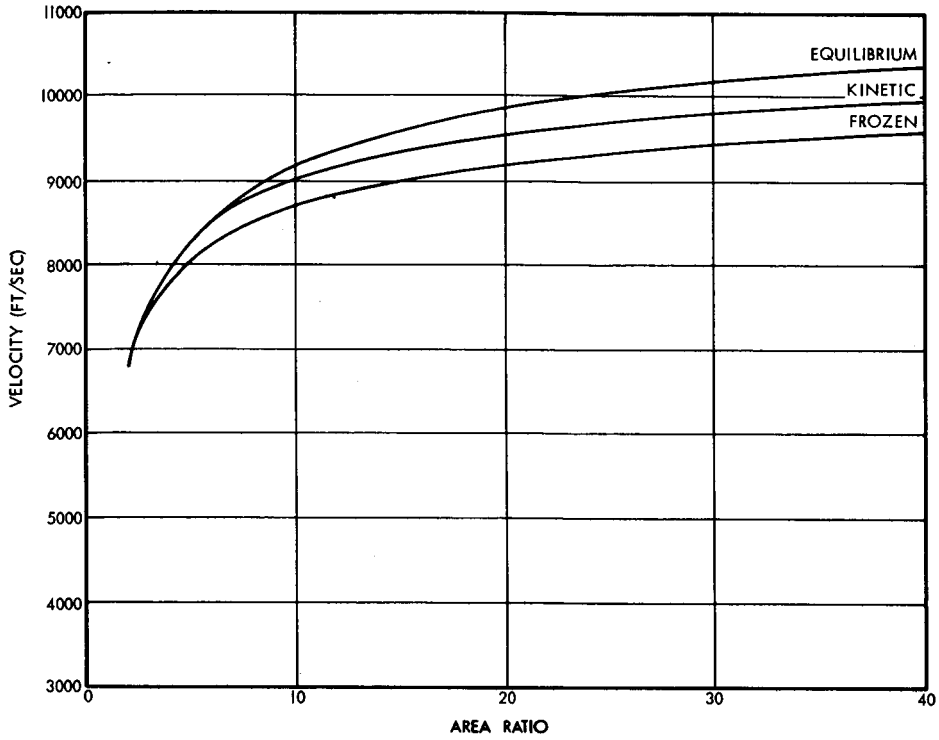

Figure 7-1. Velocity Versus Area Ratio

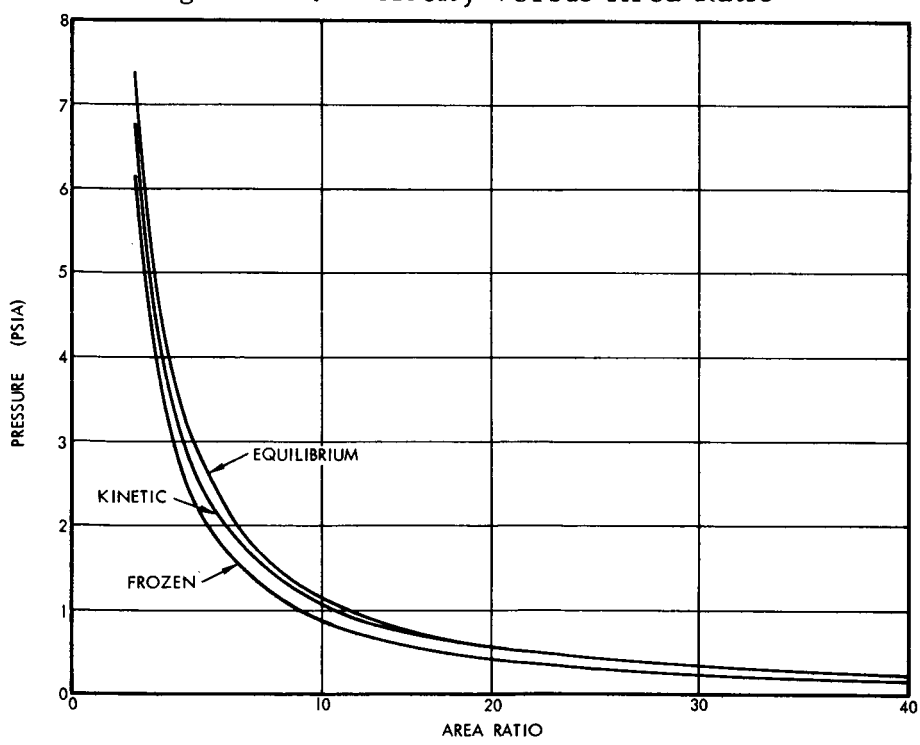

Figure 7-2. Pressure Versus Area Ratio

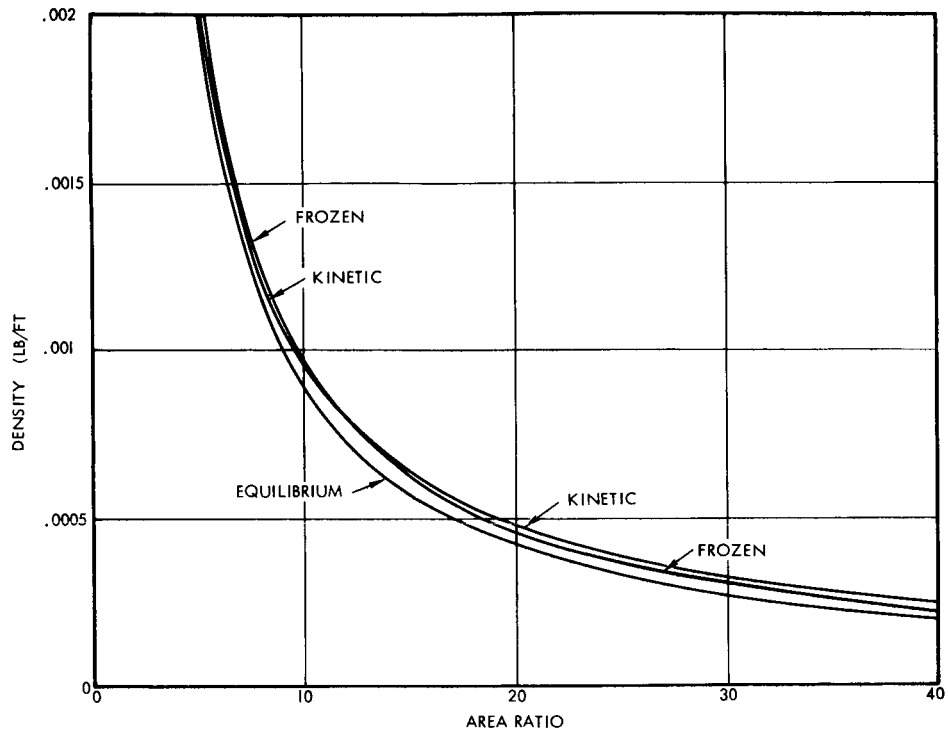

Figure 7-3. Density Versus Area Ratio

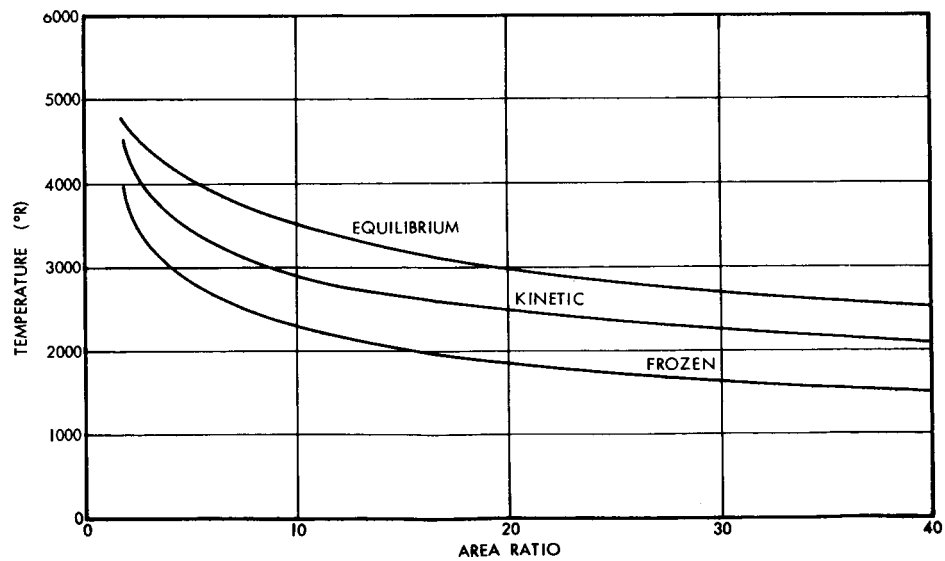

Figure 7-4. Temperature Versus Area Ratio

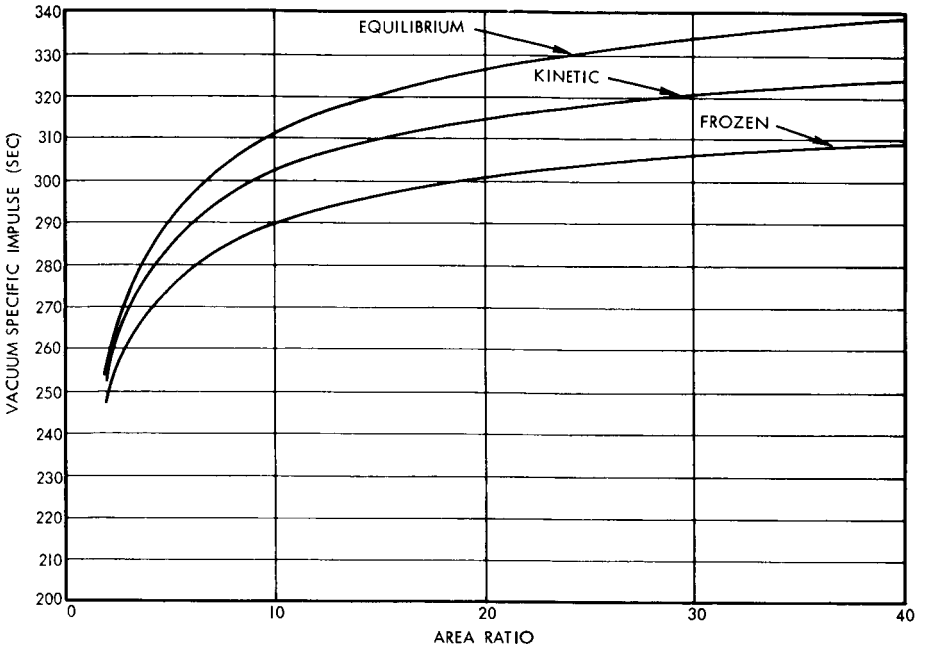

Figure 7-5. Vacuum Specific Impulse Versus Area Ratio

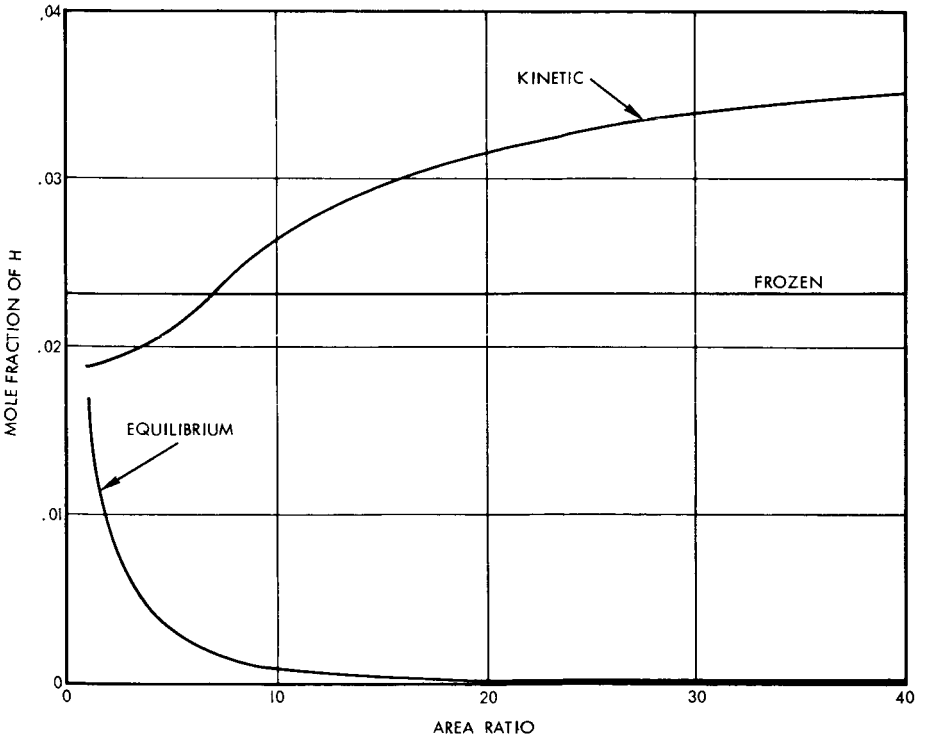

Figure 7-6. Mole Fraction of H Versus Area Ratio

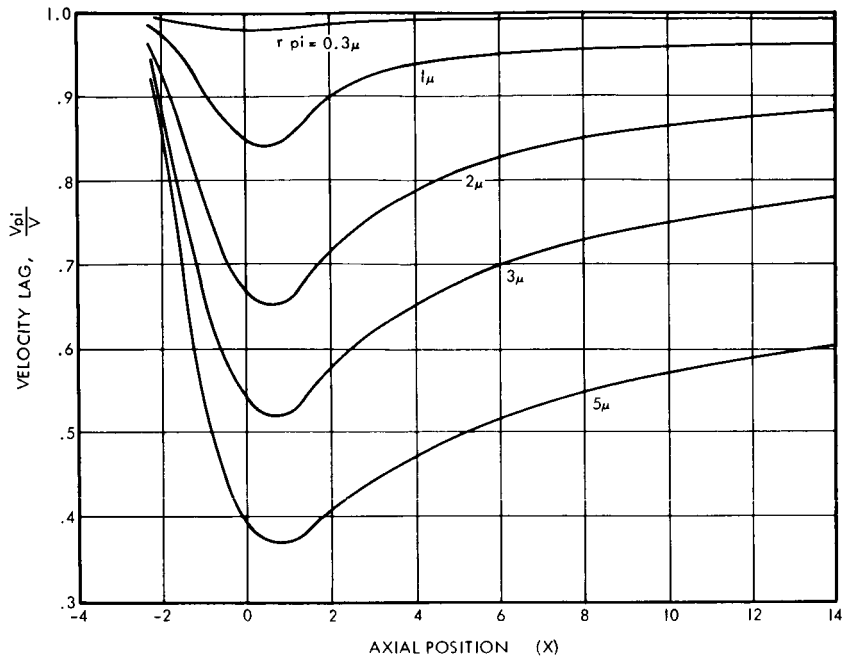

Figure 7-7. Velocity Lag Versus Axial Position

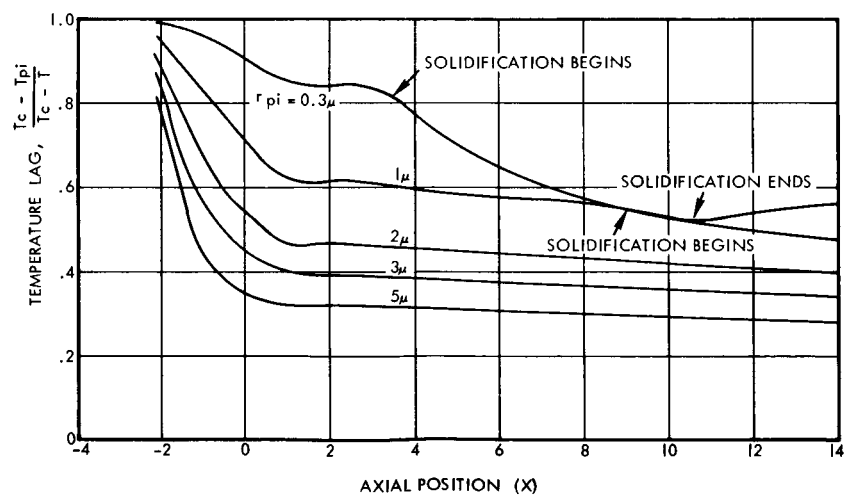

Figure 7-8. Temperature Lag Versus Axial Position

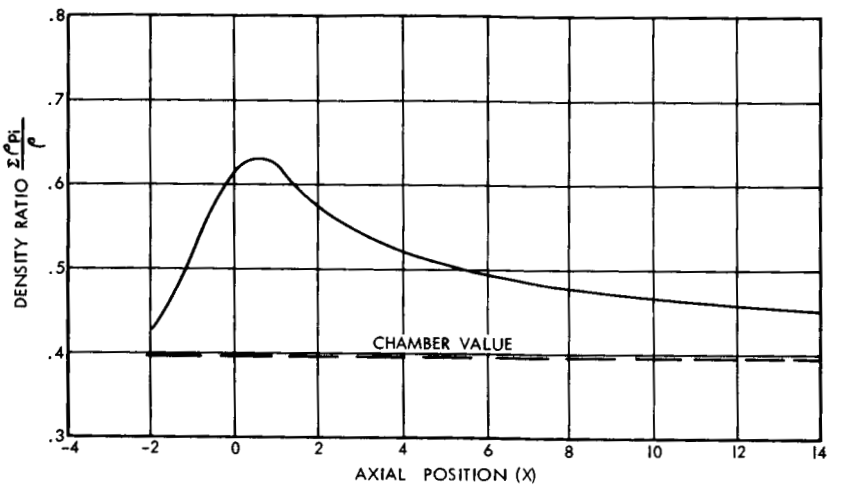

Figure 7-9. Density Ratio Versus Axial Position

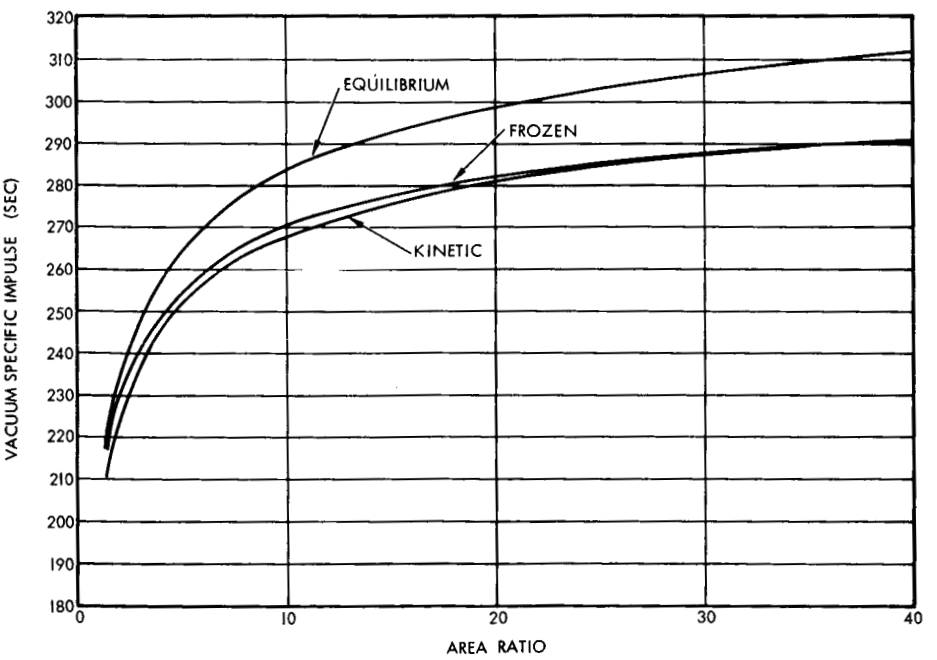

Figure 7-10. Vacuum Specific Impulse Versus Area Ratio

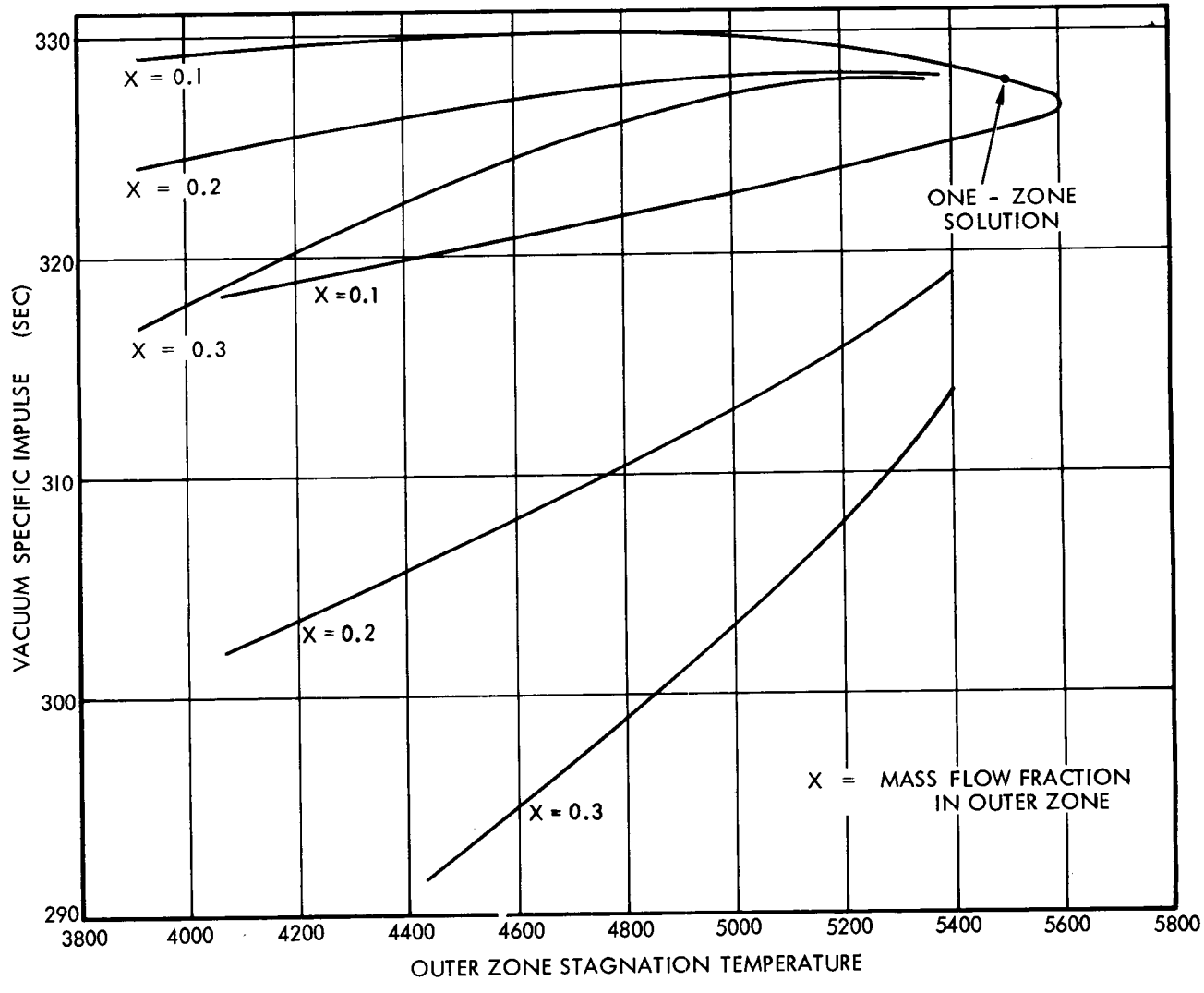

Figure 7-11. Two-Zone Nozzle Performance

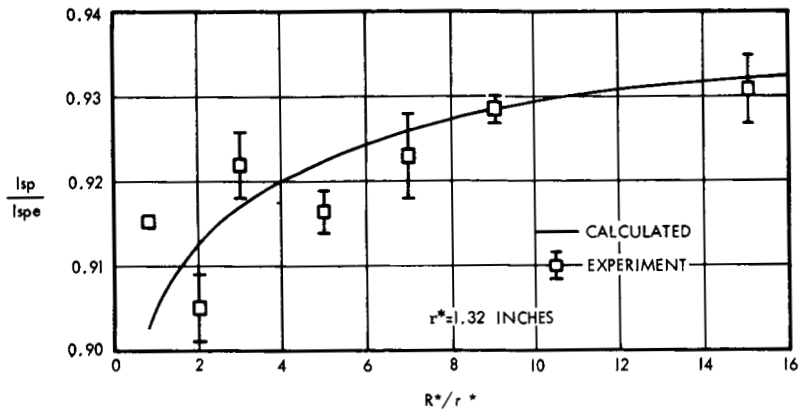

Figure 7-12. Nozzle Efficiency as a Function of Nozzle Throat Geometry

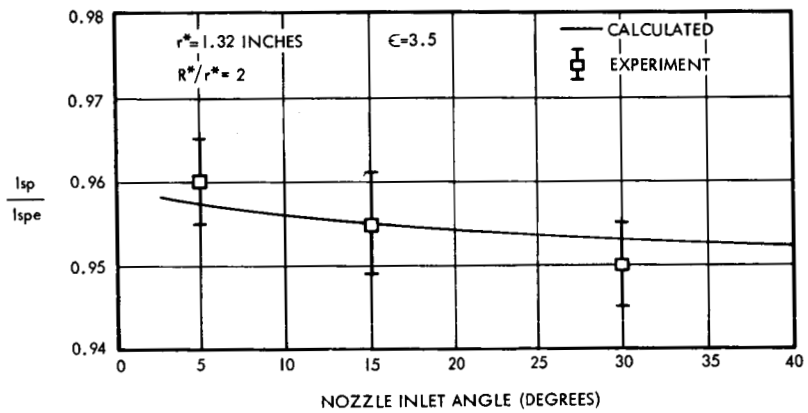

Figure 7-13. Nozzle Efficiency as a Function of Nozzle Inlet Geometry

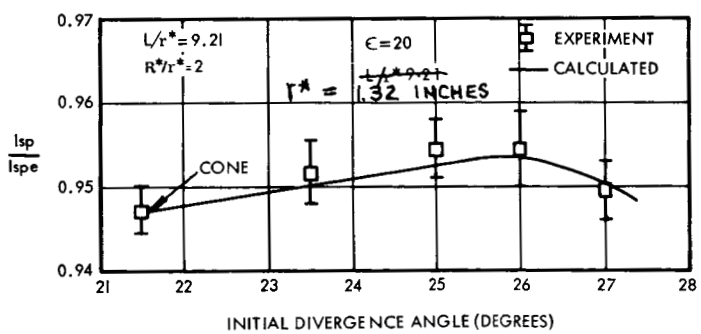

Figure 7-14. Nozzle Efficiency as a Function of Nozzle Contouring

Table 7-1. Comparison of Measured and Calculated Gas-Particle Expansion Losses in Conical Nozzles

ϵ	3.5	20	24	24	24	24
r^* (inches)	1.32	1.32	1.32	1.32	1.32	1.32
R^*/r^*	2	2	2	5	5	5
Cone angle, deg.	25.2	21.5	24	12	18	24
Calculated heat losses, %	0.6 ±0.2	0.8 ±0.2	0.9 ±0.3	1.3 ±0.4	1.1 ±0.3	1.0 ±0.3
Calculated friction losses, %	0.7 ±0.2	1.5 ±0.5	1.4 ±0.4	2.9 ±0.9	2.0 ±0.6	1.6 ±0.5
Measured engine efficiency, %	95.4 ±0.3	94.7 ±0.3	94.7 ±0.6	95.1 ±0.3	95.1 ±0.3	95.1 ±0.3
Measured expansion losses, %	3.3 ±0.7	3.0 ±1.0	3.0 ±1.3	0.7 ±1.6	1.8 ±1.2	2.3 ±1.1
Calculated expansion losses, %	5.0 ±1.0	4.8 ±1.0	4.9 ±1.0	3.5 ±1.0	4.1 ±1.0	4.6 ±1.0

8. CONCLUDING REMARKS

Four computer programs have been developed for the analytical predictions of delivered specific impulse under NASA/MSC contract NAS 9-4358. These programs are the One-Dimensional Reacting Gas Nonequilibrium Performance Program, One-Dimensional Two-Phase Reacting Gas Nonequilibrium Performance Program, Axisymmetric Reacting Gas Nonequilibrium Performance Program and Axisymmetric Two-Phase Perfect Gas Performance Program. For each of these programs, a two-volume program documentation report containing a complete engineering and programming description of the program has been issued (References 7, 12, 14, and 17).

Three analysis reports have also been issued. They pertain to the study of chemical species and chemical reactions (Reference 1), the transonic analyses (Reference 4), and the axisymmetric two-phase reacting gas nozzle flows analysis (Reference 21). Based on the analysis of Reference 21, the major components of an axisymmetric two-phase reacting gas program have been programmed also

To operate any of the computer programs developed, one should be familiar with the appropriate program documentation report which includes the user's manual and a sample case.

REFERENCES

1. P.I. Gold and C.T. Weekley, "Chemical Species and Chemical Reactions of Importance in Nonequilibrium Performance Calculations," 02874-6001-R000, TRW Systems, 6 December 1966.

2. R. Tunder, S. Mayer, B. Cook, and L. Schieler, "Compilation of Reaction Rate Data for Nonequilibrium Performance and Re-entry Calculation Programs," Aerospace Corporation, 1966.

3. T.J. Tyson, "An Implicit Integration Method for Chemical Kinetics," 9840-6002-RU000, TRW Space Technology Laboratories, September 1964.

4. J.R. Kliegel and V. Quan, "Convergent-Divergent Nozzle Flows," 02874-6002-R000, TRW Systems, 30 December 1966.

5. I.M. Hall, "Transonic Flow in Two-Dimensional and Axially-Symmetrical Nozzles, Quart. Journ. Mech. and Applied Math., Vol. XV, Part 4, p. 487 (1962).

6. R. Sauer, "General Characteristics of the Flow Through Nozzles at Near Critical Speeds," NACA Tech. Note No. 1147, 1947.

7. J.R. Kliegel and H.M. Frey, "One-Dimensional Reacting Gas Nonequilibrium Performance Program," 02874-6003-R000, TRW Systems, 1 March 1967 (Rev. September 1967).

8. J.O. Hirshfelder, C.F. Curtiss and R.B. Bird, Molecular Theory of Gases and Liquids, John Wiley and Sons, Inc., New York, N.Y., 1954.

9. S.S. Penner, Chemistry Problems in Jet Propulsion, Pergamon Press, New York, N.Y., 1957.

10. K.N.C. Bray, "Atomic Recombination in a Hypersonic Wind Tunnel Nozzle," J. Fluid Mechanics, Vol. 6, p. 1, 1959.

11. S.W. Benson and T. Fueno, "Mechanism of Atom Recombination by Consecutive Vibrational Deactivations," J. Chem. Physics, Vol. 36, p. 1957, 1962.

12. J.R. Kliegel, V. Quan, S.S. Cherry, and H.M. Frey, "One-Dimensional Two-Phase Reacting Gas Nonequilibrium Performance Program," 02874-6005-R000, TRW Systems, 15 August 1967 (Rev. September 1967).

13. J.R. Kliegel, "Gas Particle Nozzle Flows," In Ninth International Symposium on Combustion, Academic Press, Inc., New York, N.Y., 1963.

14. J.R. Kliegel, V. Quan, G.R Nickerson, and J.E. Melde, "Axisymmetric Reacting Gas Nonequilibrium Performance Program," 02874-6004-R000, TRW Systems, 8 March 1967 (Rev. September 1967).

15. R. Courant and K.O. Friedricks, Supersonic Flow and Shock Waves, Interscience Publishers, Inc., New York, N.Y., 1948.

16. J.R. Kliegel and G.R. Nickerson, "Flow of Gas-Particle Mixtures in Axially Symmetric Nozzles," In Detonation and Two-Phase Flow, Academic Press, Inc., New York, N.Y., 1962.

17. J.R. Kliegel and G.R. Nickerson, "Axisymmetric Two-Phase Perfect Gas Performance Program," 02874-6006-R000, TRW Systems, 3 April 1967 (Rev. September 1967).

18. W.G. Vincenti, "Non-equilibrium Flow Over a Wavy Wall," J. Fluid Mechanics, Vol. 6, p. 481, 1959.

19. J.R. Kliegel, "One-Dimensional Flow of a Gas-Particle System," Paper No. 60-S, IAS 28th Annual Meeting, New York, 1960.

20. K.W. Emmons, "The Theoretical Flow of a Frictionless, Adiabatic, Perfect Gas Inside of a Two-Dimensional Hyperbolic Nozzle," NACA TN 1003, 1946.

21. V. Quan and J.R. Kliegel, "Axisymmetric Two-Phase Reacting Gas Nonequilibrium Nozzle Flows Analysis," 02874-6007-R000, TRW Systems, 18 August 1967.

NASA-Langley, 1968 — 27 CR-112

NATIONAL AERONAUTICS AND SPACE ADMINISTRATION
WASHINGTON, D. C. 20546

OFFICIAL BUSINESS

FIRST CLASS MAIL

POSTAGE AND FEES PA
NATIONAL AERONAUTICS
SPACE ADMINISTRATIC

POSTMASTER: If Undeliverable (Sectior
Postal Manual) Do Not

"The aeronautical and space activities of the United States shall be conducted so as to contribute . . . to the expansion of human knowledge of phenomena in the atmosphere and space. The Administration shall provide for the widest practicable and appropriate dissemination of information concerning its activities and the results thereof."

— NATIONAL AERONAUTICS AND SPACE ACT OF 1958

NASA SCIENTIFIC AND TECHNICAL PUBLICATIONS

TECHNICAL REPORTS: Scientific and technical information considered important, complete, and a lasting contribution to existing knowledge.

TECHNICAL NOTES: Information less broad in scope but nevertheless of importance as a contribution to existing knowledge.

TECHNICAL MEMORANDUMS: Information receiving limited distribution because of preliminary data, security classification, or other reasons.

CONTRACTOR REPORTS: Scientific and technical information generated under a NASA contract or grant and considered an important contribution to existing knowledge.

TECHNICAL TRANSLATIONS: Information published in a foreign language considered to merit NASA distribution in English.

SPECIAL PUBLICATIONS: Information derived from or of value to NASA activities. Publications include conference proceedings, monographs, data compilations, handbooks, sourcebooks, and special bibliographies.

TECHNOLOGY UTILIZATION PUBLICATIONS: Information on technology used by NASA that may be of particular interest in commercial and other non-aerospace applications. Publications include Tech Briefs, Technology Utilization Reports and Notes, and Technology Surveys.

Details on the availability of these publications may be obtained from:

SCIENTIFIC AND TECHNICAL INFORMATION DIVISION

NATIONAL AERONAUTICS AND SPACE ADMINISTRATION

Washington, D.C. 20546